Evolutionary Processes in Variable Environments

by

Sebastian Novak

July, 2016

A thesis presented to the
Graduate School
of the
Institute of Science and Technology Austria, Klosterneuburg, Austria
in partial fulfillment of the requirements for the degree
Doctor of Philosophy

Institute of Science and Technology

The dissertation of Sebastian Novak, titled "Evolutionary Processes in Variable Environments", is approved by:

Supervisor: Nicholas H. Barton, IST Austria, Klosterneuburg, Austria

Signature: 

Committee Member: Séverine Vuilleumier, EPFL, Lausanne, Switzerland

Signature: 

Committee Member: Gašper Tkačik, IST Austria, Klosterneuburg, Austria

Signature: 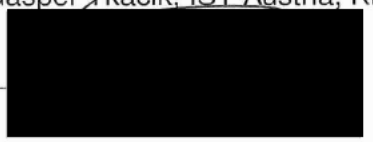

Defense Chair: Simon Hippenmeyer, IST Austria, Klosterneuburg, Austria

Signature: 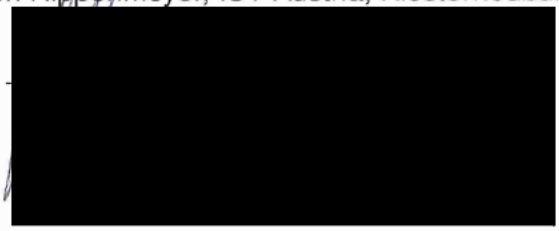

I hereby declare that this dissertation is my own work, and it does not contain other people's work without this being so stated, that this thesis does not contain my previous work without this being stated, and that the bibliography contains all the literature that I used in writing the dissertation.

I declare that this is a true copy of my thesis, including any final revisions, as approved by my thesis committee, and that this thesis has not been submitted for a higher degree to any other university or institution.

Signature: 

Sebastian Novak

July, 2016

Biographical Sketch

The author of this thesis, Sebastian Novak, was born in Tulln an der Donau, Austria. In 2004, he enrolled in the instrumental bachelor studies (accordion) at the Conservatory of Vienna and, in parallel, matriculated at the University of Vienna to study mathematics, where he specialised in Biomathematics in the ensuing years. Pursuing both studies with equal devotion, he graduated from the Conservatory in 2009 and received his master's degree in mathematics one year later, in 2010. After a short appointment as a research associate at the University of Vienna, he got accepted at the interdisciplinary graduate program of the Institute of Science and Technology Austria in 2011 to study evolutionary biology in the research group of Nick Barton.

Throughout his young career, Sebastian has proven to be a highly productive researcher with very diverse interests and the ability to collaborate across the boundaries of scientific disciplines. His publication record starts with the publication of part of his diploma thesis, and it contains articles in game theory, host-pathogen dynamics, and dispersal evolution. More recently, he has been focusing on projects on stress-induced mutagenesis and on the evolution of phenotypic characteristics in fluctuating environments. He enjoyed attending multiple international conferences to exchange ideas with colleagues and present his work to a broader community.

Sebastian is a very many-sided character which, for one thing, reflects in multiple extracurricular activities. As such, he took responsibility as representative of the IST Austria Graduate Student Association, assisted in the organization of various social and academic events, and is part of the IST Austria Works Council. For another thing, he remained true to his non-academic interests, in particular music, putting much effort in arranging pieces for his instrument, organizing his own concerts, and frequently performing in public.

List of Publications

1. **S. Novak** (2011). The number of equilibria in the diallelic Levene model with multiple demes, *Theoretical Population Biology* 79(3): 97–101 (single author)

2. **S. Novak**, K. Chatterjee, and M.A. Nowak (2013). Density games, *Journal of Theoretical Biology* 334: 26–34 (first and corresponding author)

3. **S. Novak** (2014). Habitat heterogeneities versus spatial type frequency variances as driving forces of dispersal evolution, *Ecology and Evolution* 4(24): 4589–4597 (single author)[*]

4. N.H. Barton, **S. Novak**, and T. Paixão (2014). Diverse forms of selection in evolution and computer science, *PNAS* 111(29): 10398–10399 (contributing author)

5. **S. Novak** and S. Cremer (2015). Fungal disease dynamics in insect societies: optimal killing rates and the ambivalent effect of high social interaction rates, *Journal of Theoretical Biology* 372, 54–64 (first and corresponding author)

6. B. Trubenová, **S. Novak**, and R. Hager (2015). Indirect genetic effects and the dynamics of social interactions, *PLoS ONE* 10(5), e0126907 (contributing author)

7. **S. Novak**, and R. Kollár. Type-dependent dispersal in spatial gene frequency clines (in preparation, first and corresponding author)[*]

8. M. Dravecká, **S. Novak**, and T. Paixão. Stress-induced mutagenesis: higher stress diversity leads to greater persistence of mutator genes (in preparation, joint first authorship with M. Dravecká)[*]

[*] Items marked by an asterisk are part of this thesis.

Personal Foreword

"I promise further that I will form my opinion on scholarly questions to the best of my knowledge and belief, and that I will not let my judgment be clouded by ambition, personal advantage, or other unscholarly motives."
(from: Ceremonial Vow, University of Vienna)

Evolution is a process of probing different forms and variants, putting them to the test of natural selection. It is a fluctuating process, subject to changing external conditions and obscured by the random dynamics of variants that are actually insignificant. Very similarly, my PhD studies were marked by diverse influences from different directions, various projects and interests, success and wasted efforts, yet eventually evolved into this thesis. I am confident, though, that my learning process was based on more than random mutations, and that the fluctuations that come along with an interdisciplinary environment increased the variability of my work and my versatility as a researcher.

Curiosity-driven research has accompanied me for the past five years, in its sometimes fulfilling, sometimes frustrating, yet always enthralling ways. I feel thoroughly lucky that I was not only given the opportunity and freedom to follow my interests, but also constantly encouraged to foster a broader set of skills and develop a diversified character. It is a great privilege that I've always had supportive and understanding mentors and supervisors, a family who trusted in me, and good friends to back me up. This is by no means a given, and I am deeply grateful.

Abstract

Natural environments are never constant but subject to spatial and temporal change on all scales, increasingly so due to human activity. Hence, it is crucial to understand the impact of environmental variation on evolutionary processes. In this thesis, I present three topics that share the common theme of environmental variation, yet illustrate its effect from different perspectives.

First, I show how a temporally fluctuating environment gives rise to second-order selection on a modifier for stress-induced mutagenesis. Without fluctuations, when populations are adapted to their environment, mutation rates are minimized. I argue that a stress-induced mutator mechanism may only be maintained if the population is repeatedly subjected to diverse environmental challenges, and I outline implications of the presented results to antibiotic treatment strategies.

Second, I discuss my work on the evolution of dispersal. Besides reproducing known results about the effect of heterogeneous habitats on dispersal, it identifies spatial changes in dispersal type frequencies as a source for selection for increased propensities to disperse. This concept contains effects of relatedness that are known to promote dispersal, and I explain how it identifies other forces selecting for dispersal and puts them on a common scale.

Third, I analyse genetic variances of phenotypic traits under multivariate stabilizing selection. For the case of constant environments, I generalize known formulae of equilibrium variances to multiple traits and discuss how the genetic variance of a focal trait is influenced by selection on background traits. I conclude by presenting ideas and preliminary work aiming at including environmental fluctuations in the form of moving trait optima into the model.

Table of Contents

List of Figures

1 Introduction

This thesis is a collection of selected projects I worked on during my PhD. Though diverse, they share an underlying theme, which I explain below. Most of Chapter 3 is adapted from my publication about dispersal evolution, see Novak (2014). All other projects presented here are joint work with colleagues from IST Austria and beyond: Marta Dravecká and Tiago Paixão (Chapter 2), Richard Kollár (Section 3.5), and Srdjan Sarikas and Stefanie Belohlavy (Chapter 4). Further, this entire work bears the hallmarks of Nick Barton, who provided guidance and contributed constructively and critically to each of the topics covered in this thesis.

1.1 Natural environments vary in space and time

Natural environments are never constant but subject to change on all scales. Such change may be spatial or temporal, ranging from highly diverse landscapes up to global gradients, or from the circadian cycle and yearly seasons up to recurrent glacial epochs. Human activities in the (evolutionarily) recent past have been an additional factor by increasing landscape fragmentation and transformation, and by their influence on climate change. Environmental changeability is so evident that, in fact, it is hard to imagine a natural species, or even a population, that exists under spatio-temporally constant conditions.

While the ubiquity of environmental variation is beyond question, its influence on evolutionary processes is less evident. Spatial variation may cause local adaptation and adaptive divergence, opposing the homogenizing effect of gene flow (Kawecki

and Ebert, 2004). Similarly, speciation may require a certain degree of geographic differentiation. Rapid temporal change causes populations to become maladapted, such that they may decline in numbers and face extinction unless they adapt to the new environment and restore a positive net growth rate in a process called evolutionary rescue (Bell and Gonzalez, 2009). Temporal variability also interacts with the evolution of recombination (Barton and Charlesworth, 1998) and mutation (Travis and Travis, 2002), since both these mechanisms enhance the genetic variation in a population and thus facilitate adaptation. Variation in the reproductive success of individuals due to spatial or temporal change can generally be described by genotype-times-environment ($G \times E$) interactions that provide an abstract framework for studying the effect of spatio-temporal variation on polygenic traits (Turelli and Barton, 2004).

These examples are by no means meant to be an exhaustive list, but rather an illustrative sample of the implications of spatio-temporal variation on evolutionary and ecological processes. Similarly, in the following chapters, I present three major topics that are loosely related members of the vast family of evolutionary questions, but are nevertheless connected by the theme of spatio-temporal variation. I chose them to shed light on the role of environmental variation in evolution from different angles: First, spatial and temporal environmental variation may be a constitutive factor for selection on certain traits. In other words, it generates selective forces that would be absent in a constant environment. As I explain below, this is the case in the evolution of genes that manipulate mutation rates (Chapter 2), and in the evolution of dispersal strategies (Chapter 3). When discussing the former, I consider a well-mixed population in an environment changing only in time, while in the latter, I focus on spatial variability. Second, spatio-temporal variation can be seen as modifying preexisting evolutionary phenomena. The example I discuss in Chapter 4 is concerned with the maintenance of genetic variation of quantitative traits under selection for an optimal phenotype. There, environmental variation causes the population to be maladapted and amplifies directional selection components, which in turn increases genetic variation. Environmental variation is thus instrumental in maintaining variation by interfering with selective forces that are already present in the system.

Throughout, I mostly neglect any ecological implications of changing environments

and focus on their effect on the fitnesses of (geno)types, i.e., their average reproductive success. Furthermore, environmental variation acts on the level of populations (in contrast to, e.g., variation in individual life histories), such that all individuals at a given time and location experience the same environment. I use the adjectives “heterogeneous” and “homogeneous” in context of spatially variable, and “fluctuating” and “stable” in context of temporally variable environments. When being deliberately unspecific, I write “changing” (or “variable”) and “constant”.

1.2 Environmental change as a constitutive factor

Environmental variation may give rise to evolutionary phenomena and selective pressures, which is particularly interesting for traits that are not directly under selection. For example, think of a bacterial culture under idealized laboratory conditions that are kept constant in space and time (e.g., a chemostat). If the bacteria are well-adapted to their environment, changes in their genome will typically have negative effects. Thus, considering the given physical and metabolic constraints, the culture’s rate of mutations should be as low as possible.

If the environment fluctuates in time, e.g. the mix of nutrients changes or certain antibiotics are administered, mutations that cause their carrier to better cope with the new condition will be selected for and thus spread in the population. Types that have higher mutation rates also have a higher probability of producing such favoured mutants, thus gaining an indirect selective advantage. In other words, increased mutation rates may hitch-hike to high frequency along with the beneficial mutations they produce (Taddei *et al.*, 1997); this is called the second-order selection hypothesis. The long-term potential for this effect is rooted in continuing environmental fluctuations that require the bacterial population to permanently adapt to new conditions. Overall, neglecting other factors, mutation rates should be determined as a balance between the detrimental effects of deleterious mutations and the adaptive advantage of increased mutation rates. In order to predict the mutation rates actually realized by evolution, however, these two opposing forces have to be quantified; a daunting task, in particular for the latter. As a matter of fact, it is still subject to debate if the indirect selective

advantage of increased mutation rates is a relevant factor to the evolution of mutation rates in practice (Sniegowski *et al.*, 2000).

Another example of a trait that strongly interacts with environmental variation – yet in a more intricate way – is dispersal (Ronce, 2007): Any natural species is distributed in space and individuals either migrate themselves or disperse their offspring/gametes. Oftentimes, dispersal entails increased mortality (e.g., predation risk), and it requires time and energy to disperse. However, dispersal reduces the relatedness between individuals that locally compete for resources (i.e., it reduces kin competition), which at least partially compensates these costs. In changing environments, additional factors become relevant. Spatial heterogeneities tend to reduce dispersal in two ways. First, if selection favours different features at different locations, dispersing individuals are less likely to be adapted to local requirements. Second, if the habitat consists of patches of richer and poorer quality, the former will contain more individuals. This leads to a net flux of individuals from rich to poor habitat and thus disfavours dispersal. Conversely, a temporally fluctuating environment generally leads to selection for increased dispersal. In this context, dispersal can be seen as a bet-hedging strategy against local habitat deterioration. In an extreme form, environmental fluctuations can cause local extinction events such that dispersers gain advantage from recolonizing empty habitat (Van Valen, 1971).

In both of the above examples, the challenge lies in quantifying the selection pressures created by environmental variability and to determine the evolutionarily optimal mutation or dispersal rates in the presence of the other factors. In the subsequent two chapters of my thesis, Chapters 2 and 3, I present some results that veer towards these very questions. The general approach is similar in both cases: I postulate a genetic modifier locus with two genetic variants (alleles) that alter the characteristic of interest. This characteristic is not under direct selection; selection on the modifier alleles comes from their interaction with selected alleles at other loci, or from their effect on individual life histories and behaviour. The alleles at the modifier locus are then compared to determine whether a new allele can invade, is maintained, and may even fix in the population. In the case that one allele replaces the other, new allelic variants can be introduced to study the change of the characteristic in evolutionary time in a

stepwise manner.

In Chapter 2, I discuss the second-order selection hypothesis (see above) for stress-induced mutagenesis in a panmictic (i.e. spatially not distributed) bacterial population. The difference between unconditional and stress-induced mutator genes is that the latter only increase mutation rates if their bearer experiences stress, e.g., in the form of antibiotics or other environmental challenges. Since they are inactive during non-stressful periods, they create a reduced burden of deleterious mutations. Like their unconditional counterparts, however, stress-induced mutator genes may increase in frequency along with the beneficial mutations they produce. I model this under the assumption that the modifier (mutator) locus is linked with a locus conferring resistance to the stress. Further, I assume that the mechanism of stress-induced mutagenesis is an active machinery whose genetic foundation itself degrades due to mutations, yet that does not confer a direct fitness cost. Then, the fraction of individuals showing stress-induced mutagenesis may be explained from a balance between its rate of decay and positive second-order selection. The model I present below shows how the strength of the latter crucially depends on the diversity of environmental challenges occurring over time, which may have practical implications for the evolvability of resistance to certain antibiotic treatments.

In Chapter 3, I present my work on the evolution of dispersal. I do not link the modifier for dispersal to any selected locus, and I assume that all individuals at a given location produce the same expected number of offspring. The latter implies that, locally, all individuals have the same fitness. The environmental factor of interest are spatial differences in habitat quality, expressed by spatially heterogeneous population sizes the habitat is able to sustain (i.e., a heterogeneous carrying capacity). The model I discuss elegantly captures how dispersal and heterogeneous carrying capacities interact. While this interaction has been studied before, there is more to my findings: heterogeneities in the frequencies of the dispersal modifiers themselves promote increased dispersal. This includes the phenomenon of relatedness between individuals selecting for dispersal, yet is formulated more generally, hinting at other factors stimulating dispersal that have not yet been considered.

1.3 Genetic variation and environmental change

Genetic variation, the amount by which individuals in a population differ in their genetic material, is a central concept in genetics, ecology, and evolutionary biology with widespread implications, from QTL analyses to the conservation of species. Crucially, the response of a population to selection, and hence its rate of adaptation, is proportional to its genetic variance (Barton *et al.* (2007), Ch.17). Conversely, if a population is maladapted, selection may pick out rare genetic variants that perform above average, therefore increasing the genetic variance. From an evolutionary point of view, the interplay between genetic variation and environmental change thus has two facets: genetic variation is necessary to cope with environmental change by adaptation, and environmental change causes individuals to be maladapted, hence should increase genetic variation.

Spatial structure has long been known to enhance genetic variation (Wright, 1943). For example, think of two patches of habitat, each favouring one out of two alleles at a certain locus. If migration between the patches is not too strong, each allele will be maintained in its patch, with a certain degree of admixture determined by the strengths of migration and selection. Even the simplest selection-mutation models thus have immense potential in maintaining genetic polymorphism. Also mathematically, their range of possible dynamics is extremely rich, as I showed earlier for the Levene (1953) model (Novak, 2011).

Similarly, if selection does not act on genetic loci directly, but on quantitative characters that are influenced by multiple loci, spatial heterogeneities typically increase variation in those traits. Again considering a habitat consisting of two patches, a body height H_1 might confer the highest fitness in the first patch 1, while in the second patch a different height H_2 might be optimal, with fitness declining as body height deviates from its optima. If the two patches are separated from each other, the balance between selection and mutation will lead to two distributions in body height centred around H_1 and H_2, respectively. With migration connecting the patches, the two trait distributions mix to some degree, which increases the variances of each (Lythgoe, 1997; Barton, 1999). Because of the demonstrated ability of spatial heterogeneities to maintain and promote genetic variation, I will – in the following and in Chapter 4 – restrict my atten-

tion to temporal fluctuations that are still much less explored.

In diploid organisms, genetic polymorphism can be maintained by overdominance in fitness (i.e., heterozygote individuals have higher fitness than either of the homozygotes). Note that even with additive effects, homozygotes in a beneficial mutation may overshoot the optimum and thus create heterozygote advantage (Sellis *et al*., 2011). It has been shown that, if selection acts on K phenotypic traits under stabilizing selection, at most K loci can be maintained polymorphic (Hastings and Hom, 1989). To exclude overdominance in fitness as an obvious mechanism maintaining genetic variation, I henceforth consider haploid organisms.

To secure polymorphism in haploids, some kind of negative frequency dependence of selection is required. In other words, rare alleles need to have a selective advantage to be protected from extinction. Interestingly, even if the selection coefficients are frequency-independent (i.e., the selection coefficient of an allele does not depend on the allele frequencies at its locus), fluctuating selection may give rise to negative frequency dependence. However, this requires additional structure in the system, like age structure in the population or some dormant stage (e.g. seed bank), c.f. the storage effect (Chesson and Warner, 1981). Considering a single locus under constant conditions, the allele with the largest selection coefficient simply fixes in the population. With arbitrarily many loci and alleles, there is a folkloric understanding that polymorphism cannot be maintained by constant selection. If selection is additive (i.e., the alleles contribute additively to fitness), this has been proven rigorously by Kirzhner and Lyubich (1997). In Appendix A3, I show that any form of constant frequency-independent selection on an arbitrary number of loci in linkage equilibrium (the strong recombination limit) eliminates all genetic variation. Thus in particular, my proof holds for arbitrary epistatic interactions between alleles and hence is applicable to selection on polygenic traits.

If selection is fluctuating, the situation is less simple, but it is widely assumed that fluctuations alone do not maintain polymorphism. In the simplest models, the geometric mean of fitness over time determines which of the alleles persists in the long run (Dempster, 1955; Haldane and Jayakar, 1963), but formulating a general model is hard. In a thought experiment, we may devise a pattern of fluctuating selection that keeps two alleles, P and Q, segregating at a single locus forever: Assume that

selection favours allele P for some time, then switches over to favouring allele Q for a longer time, then back to allele P for even longer, and so on. In this example, the allele frequencies oscillate between the two states where either of the two alleles is fixed, lingering there longer and longer, yet always flipping back to the other state. Clearly, this hypothetical experiment is not biologically relevant, since allele frequencies become arbitrarily low and will eventually fix in any finite population. However, it shows part of the complications of arriving at a clean mathematical statement that also fluctuating frequency-independent selection does not maintain genetic polymorphism. Anyway, in finite populations without mutations, all loci must become monomorphic eventually because of genetic drift (i.e., the change in gene frequency due to the random sampling of reproducing individuals). Thus, investigating sophisticated models of fluctuating selection alone might not be practically relevant.

Instead, it is more interesting to consider genetic variation under a balance of mutation and genetic drift, and try to quantify the impact of selection, be it conducive or destructive to genetic variation. In Chapter 4, I do this in the framework of quantitative genetics that is concerned with the variation in phenotypic characters (traits) in a population. The variance of the distribution of trait values in the population is denoted by the genetic variance (of the given trait). Quantitative characters are assumed to be determined by a (large) set of genetic loci under the influence of mutation, genetic drift, and selection. The latter is mediated by stabilizing selection on the traits, i.e., each trait has an optimal value that confers maximal fitness, and fitness declines with deviations from the optimal value. Alleles that modify the trait in the direction of the optimum are therefore positively selected, while alleles that have the opposite effect are selected against. If the population's trait mean is far from the optimum, stabilizing selection pulls the trait distribution towards the optimum by picking out genetic variants in its tip; this increases the variance in the trait distribution temporarily. Once the population's trait mean is close to the optimum, stabilizing selection acts to diminish the variance of the trait distribution, reducing the population to a single genotype that matches the optimum best. However, fluctuations in the optimal trait value may prevent the population from adapting too closely to the optimum, therefore attenuate the tendency of stabilizing selection to reduce genetic variation, and lead to higher levels

of genetic variance in the balance of selection and mutation. This principle has been demonstrated mainly in simulation studies, e.g., by Bürger and Gimelfarb (2002).

My aim is to quantify the impact of fluctuations on genetic variance analytically. I set up this project very broadly by considering more than one trait; naturally, organisms consist of multiple traits, and correlations between those matter in quantitative trait evolution. The general setup is justified in Section 4.1, see also Johnson and Barton (2005). Multivariate quantitative trait models are quite elaborate, yet I propose an approach that takes advantage of the great complexity of the problem by subsuming most of the microscopic details of the system into a stochastic process, see Section 4.2. Hence, also if the environment is constant, we may make use of a probabilistic description of fluctuating selection. In Section 4.3, I lay out the basics of genetic variances with multiple traits, which may serve as a basis for adding external fluctuations to the system. Given the stochastic description of selection mentioned above, this should be a relatively straightforward extension; in Section 4.4, I present and discuss some ideas of how to go deeper in that direction, yet leave the questions open for future research.

2 Stress-Induced Mutagenesis

2.1 Introduction

Because most mutations are deleterious, selection generally acts to lower mutation rate. There are certain forces, however, that can keep mutation rates elevated (Kimura, 1967). The most evident are physical constraints on how precise polymerases can be, or a balance between avoiding deleterious mutations and cutting down on energy costs of efficient repair. In asexual populations with complete linkage, elevated mutation rates can also exist for relatively long periods of time due to hitch-hiking with beneficial mutations they produce, consistent with the observation of strains with highly elevated mutation rates in experimental as well as clinical settings (Woods *et al.*, 2011). Theoretical studies suggest that conditions most suitable for elevated mutation rates to persist are those when beneficial mutations can have a large effect - in times of strong selection pressure. A common regime when selection pressure can be sustained despite adaptation is a setting of fluctuating selection, which includes cells experiencing bursts of stresses during antibiotic treatment or cancer chemotherapy.

There exist multiple mechanisms that result in elevated mutation rates specifically during stress (stress-induced mutagenesis, SIM). When encountering DNA damage, several species of bacteria activate an SOS response that – in addition to upregulating various repair mechanisms – activates error-prone DNA polymerases, which have been linked to a faster evolution of antibiotic resistance (Cirz *et al.*, 2005). In a study from 2003, 40% of studied isolates of *Escherichia coli* strains showed a higher than 10-fold increase in mutation rate under stress conditions, associated with ageing colonies

(Bjedov *et al.*, 2003). It has also been shown that *Streptococcus pneumoniae* activates the expression of so-called *com* genes when treated with various antibiotics. These genes allow the bacteria to readily take up DNA from the environment and incorporate it into its genome (Prudhomme *et al.*, 2006). Another example is the beneficial excision of a genomic region in the plant pathogen *Pseudomonas syringae* in response to the host's immunity (Pitman *et al.*, 2005). Similar mechanisms that link certain stresses to an increase of mutation rates have also been found in *Drosophila melanogaster* (Agrawal and Wang, 2008) and yeast (Heidenreich, 2007).

Several hypotheses may explain the prevalence of stress-induced mutagenesis mechanisms. The first is a pleiotropic argument, where these mechanisms primarily carry benefits of faster repair or nutritional gain (for error-prone polymerases in SOS response, and uptake of foreign DNA with the *com* system respectively); then, the elevation of mutation rates is a side effect (e.g. Torres-Barceló *et al.*, 2015). MacLean *et al.* (2013) suggest an alternative hypothesis to explain the stress-linked induction of error-prone DNA polymerases: DNA polymerases that are linked to specific stress situations and that are used less often may be subject to weaker selection, and become error-prone by accumulation of slightly deleterious mutations. Another intriguing hypothesis, the second-order selection hypothesis, states that stress-induced mutagenesis has evolved thanks to its benefit of combining elevated mutation rates with those situations when they give most benefit (Rosenberg, 2001; Ram and Hadany, 2012). Exactly like in the case of second-order selection explanations of constitutive mutator strain prevalence, an allele that causes elevated mutation rates hitch-hikes with the beneficial mutations it produces. By elevating mutation rates in times of stress, when beneficial mutations are more likely to have large effects, a SIM mechanism is more likely to rise in frequency. By keeping mutation rates down at times of no stress, it decreases the mutational load from excessive deleterious mutations. There is no reason to think that only one of these hypotheses is correct; it is plausible that an interplay of these factors is responsible for the prevalence of SIM mechanisms in many organisms.

The aim of our investigation is to explore the basic principle behind the second-order selection hypothesis of stress-induced mutagenesis: How can a mechanism that increases mutation rates under stress evolve? Under which conditions and at what lev-

els can it be sustained in a population? What stress patterns and regimes promote it the most? The relevance of these questions is beyond doubt: stress-induced mutagenesis facilitates the adaptation of a population subjected to changing conditions. This is relevant for cancer therapy or antibiotic treatment, for example. Much effort goes into identifying strategies that keep the treatment effective for as long as possible, i.e., that impede the evolution of resistant strains (Bonhoeffer *et al.*, 1997; Chait *et al.*, 2007; Bollenbach, 2015). If second-order selection is a key factor in the emergence and maintenance of SIM genes, however, different treatment regimes also affect the evolution of mutagenesis, and thus the evolvability towards resistant strains in the long term. It is therefore essential to understand to what extent different patterns of changing conditions cause second-order selection on stress-induced mutagenesis.

2.2 A population genetics model for SIM alleles

We thus set up a model of a hypothetical stress-induced mutator (SIM) allele; its properties are based on the features of existing SIM mechanisms, yet the model is not meant to truthfully represent any one particular system. We are interested in exploring specifically the effectiveness of second-order selection in the evolution of a SIM allele. To do so effectively, we need to isolate second-order selection from any direct benefit of the SIM system. Direct effects are likely a major determinant of the persistence of SIM mechanisms in the wild, but such dynamics have also been extensively studied with existing evolutionary models (e.g. Hegreness *et al.*, 2006). We therefore assume that the SIM allele does not confer any direct fitness cost or benefit, and consider a population of haploid individuals with two non-recombining loci. At the first, the SIM allele can be present or absent (alleles M or m, respectively), and the second may or may not grant resistance to a given stress (alleles R or r). The resulting four possible genotypes are displayed in Figure 2.1.

In the absence of stress, we assume that transitions between the genotypes are only due to mutations as indicated by the arrows in Figure 2.1a; thus in particular, there is no cost to being resistant. Individuals may lose or gain resistance at rates μ_R and ν_R, respectively. The SIM allele M may lose its function at rate μ_M; since we are

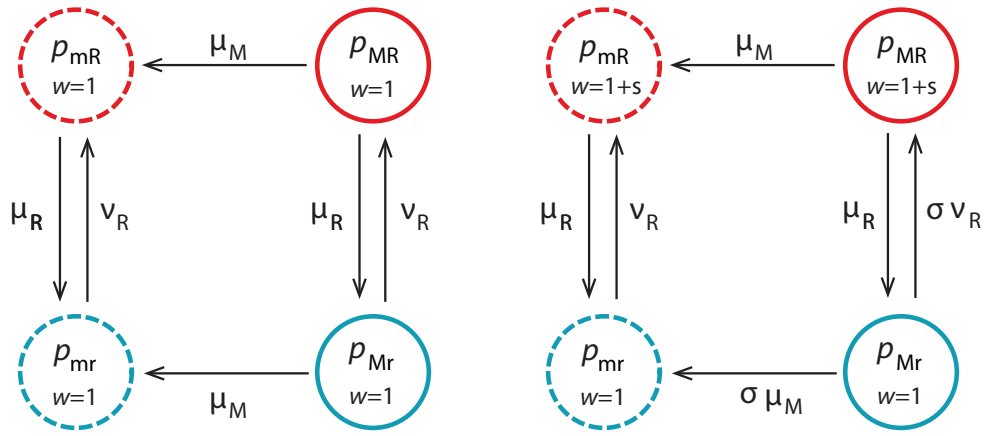

(a) No-stress environment (b) Stress environment

Figure 2.1: Schematic description of the genotype dynamics under no stress and stress. (a) Under no stress, all genotypes have the same fitness $w = 1$ and transitions between the states are solely due to mutations. Resistance is lost and gained at rates μ_R and ν_R, respectively. Furthermore, the SIM allele degrades at a rate μ_M. (b) In the stress environment, individuals that are resistant to the stress gain a selective advantage s (fitness $w = 1 + s$). In addition, the genotype that is susceptible to the stress and carries the SIM allele (p_{Mr}) increases its outgoing mutation rates by a factor $\sigma > 1$.

interested in conditions for the ultimate loss of the SIM allele, we neglect back-mutation from m to M.

In the stress environment, genotypes containing the resistance allele R have increased fitness $w = 1 + s$ relative to susceptible genotypes. Furthermore, the Mr genotype increases all outgoing mutation rates by a factor $\sigma > 1$ due to stress-induced mutagenesis, see Figure 2.1b. There are two assumptions behind this modelling approach: First, stress does not activate the SIM allele in resistant individuals. This is reasonable if, for example, the stressor is effective inside the cell but the resistant mutation makes its membrane impermeable. Were the SIM allele also active in resistant individuals, it would rapidly degrade itself and be lost from the population in our model.

Second, the only cost of an active SIM allele is that the mechanism degrades itself. This may at best partially compensate for the detrimental effects of elevated mutation rates not considered in this model. In any natural system, the load due to deleterious mutations may be substantial and restrain the evolution of SIM alleles. This effect could be included in our model by adding additional classes of individuals with reduced

fitness. However, artificially creating an idealised situation for the SIM allele allows for a clean and mathematically tractable model of positive second-order selection, which is or focal concern. We may thus interpret our results as an upper bound on how effective positive second-order selection can be.

We cast the schematic dynamics of Figure 2.1 into two sets of differential equations for the variables $p = \{p_{mr}, p_{Mr}, p_{mR}, p_{MR}\}$. Using the classical mutation-selection dynamics of population genetics, they take the form

$$\dot{p} = p\,(w - \bar{w}) + \mathcal{M}.p, \tag{2.1}$$

where w is the vector containing the marginal fitnesses of the genotypes, $\bar{w}$ is the mean fitness of the population, and $\mathcal{M}$ is a matrix encoding the mutation scheme (c.f. Appendix A1.1). It seems reasonable to assume the following hierarchy among the parameters:

$$s \gg \mu_M, \mu_R \gg \nu_R. \tag{2.2}$$

Hence first, we assume that selection is strong compared to mutation. From a conceptual point of view, this implies that selection is the main driving force under stress; if mutations that deactivate an existing resistance mechanism were too frequent, they would "swamp" the population and resistance could not evolve. Since antibiotics typically exert high selection pressures, our assumption is justified in many cases. Second, we assume that resistance mechanisms are lost more readily than they are gained by mutation. This is intuitive, since by random genetic modifications it is more likely to disable a functional mechanism than to create one. Assuming a functional resistant mechanism to consist of 10^5 base pairs and a per-base mutation rate of 10^{-8} leads to a rough estimate of $\mu_R \approx 10^-3$ (and similarly for μ_M). To obtain resistance, however, a few very specific point mutations may be required, such that ν_R may not be much larger than 10^{-8}. The relative magnitudes of μ_R and μ_M do not impact our results qualitatively, although clearly a higher decay rate μ_M of the SIM allele hinders its prevalence.

Given the hierarchy (2.2), it can be shown that the SIM allele is maintained in none of the two environments separately. Switching the stress and no-stress environments, however, gives rise to non-trivial dynamics. During a stress phase, the SIM allele may increase in frequency along with the resistance mutations it produces. Note that even if the SIM allele is rare, it may contribute much of the resistance acquired during

stress. As resistance levels in the population rise, its effect weakens and the SIM allele frequency falls off because of mutations degrading the SIM mechanism. Periods of no stress allow resistance levels to decline, such that the SIM allele becomes effective again at the next stress phase.

2.3 Maintenance of the SIM allele

2.3.1 Recurrent and non-recurrent stress

We describe a hypothetical evolutionary experiment, in which we repeatedly subject an effectively infinitely large bacterial population to stress. We apply stress for τ_S time units, followed by τ_{NS} time units of no stress. Under no stress and stress, the genotype frequencies evolve as described by the dynamical system (2.1) and according to the schematics in Figures 2.1. Iterating this procedure leads to oscillations in the SIM allele frequency $p_M = p_{Mr} + p_{MR}$ as depicted in Figure 2.2. We measure genotype frequencies at discrete time points directly before the onset of each stress (bold points in Figure 2.2). The long-term equilibria of this time series thus describe the long-term prevalence of the SIM allele, which we denote by $\hat{p}_M$. Note that sampling at the end of the no-stress phases gives only approximately the minimal SIM allele frequencies of the corresponding cycle, since they may continue dropping at the onset of stress before they can hitch-hike to higher frequencies along with the resistance mutations they produce. As our model assumes an effectively infinite population, however, the SIM allele cannot be lost within one cycle. Nevertheless, it is possible that $\hat{p}_M = 0$, i.e., that the SIM allele frequency declines to zero as the cycles are iterated.

To be able to study the impact of stress diversity on the evolution of SIM alleles, we first cover the two extreme cases of always the same stress re-occurring, and of an infinite variety of stresses such that the population never experiences the same kind of stress twice. We denote the first case by the recurrent (R) stress regime; it corresponds to repeatedly triggering the same stress, for example, applying a certain antibiotic. The second case can be seen as drawing each stress from an infinite pool of possibilities, where each of them requires a different resistance mutation. We call this case the non-recurrent (NR) stress regime. In Section 2.3.2, we numerically

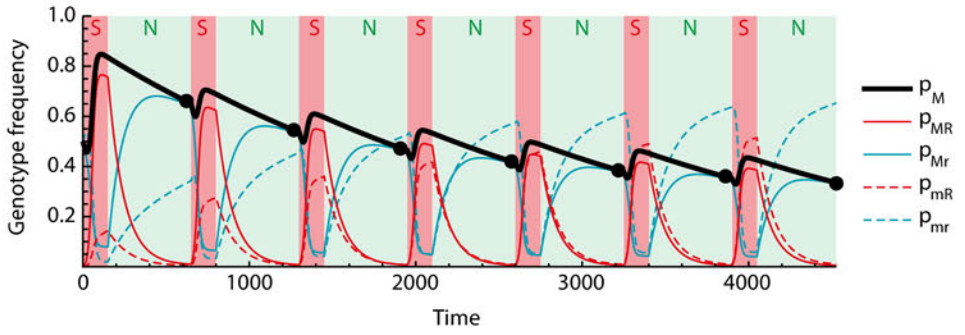

Figure 2.2: Illustration of the temporal dynamics of genotype frequencies. Periods of stress (S, red shading) and no stress (N, green shading) are alternated and the dynamics of genotype frequencies is simulated according to the schematic Figure 2.1 and equation (2.1). During stress, resistant genotypes increase in frequency (red lines), and the SIM allele frequency p_M hitch-hikes to some extent (black line). If there is no stress, both resistance and SIM allele frequency levels decay. Over time, the SIM allele frequency thus fluctuates, possibly converging to stable oscillations. We sample the SIM allele frequency p_M at the end of each no-stress phase (black points), thus obtaining a discrete system in which the time between two successive measurements is given by the iteration of one cycle of stress and no stress. (Parameters: $\sigma = 10$, $s = 0.1$, $\mu_P = 5 \times 10^{-4}$, $\mu_R = 10^{-2}$, $\nu_R = 10^{-4}$).

interpolate between the (R) and (NR) regimes by simulating finite numbers of different stresses.

Assuming that stresses are intense but of short duration, and that the effect of the SIM allele is large (i.e., s and σ are large, τ_S is small), we argue in Appendix A1.2 that the long-term prevalences of the SIM allele in the (R) and (NR) regimes are well approximated by

$$\hat{p}_M^{(R)} = \max\left\{0\,,\, e^{-\mu_M \tau} - \aleph\left(1 - e^{-\mu_M \tau}\right)\left(1 + \frac{\mu_R + \nu_R}{\nu_R}\left(e^{(\mu_R+\nu_R)\tau} - 1\right)^{-1}\right)\right\}, \quad \text{(2.3a)}$$

$$\hat{p}_M^{(NR)} = \max\left\{0\,,\, e^{-\mu_M \tau} - \aleph\left(1 - e^{-\mu_M \tau}\right)\right\}, \quad \text{(2.3b)}$$

where $\tau = \tau_S + \tau_{NS}$ is the length of one cycle of stress and no-stress, and

$$\aleph = \frac{s/\sigma + \mu_M + \nu_R}{\mu_R}. \quad \text{(2.4)}$$

In particular, we thus see that the parameters s and σ enter the long-term SIM allele prevalences only via their ratio s/σ.

To test our analytical predictions, we explicitly simulate the dynamics (2.1), alternating stress and no-stress phases according to the schematics in Figure 2.1. Note that

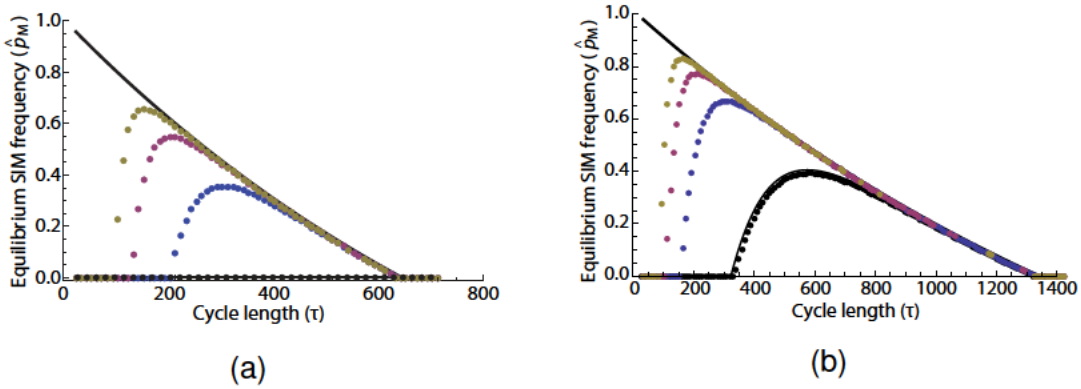

Figure 2.3: Long-term prevalence of the SIM allele. Two representative parameter sets (σ, s, μ_M, μ_R, and ν_R) were simulated for different values of $\tau = \tau_S + \tau_N S$. The solid black lines represent the analytical predictions from equation (2.3) for the (R) and (NR) regimes. For our numerical simulations, we chose $\tau_S = 10$ and varied $\tau_N S$ accordingly. The simulation results of the (R) and (NR) regimes (black points) fit their corresponding predictions well. The blue, red, and yellow points represent simulation results for two, three, and four different stresses occurring cyclically (see Section 2.3.2). Clearly, increasing the number of stresses gradually increases the SIM prevalences up to a maximum given by the prediction for the (NR) regime. (a) In the (R) regime, the SIM allele is not maintained for any choice of τ. (Parameters: $\sigma = 100$, $s = 1$, $\mu_M = 0.001$, $\mu_R = 0.01$, $\nu_R = 0.0001$.) (b) In the (R) regime, the SIM allele is maintained for an interval of values of τ. This is possible because μ_M is sufficiently small such that $\mu_M \approx \nu_R$, which is in conflict with our assumptions in equation (2.2). (Parameters: $\sigma = 100$, $s = 1$, $\mu_M = 0.0005$, $\mu_R = 0.01$, $\nu_R = 0.0001$.)

we simulate the full model, without requiring the simplifications (see Appendix A1.2) that lead to the above formulae. Throughout, we used multiple initial conditions to ascertain that our simulation results are independent of the initial genotype frequencies.

To simulate the recurrent (R) regime, it suffices to alternate the stress and no-stress dynamics on the vector of genotype frequencies, $p = \{p_{mr}, p_{Mr}, p_{mR}, p_{MR}\}$. For the non-recurrent (NR) regime, we may use the same procedure, but replace $\{p_{mr}, p_{Mr}, p_{mR}, p_{MR}\}$ by

$$\{(1-\varepsilon)(p_{mr}+p_{mR}), (1-\varepsilon)(p_{Mr}+p_{MR}), \varepsilon(p_{mr}+p_{mR}), \varepsilon(p_{Mr}+p_{MR})\}$$

before every new stress, because if the particular kind of stress has never occurred before, the probability of being resistant to it is given by the balance between the rates of gaining and losing resistance by chance (mutation equilibrium), $\varepsilon = \nu_R/(\mu_R + \nu_R)$.

Figure 2.3 shows the long-term SIM prevalences as functions of the cycle length τ

for two representative choices of the remaining parameters. For both the (R) and (NR) regimes, the simulated values (points) align well with the above formulae (solid lines). In the non-recurrent regime, the SIM allele is maintained in the population as long as stresses occur frequently enough; more precisely, there is a critical cycle length τ_c such that the SIM allele is not maintained for cycle lengths exceeding τ_c,

$$\hat{p}_M^{(NR)} = 0 \qquad \text{if} \qquad \tau > \tau_c = \frac{1}{\mu_M} \log\left(1 + \frac{1}{\aleph}\right). \tag{2.5}$$

Furthermore, in this regime there is a strictly monotone dependence between the SIM allele frequency and the frequency of stress occurrence; in particular, the SIM allele becomes fixed in the population in the limit of infinitely rapid stress occurrence (i.e., $\hat{p}_M^{(NR)} \to 1$ for $\tau \to 0$).

The dependence of the long-term SIM prevalence $\hat{p}_M^{(R)}$ in the recurrent regime on the cycle length τ is less simple. If the rate of gaining resistance without the SIM allele is sufficiently low (i.e., $\nu_R \ll 1$, in particular $\nu_R \ll \mu_R$), we can show that the SIM allele is not maintained in the population for any choice of τ (see Appendix A1.3). This is the case in Figure 2.3a. In other cases, e.g., in Figure 2.3b, the SIM allele may be maintained in the recurrent regime for intermediate values of τ. Such cases, however, are not in concordance with our basic ranking of parameters, inequality (2.2): To obtain Figure 2.3b, we chose a very small decay rate of the SIM allele such that $\mu_M \approx \nu_R$. Hence, there is no contradiction to the previous statement. Furthermore, we mathematically show in Appendix A1.3 that the non-recurrent regime generally maintains a higher SIM prevalence than the recurrent regime, i.e., $\hat{p}_M^{(NR)} \geq \hat{p}_M^{(R)}$ for any choice of parameters.

2.3.2 Finite stress cycles

In the next step, we explore the prevalence of the SIM allele when subjected to a finite number of stresses. To this end, we simulate the full system as explained earlier for the (R) and (NR) regimes, but for a finite number χ of stresses. This is done by taking into account a separate resistance locus for every stress. As in the (NR) regime, we assume no cross-resistance and there is complete linkage between all loci. Hence, there are $2^{\chi+1}$ different genotypes to consider. The SIM allele is lost at rate μ_M, and

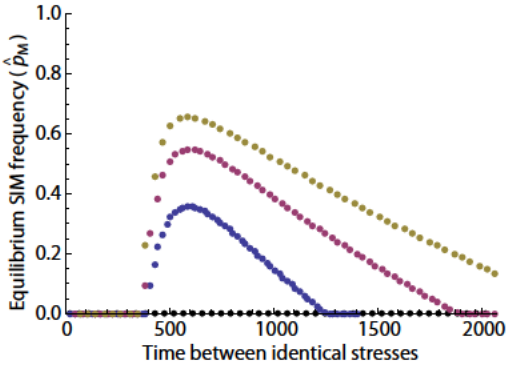

Figure 2.4: The long-term SIM allele prevalences as functions of the time between the occurrence of two identical types of stress. The data and colours are identical to those displayed in Figure 2.3a. For two (three, four) stresses, the time between two stresses of the same type is 2τ (3τ, 4τ). Rescaling the values on the horizontal axis accordingly indicates that the time between identical stresses is pivotal for determining the minimal stress occurrence time above which the SIM allele may be maintained (given a sufficient number of stresses χ, here $\chi \geq 2$).

resistance to a stress is gained at rate ν_R and lost at rate μ_R, independently between stresses. We ignore cross-resistance between stresses, i.e., mutations that confer resistance to multiple stresses. Iterating stress and no stress as above, the next stress to occur is chosen in a deterministically cycling manner. Each stress period is of a constant length τ_S, and each stress period is followed by a no-stress period of length τ_{NS}.

The results interpolate between the (R) and (NR) regimes, where every increase in the number of stresses, χ, also increases the SIM allele equilibrium frequency and the parameter regime where it is maintained, see Figure 2.3. In particular, the simulations suggest a simple way to generalize our analytical results. When varying the length of one iteration of stress and no stress ($\tau = \tau_S + \tau_{NS}$), we find three dynamical regimes.

First, for small values of τ, we observe the loss of the SIM allele. The upper bound of this region is inversely proportional to the time it takes for the same stress to recur. Keeping the cycle length τ constant and increasing the number of stresses χ also increases this time and therefore permits the maintenance of the SIM allele for smaller values of τ. The scaling with the time between two stresses of the same type can be seen clearly in Figure 2.4; we may deduce that a too frequent occurrence of the same stress is not beneficial for the SIM allele. This is not surprising; the SIM allele has no

fitness advantage on its own and therefore can only rise in frequency if the relevant resistance levels in the population are low. When stresses re-occur frequently, the resistance levels are kept high, preventing the SIM allele from hitch-hiking.

Second, if there is a sufficient number of stresses available, a SIM allele can be kept for intermediate frequencies of stress occurrence. The size of this region expands with increasing stress diversity up to the level of the (NR) regime of infinite stress diversity. The maximum allele frequency that can be kept also increases with increasing stress diversity, geometrically approaching the analytically determined value of the (NR) case. Third, if stresses occur too infrequently, the SIM allele is lost. The critical time between two consecutive stresses, above which the SIM allele is lost for any number of stresses χ, was calculated analytically as τ_c, see equation (2.5).

We may randomize our model by choosing one out of the χ stresses at each iteration of the simulation. Qualitatively, this leaves the picture unchanged, see Figure 2.5a: The SIM prevalence levels $\hat{p}_M$ and the interval of stress occurrence times τ that maintain the SIM allele both increase with increasing stress diversity, though not as readily as in the deterministic case. Generally speaking, given a fixed number χ of stresses, a strict cycle of stress occurrence is capable of maintaining the SIM allele at a higher level than randomly choosing the next stress to occur. We obtain qualitatively very similar results if we keep the ordering of stresses intact, yet choose the stress occurrence times τ randomly at each iteration (not shown).

For practical questions in antibiotic therapy, for instance, it is of interest to investigate treatment scenarios in which a set of pharmaceuticals is applied simultaneously or administered separately over a given period of time (combined versus sequential treatment, Bonhoeffer *et al.*, 1997; D'Agata *et al.*, 2008; Perron *et al.*, 2012). To this end, we simulate and compare four stresses either occurring simultaneously, being grouped in two pairs, or being applied separately. We assume that the stresses do not allow for cross-resistance mutations (i.e., single mutations that provide resistance to multiple stresses), that their effects on fitness are additive, and that one cycle through all stresses or stress combinations takes τ time units in each case. The results of our simulations are depicted in Figure 2.5b; while applying all stresses at once does not maintain the SIM allele for our choice of parameters (blue), the SIM allele prevalence

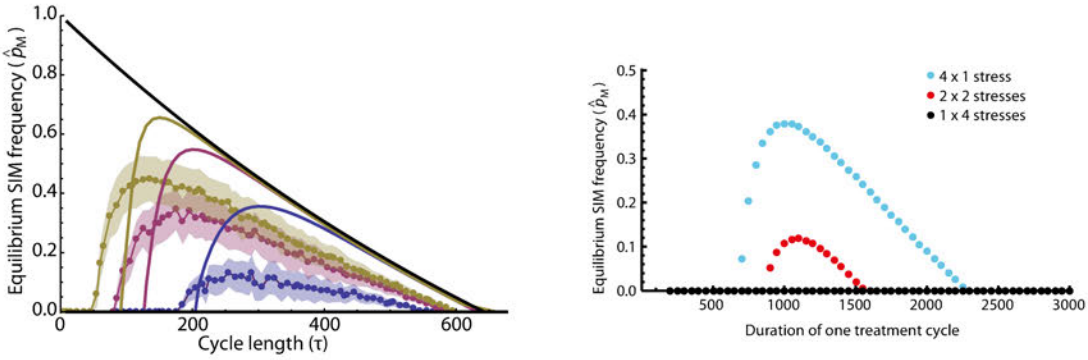

(a) Randomizing stresses (b) Hypothetical treatment regimes

Figure 2.5: Generalized simulations of long-term SIM prevalence. (a) The solid lines represent the same data as Figure 2.3a. In addition, we randomized the simulation by choosing the next stress randomly from the set of available stresses (instead of a deterministic periodic stress cycle). $10,000$ iterations of randomly chosen stress and no stress were performed, and the SIM prevalences over the last $1,000$ were calculated (blue, red, and yellow points for two, three, and four different stresses). There is some variation around these values (the shaded areas indicate the standard deviations in the samples), yet there is a clear increase in SIM prevalence levels for increasing numbers of different stresses. However, the mean SIM prevalences are significantly lower than the corresponding long-term SIM prevalences from the deterministic simulations. (b) To mimic various treatment regimes, we simulated the simultaneous versus sequential occurrence of four different stresses. We assumed that resistance to each stress confers a selective advantage s. If multiple stresses occur simultaneously, their effects add up such that, for instance, being resistant against two simultaneously occurring stresses provides an advantage of $2s$. If all four stresses occur simultaneously (combined treatment) every τ time units, the SIM allele is not maintained for our chosen set of parameters (black points). In contrast, if the four stresses are applied in sequence (sequential treatment) with $\tau/4$ time units between consecutive stresses (such that one cycle through all stresses takes τ time units), the SIM allele is maintained at considerable frequency for a wide range of values of τ (blue points). Grouping the four stresses in two pairs and alternating those at half the previous rate ($\tau/2$; each pair of stresses re-occurs every τ time units) leads to intermediate SIM allele maintenance levels (red points). (Parameters: $\sigma = 100$, $s = 0.5$, $\mu_M = 0.001$, $\mu_R = 0.005$, $\nu_R = 0.0001$.)

increases if stresses occur more frequently, yet in a less clustered fashion (orange and green).

Note that, to simulate the three scenarios presented here, we varied not only the number of different stress combinations varies, but also the selection intensities due to each stress combination and hence the fitnesses of the genotypes. Thus, a simple comparison between the different cases – as we carried out for the simpler case of an increasing stress diversity (Figures 2.3 and 2.4) – becomes infeasible. Generally, the dynamics behind these simulations are intricate; each of the $\chi = 4$ stresses requires its own resistance allele, hence there are $2^{\chi+1} = 32$ genotypes (equations) to consider. Therefore, we do not aim at analysing the dynamics in detail and more complicated dynamic behaviour (e.g. limit cycles) cannot be excluded, yet the emerging qualitative insight is interesting and may initiate more targeted investigations.

2.4 Discussion

Our study investigates the fate of a hypothetical stress-induced mutagenesis (SIM) mechanism under various schemes of environmental fluctuations. We assume that stress-induced mutagenesis is brought about by an active mechanism that increases mutation rates as a response to stress, modeled by a modifier allele for stress-induced mutagenesis that is much easier lost than gained. As a consequence, it decays over time unless maintained by recurrent second-order selection due to changes in the environment. A similar model was analysed by Masel *et al.* (2007). Conversely, unconditional hyper-mutating strains are most often produced as a result of a loss of function in methyl-directed mismatch repair, hence the hypermutator phenotype is much easier gained than lost. One thus has to be cautious when extrapolating our model to such strains, yet our results about the qualitative effect of environmental fluctuations on positive second-order selection can be expected to apply to unconditional mutator phenotypes also.

Under our assumptions, environmental fluctuations are essential for the SIM allele to be maintained in the population: in the absence of environmental challenges (stresses), the SIM allele is lost. Repeatedly occurring stresses, however, give rise

to second-order selection on the SIM allele. Under reasonable assumptions on the model parameters, c.f. equation (2.2), we show that simple fluctuations caused by a repetitive stress generally fail to maintain the SIM allele. As the stress diversity – i.e., the number of different stresses available – increases, the SIM allele may be maintained at increasingly high levels, see Figure 2.3. In the limit of infinite stress diversity, the SIM allele is maintained for any frequency of stress occurrence above a given threshold, which we characterized analytically by τ_c. It is hard to assess how many different stresses may invoke the same mutator allele in practice, but it is plausible that multiple stresses activate the same stress response, yet require different resistance mechanisms. Furthermore, we assume that there are no mutations conferring resistance to more than one stress at a time; realistic cases will be more intricate due to cross-resistance mutations.

Interestingly, choosing the stresses from the pool of available stresses at random, or randomizing the stress occurrence times, generally decreases the levels at which a SIM allele can be maintained compared to a deterministic cycling pattern (see Figure 2.5a). This helps identifying the aspects of environmental fluctuations that promote second-order selection on SIM alleles: The relevant quantity leading to higher SIM allele prevalences is stress diversity. Random fluctuations in either the type of stress occurring or in the timing of stresses typically lowers the mean levels at which the SIM allele is maintained.

Our results focus on how the maintenance of a SIM allele depends on the frequency of stresses. We find that in the case of cycling a finite number of stresses, the SIM allele is only maintained at intermediate stress frequencies. Irrespective of the number of available stresses, a lower bound for the stress frequency can be determined analytically as $1/\tau_c$. For the upper bound, we find that the time between two stresses of the same kind is crucial (Figure 2.4). This could inform the choice of treatment strategies by identifying the schemes that could exert extensive selection pressure to keep a SIM allele and possibly strengthen its effect. Somewhat intuitively, restricting the use of antibiotics for long periods of time allows both resistance and SIM alleles to be lost, adding another reason to limit antibiotic use to situations where it is necessary.

To date, various temporal treatment strategies have been investigated to counter

the current antibiotic resistance crisis (Kim *et al.*, 2014; Nichol *et al.*, 2015; Roemhild *et al.*, 2015). However, it is not only necessary to impede the evolution of resistant strains, but also to assess the effect of these treatment schemes on evolvability, for example in the form of SIM mechanisms. Hence, our results may contribute to the growing debate on developing new strategies to fight drug resistance.

To prevent the emergence of resistant strains, one approach is to inhibit known resistance mechanisms directly (Reading and Cole, 1977). Another is to use combinations of existing drugs in treatment regimes that are rationally designed to suppress resistance levels (Bergstrom *et al.*, 2004; Baym *et al.*, 2016). However, to keep drugs effective in the long term, it is desirable to develop strategies that not only decrease resistance levels, but also restrict evolvability. To this end, there have been efforts to directly inhibit SIM mechanisms, e.g. Cirz *et al.* (2005); Alam *et al.* (2016). Our study complements this approach by assessing temporal treatment schemes on how well they prevent second-order selection on a SIM mechanism. We find that an increasing diversity of stresses encountered increases long-term SIM frequencies, see Figures 2.3 and 2.5b. This suggests a trade-off between controlling resistance and controlling evolvability: In most proposed schemes, it is the stress diversity and the resulting need for new resistance mutations that help keep resistance levels low, at least in the short term (Kim *et al.*, 2014; Nichol *et al.*, 2015; Roemhild *et al.*, 2015). Our model predicts that the sequential occurrence of stresses strengthens second-order selection on a SIM allele compared to simultaneous stress occurrence. Experimental work is needed to further characterize this trade-off and assess its relevance in a clinical setting. Since the dynamics of SIM alleles are presumably much slower than that of resistance acquisition, such experiments could be challenging, yet not impossible. Our results may inform such experiments to confirm the suggested trade-off between the evolution and evolvability of resistance.

It has been proposed that the simultaneous application of drugs that exhibit no cross-resistance may be more effective against resistant strains than their sequential application (Bonhoeffer *et al.*, 1997; D'Agata *et al.*, 2008; Perron *et al.*, 2012). In our model, the same applies to reducing positive second-order selection on SIM alleles. This is an intriguing prospect, which should be explored further and may provide a

resolution of the trade-off between fighting resistance and evolvability, at least for those drug combinations that allow for simultaneous application despite common toxicity or dosage problems.

3 Evolution of Dispersal

3.1 Introduction

The dispersal of individuals is a ubiquitous trait of any species. It embeds natural populations into their environment by setting a scale for geographic distance, and it dictates to what extent habitat heterogeneities are experienced as such or are averaged out. Furthermore, it determines the degree of admixture of a spatially structured population by providing an estimate of how many individuals interact locally. Understanding the evolution of dispersal is therefore crucial for understanding the dynamics of spatially structured populations, speciation, and the evolution of many other life-history traits. Furthermore, it helps us predict the impact of environmental change or invasions of alien species.

The propensity to disperse is variable and heritable, and hence subject to natural selection. The evolution of dispersal has attracted much interest in the past few decades, see the reviews by Bowler and Benton (2005); Dieckmann *et al.* (1999); Johnson and Gaines (1990); Ronce (2007). Positive dispersal must entail significant benefits, since substantial costs are associated with dispersal (Bonte *et al.*, 2012). These costs come from the time and energy needed for dispersal, as well as from increased mortality during the dispersal phase (Johnson and Gaines, 1990; Ronce, 2007). In addition, local adaptation causes indirect costs for dispersers, since they are less likely to carry alleles locally favoured at their destination and thus have a disadvantage in new environments (Billiard and Lenormand, 2005).

Two main driving forces of dispersal evolution have been identified (Bowler and Benton, 2005; Ronce, 2007). First, dispersal can be seen as a mechanism to avoid competition between relatives. By reducing the relatedness, dispersal alleviates kin competition, as first proposed by Hamilton and May (1977) and studied in more detail in subsequent articles, e.g., Gandon and Michalakis (1999); Rousset and Gandon (2002); Taylor (1988). Also, inbreeding depression is ameliorated by increased dispersal (Gandon, 1999; Roze and Rousset, 2005; Szulkin and Sheldon, 2008). In practice however, the relative impacts of inbreeding and kin competition on the evolution of dispersal are difficult to separate since both are based on the relatedness between individuals (Perrin and Goudet, 2001).

Second, spatio-temporal variation of the environment interacts strongly with dispersal. If local extinction events occur, dispersal is necessary to recolonize empty habitat, and thus is maintained even if it is costly (Van Valen, 1971). This is an extreme form of temporal habitat variability, which has been shown to promote dispersal (Bach *et al.*, 2007; Blanquart and Gandon, 2011; Cadet *et al.*, 2003; Jansen and Vitalis, 2007; Mathias *et al.*, 2001; Parvinen *et al.*, 2012). By spatial habitat heterogeneity, I refer to spatial differences in habitat quality, expressed by variable resource availability or carrying capacity, for example. In particular, I do not consider spatial heterogeneity in selection (Balkau and Feldman, 1973). However, the effects of these two types of habitat heterogeneity on the evolution of dispersal are very similar. Conversely to temporal habitat variability, spatial habitat heterogeneities select against dispersal (Dockery *et al.*, 1998; Holt, 1985). Hastings (1983) argued that zero dispersal is the only evolutionarily stable dispersal strategy if the habitat is heterogeneous in space but temporally stable (see e.g. Waddell *et al.* (2010) for a weighting between these two kinds of variability). This is because high-quality habitat contains relatively many individuals and thus dispersal leads to a net flux of individuals into low-quality habitat. However, Hastings pointed out that non-zero dispersal rates can be maintained under conditional, e.g., density-dependent, dispersal. This idea is confirmed by McPeek and Holt (1992), demonstrating that spatial heterogeneity can select for dispersal if dispersal depends on carrying capacity. Note that at the margins of a species' range, additional factors govern the evolution of dispersal (Dytham, 2009). However, I do

not consider those but focus on a population that has become established within its habitat.

In the context of dispersal evolution, the ideal free distribution (Kacelnik *et al.*, 1992) has gained significant importance. The ideal free distribution is a spatial distribution of a population with the property that individuals cannot increase their reproductive output by changing their location. As a result, all individuals have the same reproductive output and the population is distributed as if there was no dispersal. In particular, this implies that a homogeneous population, whose growth is limited by the abundance of a fixed resource, is at its carrying capacity. Under reasonably general assumptions, dispersal strategies that lead to an ideal free distribution are evolutionarily stable (Cantrell *et al.*, 2007, 2010; Cressman and Křivan, 2006), i.e., they are the expected ultimate outcomes of evolutionary trajectories. Zero dispersal as found by Hastings (1983) and the positive dispersal strategy described by McPeek and Holt (1992) are examples in support of this theory.

The dispersive ability of a population is usually characterized by its dispersal rate (migration rate) that denotes the fraction of individuals leaving their habitat patch per time unit. Classical discrete models, like Wright's island model and the stepping stone model (Kimura and Weiss, 1964), use this description of dispersal. To describe more detailed modes of dispersal, the notion of dispersal distance determines how far individuals displace from their original patch (Gandon and Rousset, 1999; Murrell *et al.*, 2002; Rousset and Gandon, 2002). More generally and more commonly used in continuous models of dispersal, dispersive behaviour is described by dispersal kernels. They denote probability distributions for the displacement of individuals within a time unit. A few authors have studied the evolution of whole dispersal kernels either of a fixed shape (Gros *et al.*, 2006), or changing their shape (Hovestadt *et al.*, 2001), mainly using numerical simulations. In the following, I present a deterministic diffusion model of type-dependent dispersal in which the mean and variance of the dispersal kernel alone determine the dispersive behaviour of the population. I will denote the mean of the dispersal kernel by the mean displacement, since it describes the mean distance and direction of individual movement. The variance of the dispersal kernel I call diffusiveness. It can be interpreted as the extent to which individuals spread in space, or

as a measure of variability in dispersal distance among individuals. The evolution of these two determinants, mean displacement and variance of dispersal, is studied.

3.2 The model

Consider a population consisting of n dispersal types that occupy a habitat Ω in 1-dimensional space. By $N_i(x,t)$ denote the densities of adults of type i at location x and time t, and by $p_i(x,t)$ their relative frequencies. $N_T(x,t) = \sum N_i(x,t)$ is the total population density. Local birth and death rates of individuals are assumed to be identical for all types, and I collapse them into a single per-capita growth rate $r(x, N_T)$ that depends on the spatial variable x and the total population density N_T. Hence, there is no direct selection on any trait. For any given position x, a zero of the growth rate function $r(x, N_T) = r_x(N_T)$ determines a carrying capacity κ_x, i.e., $r_x(\kappa_x) = 0$. Let this zero be unique to exclude, e.g., strong Allee effects, and let $r_x(N_T) > 0$ if $N_T < \kappa_x$ and $r_x(N_T) < 0$ if $N_T > \kappa_x$. Given that $r(x, N_T)$ is smooth, we can define a smooth carrying capacity profile $\kappa(x) = \kappa_x$ for $x \in \Omega$. In the following, I require κ to be strictly positive in the interior of the habitat Ω.

The dispersive behaviour of each type in the population is described by a dispersal kernel $\mu_i(x,t;y,t+\Delta t)$, which gives the probability that an individual of type i located at position x at time t disperses to y within a short time interval Δt. Let the dispersal kernels fulfil the following three assumptions, which are standard in diffusion theory. First, individuals must not move at infinite speed, that is, no finite distances can be covered in infinitesimally small time. Hence, for $\varepsilon > 0$ we postulate

$$\lim_{\Delta t \to 0} \frac{1}{\Delta t} \int_{|y-x|<\varepsilon} \mu_i(x,t;y,t+\Delta t)\, dy = 0. \tag{3.1a}$$

Moreover, let the μ_i have (truncated) means and variances, $M_i(x,t)$ and $V_i(x,t)$, i.e.,

$$M_i(x,t) = \lim_{\Delta t \to 0} \frac{1}{\Delta t} \int_{|y-x|<\varepsilon} (y-x)\, \mu_i(x,t;y,t+\Delta t)\, dy < \infty, \tag{3.1b}$$

$$V_i(x,t) = \lim_{\Delta t \to 0} \frac{1}{\Delta t} \int_{|y-x|<\varepsilon} (y-x)^2\, \mu_i(x,t;y,t+\Delta t)\, dy < \infty. \tag{3.1c}$$

The expected directional movement (mean displacement) and the diffusive effect of dispersal (diffusiveness) of type i are captured by $M_i(x,t)$ and $V_i(x,t)$, as defined

in equations (3.1b) and (3.1c)). If mean displacement M_i and diffusiveness V_i are constant, I speak of unconditional dispersal. Conversely, with conditional dispersal, individuals base their dispersal decisions on environmental cues such that M_i and V_i may vary in space and time. This dependence can be explicit or emerge implicitly from conditioning on, e.g., the current population density or resource abundance. To indicate this – possibly indirect – spatio-temporal dependence of mean displacement and diffusiveness, I will write $M_i(\cdot)$ and $V_i(\cdot)$ in the case of conditional dispersal (rather than $M_i(x,t)$ and $V_i(x,t)$).

Under the assumption that we can approximate the life cycle described above by a diffusion equation – namely that the population can be characterized in terms of densities, the local influences $r(x, N_T)$ are weak, and the μ_i satisfy (3.1), details in Appendix A2 – the dynamics of population density N_T and dispersal type frequencies p_i are given by

$$\partial_t N_T = -\partial_x J_T + N_T r, \tag{3.2a}$$

$$\partial_t p_i = \frac{1}{N_T}(-\partial_x J_i + p_i\, \partial_x J_T), \qquad i = 1, ..., n, \tag{3.2b}$$

where

$$J_i = M_i N_i - \frac{1}{2}\, \partial_x (V_i N_i) \tag{3.3}$$

is the flux of individuals of type i, and $J_T = \sum_i J_i$ is the total flux of individuals. For the ease of notation, I dropped the arguments x and t throughout. Similar models have been employed by, e.g., Dockery *et al.* (1998); Pigolotti and Benzi (2014).

The equations (3.2) are reaction-diffusion equations. The population disperses according to the gradient of its flux, $-\partial_x J_T$, and is locally regulated by the per-capita growth rate r. I do not impose any particular regulation mechanism on population density; population regulation arises from the specification of density dependence of the growth rate $r = r(x, N_T)$. Similarly, spatial heterogeneity comes from the dependence of the growth rate on the spatial variable x. Interestingly, the reaction terms in the equations for the type frequencies p_i are determined by the total flux of individuals, $\partial_x J_T$. Hence, $\partial_x J_T$ represents a force selecting on dispersal that is detailed below. If dispersal were type-independent and unconditional (i.e., $M_i(\cdot) \equiv M$ and $V_i(\cdot) \equiv V$ for all i, and M and V constant), and $r = r(N_T)$ spatially homogeneous, equation (3.2b)

simplifies to the standard diffusion equation, $\partial_t p_i = (V/2)\partial_{xx} p_i$. Note that from the dispersal kernels μ_i, only M_i and V_i enter the equations. Hence, I do not restrict to any particular shape of dispersal kernel; a dispersal strategy is characterized solely by $M_i(\cdot)$ and $V_i(\cdot)$.

For the equations (3.2), we need to specify boundary conditions. Throughout this chapter, I require that the habitat Ω is closed, e.g., a bounded interval or a circular habitat. In the first case, no individuals must enter or leave the habitat, such that all fluxes vanish at the interval's endpoints. In the latter case, we can imagine an interval glued together at its endpoints, such that the values of all expressions and their derivatives coincide there.

In Appendix A2, I argue that the two equations (3.2a) and (3.2b) can be separated by separating their time scales, given that the dispersal patterns of all types are sufficiently similar. Then, population density equilibrates in a rapid initial phase and can be assumed to be constant, hence $\partial_x J_T = N_T\, r$, as type frequencies evolve on a slower time scale. In the following, I consider a resident population with a dispersal strategy characterized by mean displacement $M_0(\cdot)$ and diffusiveness $V_0(\cdot)$. This population is invaded by a dispersal modifier with frequency $p_I(x,t)$ that changes the dispersal strategy to $M_I(\cdot) = M_0(\cdot) + m(\cdot)$ and $V_I(\cdot) = V_0(\cdot) + v(\cdot)$, where $m(\cdot)$ and $v(\cdot)$ are sufficiently small. The invasion corresponds to a perturbation of the dispersal type frequencies around $p_I(x,t) = 0$; the exact pattern of the perturbation (e.g., local or global) is irrelevant for the long-term outcome in our continuous model. Since all types at location x have the same growth rate $r(x, N_T)$, changes in modifier frequencies will be due to dispersal effects rather than different growth rates. In my study, dispersal hence does not incur any explicit cost, which could be added to the model in a straightforward way by introducing distinct growth rates $r_i(x,t)$ for different types, see Appendix A2, in particular equation (A2.7).

3.3 Results

I use the terminology introduced in the previous section. In addition, I denote by N_I the number of dispersal modifiers (invaders), and by J_I their flux. For the sake of improved

readability, I will often omit the spatial and temporal dependence of these and similar quantities in the following. Generally however, they will not be constant unless stated explicitly.

3.3.1 Temporal change of modifier abundance

The total number of modifiers in the habitat is obtained by integrating $N_I = p_I N_T$ over the habitat Ω. Using (3.2), this yields

$$\partial_t \int_\Omega N_I \, dx = \int_\Omega p_I \, \partial_x J_T \, dx, \tag{3.4}$$

since $N_T \, r = \partial_x J_T$ at equilibrium of N_T. Note that integration of the flux term in (3.2) gives $-J_I|_\Omega$, which vanishes since the habitat is closed. Equation (3.4) shows that the modifier will not increase in total numbers if either the total flux of individuals, J_T, or, after partial integration, if its frequency p_I is constant throughout the habitat. Thus, invasion stops if the modifier's frequency spreads out evenly, but note that spatial heterogeneities in dispersal patterns or population density profiles can deform initially constant frequency profiles. Furthermore, a modifier increases if it invades regions where $\partial_x J_T$ is positive. Since N_T is at equilibrium, these areas coincide with those where the growth rate r is positive. Thus, this finding is very natural and, in particular, does not depend on the dispersal pattern of the invading type. In general, the invader increases in numbers if the change of flux weighted by its frequency is positive. Thus, heuristically, the dispersal pattern must have the effect of keeping the invader's frequency above average in areas of positive growth rates to ensure its continuing spread.

3.3.2 Ideal free distributions and stability of balanced dispersal

In the modelling section, I defined the carrying capacity profile $\kappa(x)$. I call a dispersal strategy balanced (Doncaster *et al.*, 1997) if $N_T = \kappa$ is a stable solution for the dynamics of a population entirely adopting this strategy. Recalling the definition of the ideal free distribution (Kacelnik *et al.*, 1992), a population using a balanced dispersal strategy is hence maintained at an ideal free distribution under perturbations of N_T. From

equation (3.2a), together with equation (3.3), we see that a dispersal strategy given by $V(\cdot)$ and $M(\cdot)$ is balanced if the change in total flux, $\partial_x J_T$, vanishes if the population (entirely adopting it) is at carrying capacity κ; that is if

$$\Phi = \frac{1}{2}\,\partial_x(V\kappa) - M\kappa \equiv C, \tag{3.5}$$

where $C \in \mathbb{R}$ is, in particular, constant with respect to space – see also Cantrell *et al.* (2010). Note that an inhomogeneous composition of two or more balanced dispersal strategies at carrying capacity generally does not imply vanishing $\partial_x J_T$.

In Appendix A2, I prove mathematically that the class of balanced dispersal strategies is protected against invasion by (sufficiently similar) non-balanced dispersal strategies. In this sense, balanced dispersal strategies that produce an ideal free distribution are evolutionarily stable outcomes of dispersal evolution. Evolutionary stability of balanced dispersal strategies has been shown for similar models of dispersal evolution, e.g., Cantrell *et al.* (2007); Cressman and Křivan (2006).

3.3.3 Dynamics at ideal free distribution

Between two balanced dispersal strategies, the previous stability analysis does not provide a definite statement. In the following, I investigate dispersal evolution within the class of balanced dispersal strategies, i.e., the evolution of dispersal at ideal free distribution. Assume that both the original and the modified dispersal strategies are balanced, i.e., they satisfy (3.5). In particular, this implies that $1/2\,\partial_x[v(x)\kappa(x)] - m(x)\kappa(x)$ is constant. Replacing for the total flux J_T, we obtain from equation (3.4)

$$\begin{aligned}
\partial_t \int_\Omega N_I\,dx &= -\int_\Omega p_I\,\partial_x\left[(M + p_I m)\kappa - \frac{1}{2}\partial_x(V + p_I v)\kappa\right] dx \\
&= -\int_\Omega p_I\,\partial_x\left(p_I C + \frac{v\kappa}{2}\,\partial_x p_I\right) \\
&= -\frac{p_I^2}{2}\bigg|_\Omega - \int_\Omega \frac{v\kappa}{2}\,p_I\,\partial_{xx} p_I\,dx \\
&= -\int_\Omega \frac{v\kappa}{2}\,p_I\,\partial_{xx} p_I\,dx.
\end{aligned} \tag{3.6}$$

This expression is independent of the modification to mean displacement m. Therefore, the mean displacement does not contribute to the success or failure of the modifier as long as it adjusts a potential mismatch in diffusiveness to retain a balanced dispersal strategy.

It is remarkable that changes in diffusiveness (non-zero v) lead to changes in the number of modifiers as long as their frequency profile, p_I, is not spatially constant. In full generality, the sign of this change depends on the shape of p_I. However, if $v\kappa$ is constant, equation (3.6) can be partially integrated to yield

$$\partial_t \int_\Omega N_I \, dx = \frac{v\kappa}{2} \int_\Omega (\partial_x p_I)^2 \, dx. \tag{3.7}$$

The second term from the partial integration vanishes due to the boundary conditions. This equation is analogous to equation (5) by Pigolotti and Benzi (2014), who analysed stochastic noise in a finite population. The occurrence of equation (3.7) here, however, demonstrates its relevance more broadly. It shows that a growth rate of the modifier abundance proportional to $v\kappa$ is induced if the modifier changes its diffusiveness such that dispersal stays balanced. This change is fuelled by heterogeneities in the modifier's frequency, $\partial_x p_I \neq 0$. Consequently, it is only transient if the dispersal type frequency profile diffuses out over time. Thus, under a purely deterministic model without explicit costs of dispersal, or selection on a genetic background, balanced dispersal strategies are neutral with respect to each other.

However, the flattening-out of the frequency profile can be counteracted by factors not yet considered in the model, tipping the balance between the competing types. If these factors generate or maintain spatial differences in the frequency profile, they thereby make the transient effect of a variant dispersal strategy permanent. For example, selection on linked traits takes a complex role in dispersal evolution. While local adaptation is known to select against dispersal, equation (3.7) indicates that selective processes on a genetic background that perturb the frequency profile of dispersal modifiers thereby can favour increased dispersal. First, selection against heterozygotes can maintain frequency heterogeneities in the form of clines (Barton, 1979) in which type-dependent dispersal can operate. Note that these clines do not require spatial heterogeneity in selection but emerge, e.g., after secondary contact between differentiated species. Second, transient selection patterns on a selective background linked to the dispersal modifier can directly perturb modifier frequencies away from uniformity. Third, if beneficial mutations appear on the selective background, they sweep to fixation. Since recombination gradually breaks down linkage between the beneficial mutation and the dispersal modifier, the sweep has an impact on the latter's frequency

profile (Barton, 2000). Even though, on average, the effect of such sweeps – often termed ”genetic draft” (Gillespie, 2001) – cancels out, it hence leads to a systematic increase of modifiers that enhance dispersal.

Finally, genetic drift in finite populations perturbs type frequencies away from spatial uniformity. It has been observed that relatedness may emerge from genetic drift in a structured population (Lenormand *et al.*, 2009). Accordingly, the variability in type frequencies due to genetic drift constitutes a measure of relatedness between individuals in the population (Barton and Clark, 1990). Hence, equation (3.7) relates to the body of literature that dates back to Hamilton and May (1977) and predicts the promotion of positive dispersal to escape from kin competition.

3.4 Discussion

As dispersal evolves, different dispersal strategies in a population compete against each other in a selective process. The two main factors of influence are known to be the relatedness between individuals, and spatio-temporal variability of the environment. Here, by spatial heterogeneity I referred to local differences in resource availability or carrying capacity. Other types of spatial habitat variability require additional information put into the model. For example, selection for a spatially shifting optimum requires to link dispersal to a second trait under direct selection. However, the consequences for dispersal are analogous to a variable carrying capacity: Gene flow causes individuals to be locally maladapted and hence induces a dispersal load (Kirkpatrick and Barton, 1997) that enhances the pressure for lower dispersal. Historically, investigations have focused on either effects of relatedness or spatio-temporal variability of different kinds rather separately – but see, e.g., Gandon and Michalakis (1999); Leturque and Rousset (2002); Morris *et al.* (2001); Blanquart and Gandon (2014). In this study of the evolution of dispersal, I demonstrated how the effects of environmental heterogeneity and type frequency variances, e.g. due to genetic drift and relatedness, can be linked within the same model.

Throughout this chapter, I assumed that population density is temporally constant. This can be justified if the differences in dispersal behaviour between types are small.

Then, population density will quickly equilibrate and we recover a fast-slow dichotomy in which the ecological dynamics of population density can be decoupled from the dynamics of dispersal type frequencies. The assumption of small differences in dispersal strategies is reasonable if we accept that dispersal evolution proceeds in small steps. It allows us to treat population density as given while type frequencies evolve. Simulations confirm that the approximation is robust; as long as the deviations between dispersal patterns are small, simulations of the full system (3.2) and of equation (3.2b) with population density N_T fixed produce virtually identical outcomes. In particular, however, the assumption of temporally constant population density precludes most aspects of environmental stochasticity, which is not considered in this chapter.

Intuitively, dispersal strategies that let the population more efficiently exploit the resources that are present in the habitat should be successful. That is, strategies that minimize the spatial discrepancies in growth rates and hence the experienced differences in habitat quality can be expected to be selectively favoured. This intuition is confirmed by equation (3.4), which gives an analytical expression for the change of the total abundance of dispersal strategies present in the habitat. The number of individuals of a specific dispersal strategy increases if the mean derivative of the total flux, $\partial_x J_T$, weighted by the type's frequency, is positive. Since $\partial_x J_T$ is proportional to the local growth rate, this result simply states that a successful type must be overrepresented in regions of positive growth rate. It follows that an evolutionarily stable dispersal strategy homogenizes the total flux J_T, and hence equalizes local growth rates. That is, it causes the population to attain an ideal free distribution (Kacelnik *et al.*, 1992).

In principle, this can be achieved in two ways. Zero dispersal trivially homogenizes the total flux J_T. One of the first contributions to this aspect of dispersal evolution was by Hastings (1983), who showed that a heterogeneous environment leads to zero dispersal if dispersal is unconditional. This is because positive unconditional dispersal leads to a net flux of individuals from regions of positive growth rates (high carrying capacity) into regions of negative growth rates (low carrying capacity) and is thus to the disadvantage of the population. Accordingly, dispersal types with reduced diffusiveness exploit their environment more efficiently and therefore out-compete more

mobile types. This statement is a special case of the present analysis, restricting to unconditional dispersal strategies. It has been proved earlier by Dockery *et al.* (1998) for a specific choice of local growth function $r(x, N_T)$. An illustrative description of the mechanism in a discrete setting is given by Holt (1985).

More generally, balanced dispersal strategies take the population to an ideal free distribution by matching dispersal behaviour to the spatial carrying capacity profile. This class of strategies has been shown to be evolutionarily stable in previous studies, e.g. by Cantrell *et al.* (2010); McPeek and Holt (1992). If the population is at an ideal free distribution, any non-balanced dispersal strategy changes the flux J_T to its own disadvantage. Accordingly, I characterized the class of balanced dispersal strategies for the present model, equation (3.5), and showed that it cannot be invaded by strategies from outside this class. Hence, it is evolutionarily stable and an expected long-term outcome of dispersal evolution.

Confirming this prediction in practice, however, is difficult. In principle, mean displacement M and variance of dispersal V can be estimated directly by recording the movement behaviour of large numbers of individuals. However, the carrying capacity of the habitat can hardly be inferred in most cases. Unless there is a clear upper bound to the number of individuals an area may sustain (e.g., a limited number of nesting places), the availability of resources and their effect on carrying capacity in natural environments are likely to be crudely estimable at best. In experimental approaches, there is only little empirical evidence for balanced dispersal strategies, reviewed by Diffendorfer (1998). Rather, experiments with bacteria and protozoa (Donahue *et al.*, 2003) seem to support a source-sink dispersal type (Pulliam, 1988). However, given the complexity of the interaction of dispersal with other traits and the time it would take to reach an evolutionarily stable state even under controlled conditions, it is questionable if balanced dispersal is feasible to evolve in the laboratory.

Not all balanced dispersal strategies do equally well so that we can establish a selective hierarchy between them whenever dispersal type frequencies are variable in space. Analytically, this is formulated in equation (3.6) and, for an important special case, in equation (3.7). The latter shows that the total number of individuals with increased diffusiveness never declines. In fact, this number increases whenever disper-

sal type frequencies vary in space. In our deterministic setting, the effect levels out as frequencies diffuse in space and stalls once the frequency profiles are completely flat. In practice however, various forces (e.g. selection on a genetic background and different sources of stochasticity) continuously perturb the frequency profiles and hence induce a variance that sustains the increase in numbers of individuals with increased diffusiveness. Thus, roughly speaking, elevated dispersal is selected for amongst balanced dispersal strategies.

The two forces exerted by the variability in the habitat and the variability in dispersal type frequencies can be seen as opposing each other. Spatial heterogeneity in the habitat exert a selection pressure for reduced dispersal, at least if the possibility of conditional and hence balanced dispersal is limited, as is likely the case in many natural populations. Once sufficiently close to an ideal free distribution, the variability in the dispersal type frequency profile of the population counters this force. The magnitude of the pressure for increased dispersal will depend on the balance between the size of the perturbations of frequencies away from uniformity, and the homogenizing effect of dispersal.

A particular issue of dispersal evolution is whether dispersal evolves in a population that initially does not disperse at all, i.e., $M_0 = V_0 = 0$. My results answer this question for the scenario studied here: Given that the population is capable of adjusting its dispersal to the demographic heterogeneities, any non-zero balanced dispersal strategy is selectively favoured over the zero-dispersal strategy, as long as dispersal type frequencies are variable in space.

Spatial heterogeneities in the type frequencies can emerge due to many reasons. If the type frequencies fluctuate because of genetic drift, the variance in type frequencies constitutes a measure of relatedness (Barton and Clark, 1990). The fact that relatedness selects for dispersal in finite populations is well known (Billiard and Lenormand, 2005; Gandon and Michalakis, 1999; Roze and Rousset, 2005). Equation (3.7) demonstrates an alternative approach to identifying effects of relatedness in dispersal evolution via type frequency variances emerging from stochastic sampling. To illustrate how the effects of kin competition and genetic drift relate to spatial heterogeneities in type frequencies, briefly consider two examples.

First, consider a simple two-patch model with different patch sizes. In a classical paper, McPeek and Holt (1992) showed that balanced dispersal strategies, which cause the number of emigrants to equal the number of immigrants in each patch, are evolutionarily stable. Extending this model to finite populations, Leturque and Rousset (2002) defined a fitness measure taking relatedness into account. In this case, a single dispersal strategy is selected for, which both is balanced and leads to panmixia, i.e., the population behaves as if mating happened randomly in a single mating pool. Assume that the population consists of two types of identical clones, one of which is present at frequencies p_A and p_B in patches A and B. Then, the quantity $\chi = (p_A - p_B)^2$ is a measure of type frequency variability between the two patches, analogous to $(\partial_x p_I)^2$ in equation (3.7). One can easily show that χ is minimized for panmixia with $\chi = 0$, hence dispersal increases as long as this quantity is positive and equilibrates when $\chi = 0$. The variability of type frequencies between the patches thus plays an interesting role and could be used as a measure for the benefit of dispersal in alleviating kin competition in this example.

Second, one could incorporate genetic drift directly into the model (3.2). This has been done by Pigolotti and Benzi (2014), who obtained equation (3.7) from their resulting stochastic partial differential equation. However, to evaluate this quantity, they had to introduce a cutoff ϵ, which is hard to interpret biologically. Considering a stepping stone model (Kimura and Weiss, 1964) as a discrete version of the continuous model (3.2) shows that the expected change in the total abundance, $\mathcal{N}_I^{total}$, of a dispersal modifier that increases the migration rate between patches from $\mathcal{M}$ to $\mathcal{M} + m$ is given by

$$\mathbb{E}\left[\Delta \mathcal{N}_I^{total}\right] = m\mathcal{J}\mathcal{N}\sigma_p^2\big(1-\rho\big), \tag{3.8}$$

(cf. Appendix A2 for details) where $\mathcal{J}$ is the number of patches the habitat consists of, and $\mathcal{N}$ is the number of individuals present in each patch. Furthermore, σ_p^2 denotes the spatial variance of type frequencies, and ρ is the correlation between type frequencies in adjacent patches. The expression $\sigma_p^2(1-\rho)$ is the discrete space equivalent to $(\partial_x p_I)^2$ in equation (3.7). The fact that σ_p^2 is a measure of relatedness was already noted by Kimura and Weiss (1964). Driving the analysis further (cf. Appendix A2), one can derive a selection coefficient for dispersal modifiers as $s = m/(4\mathcal{N}\mathcal{M})$. This

shows that the cutoff in the article by Pigolotti and Benzi (2014) needs to be chosen as $\epsilon = (\Omega/\jmath)^2/(V\pi)$, where $V = \mathcal{M}(\Omega/\jmath)^2$, to establish the correspondence between a discrete stepping stone model and its approximation, the diffusion model (3.2). Hence, a possibility for measuring the selective benefit of dispersal modifiers due to relatedness is provided by the present framework.

Overall, the spatial heterogeneities of type frequencies take a central role in translating stochastic effects into selective forces promoting dispersal. Previous studies developed rather specialized models to analyse the impact of different stochastic factors on the evolution of dispersal. Direct methods are crucial for understanding the detailed process of how they influence dispersal evolution, but make it difficult to compare their relative importance. However, the stochastic factors are reflected in the same variability of type frequencies. Thus, their mode of promoting increased dispersal is channelled through the same phenomenon, as noted already by Waddell *et al.* (2010). Identifying their contributions to the variability of type frequencies hence puts these stochastic factors on a single scale.

In summary, my study shows that many of the main factors of dispersal evolution can be brought together in a single modelling framework. The effect of spatially varying resource availability and the consequent spatial density variations are phrased in terms of the fluxes J_I and J_T. Environmental stochasticity is not considered in this chapter, but could be implemented directly into the equation for the total population size, equation (3.2a). Genetic drift and relatedness are reflected in the variability of dispersal type frequencies, $(\partial_x p_I)^2$, that exerts a selection pressure for increased dispersal. In many cases, selection on a genetic background can lead to heterogeneities in dispersal modifier frequencies, e.g. in hybrid zones, if selection transiently favours a certain part of the population, or by sweeping beneficial alleles. Indirectly, selection on a genetic background hence can also exert a positive selection pressure on dispersal modifiers that is channelled through the spatial variability of type frequencies. On top of that, dispersal evolution is limited by direct costs of dispersal in practice, which can be added to the model straightforwardly by introducing distinct growth rates $r_i(x,t) \neq r_j(x,t)$ for different types i and j. This is indicated in Appendix A2, but I did not consider direct costs of dispersal otherwise.

The results described here suggest that future studies should focus on the variability of type frequencies as a force promoting increased dispersal and establish its connection to demographic and environmental stochasticity more closely. I argued that selective pressures on traits linked to dispersal may maintain spatial patterns that dispersal differences can act on. The complexity of interactions between selection and type-dependent dispersal is hard to assess, but can be relevant in nature, in particular if individuals base dispersal decisions on their fitness. The correlations between fitness and dispersal are virtually unexplored and it is unclear to what extent the ability to detect and interpret fitness conditions can be based on a genetic level. In the presence of density-dependent selection, type-dependent dispersal might tip the balance by pushing population density above thresholds and lead to interesting phenomena.

3.5 Excursion: Type-dependent dispersal in clines

In the final section of this chapter, I consider spatial patterns of gene frequencies that are maintained by selection, and assume that the same genes concurrently determine dispersal behaviour. This reveals the impact of type-dependent dispersal on moving gene frequency clines, i.e., stable heterogeneities in gene frequency. At the same time, however, it relates back to dispersal evolution: We show that in the presence of clines, fast dispersing types have an advantage over slow dispersers, thus drawing the parallel to the previous sections.

Most theoretical models in population genetics assume that dispersal is random with respect to genotype (Slatkin, 1985). Such random gene flow homogenizes populations, eroding genetic dissimilarities. However, as pointed out by Edelaar and Bolnick (2012), gene flow can have a much more complex role. Type-dependent dispersal appears naturally in numerous organisms, e.g., aquatic species (Bolnick *et al.*, 2009; Lutscher *et al.*, 2007), butterflies (Haag *et al.*, 2005), and plants that are polymorphic in flower shape and/or colour (Stanton, 1987). It thus arises naturally to ask about the impact of type-dependent dispersal on processes of natural selection in spatially extended populations.

Advantageous mutations spread locally and propagate in the form of travelling waves (Fisher, 1937). These spatial changes in gene frequencies are commonly called clines (Haldane, 1948); they may move, but have a stable shape that describes the transition between areas where different alleles are predominant. Clines also emerge due to spatial heterogeneities in selection, when different alleles are favoured in different places (Nagylaki, 1975; Slatkin, 1973), or in the case of selection against hybrids, e.g., in hybrid zones that emerge after secondary contact between populations (Barton, 1979). Spatial gene frequency clines are frequently observed in many natural populations and provide insight into evolutionary patterns, e.g., Bridle *et al.* (2001); Szymura and Barton (1986); Teeter *et al.* (2008); Whibley *et al.* (2006).

We study the effect of type-dependent dispersal on clines. As we will see, type-dependent dispersal can affect both the shape of a cline and the speed at which it moves; hence, the presence of different dispersal patterns can bias our predictions drawn from the analysis of clines. Any model of type-dependent dispersal and selection requires a connection between the dispersal trait and individual fitness. We will choose the simplest approach by assuming that they are completely linked, i.e., the trait under selection also controls the dispersal behaviour of the individual. This is a reasonable assumption, since alleles affecting dispersal are likely to pleiotropically also affect fitness – for instance in the case of flowering plants, when flower shape both determines how successfully to attract pollinators, and what kind of pollinators to attract. The assumption is also justified if separate alleles determining fitness and dispersal are sufficiently closely linked, at least for a limited period of time.

3.5.1 The model

Throughout this section, we consider a spatially homogeneous environment with (spatially and temporally) constant population density. The classical continuous model for selection and dispersal in unidimensional space assumes that all individuals follow the same spatially homogeneous dispersal pattern, which is characterized by a mean displacement (directional movement coefficient) M, and a variance of dispersal (diffusion coefficient) V. If the population consists of two genotypes with frequencies $p(x,t)$ and $1-p(x,t)$ at location x and time t, the diffusion limit of the selection-dispersal dynamics

is

$$\partial_t p = \frac{V}{2}\,\partial_{xx} p - M\,\partial_x p + F(x;p). \tag{3.9}$$

Here, the function $F(x;p)$ describes selection: at position x, the frequency p grows at rate F relative to the frequency of the other genotype. If no selective force is active ($F = 0$), gene frequencies spread in space and equilibrate to a spatially constant value at a rate proportional to V. The parameter M adds a directional component that can emerge due to an active individual preference or due to the presence of a slope, wind, or the current of water in the habitat. Since this is a constant shift of the system, M disappears from the equation when transforming $x \mapsto x - Mt$.

Equation (3.9) can be generalized to different dispersal strategies for the two types, including the possibility of conditional dispersal strategies that depend, e.g., on space and time (Nagylaki and Moody, 1980). We briefly sketch a derivation of the dynamics that leads to an equation analogous to (3.2b), but with an additional selection term (see also Appendix A2). Assume that the two genotypes have mean displacements $M_1(x,t)$ and $M_2(x,t)$, and variance of dispersal $V_1(x,t)$ and $V_2(x,t)$. If the abundances of the two types are denoted by N_1 and N_2, their reaction-diffusion dynamics can be written as

$$\partial_t N_1(x,t) = \frac{1}{2}\,\partial_{xx}\left[V_1(x,t)N_1(x,t)\right] - \partial_x\left[M_1(x,t)N_1(x,t)\right] + G_1(x;N_1,N_2), \tag{3.10a}$$

$$\partial_t N_2(x,t) = \frac{1}{2}\,\partial_{xx}\left[V_2(x,t)N_2(x,t)\right] - \partial_x\left[M_2(x,t)N_2(x,t)\right] + G_2(x;N_1,N_2), \tag{3.10b}$$

where G_1 and G_1 are the growth rates of the two types. Here, we consider unconditional dispersal strategies, which are defined by constant $M_i(x,t) \equiv M_i$ and $V_i(x,t) \equiv V_i$. This assumption is justified since unconditional dispersal strategies are balanced in a spatially homogeneous environment and thus are not selected against directly, see Cantrell *et al.* (2010) or the previous sections of this chapter. Furthermore, since we assume that the environment is spatially homogeneous, selection does not explicitly depend on x, hence $G_1(x;N_1,N_2) = G_1(N_1,N_2)$ and $G_2(x;N_1,N_2) = G_2(N_1,N_2)$ (and thus $F(x;p) = F(p)$, see below). If the total population size $N_T = N_1 + N_2$ is regulated and remains constant, we may write the system (3.10) in terms of the single variable $p = N_1/N_T$. This generalizes the gene frequency dynamics (3.9) to type-dependent

dispersal as follows:

$$\partial_t p = \frac{V(p)}{2}\,\partial_{xx} p - M(p)\,\partial_x p + F(p), \tag{3.11}$$

where $M(p) = p\,M_2 + (1-p)\,M_1$ and $V(p) = p\,V_2 + (1-p)\,V_1$ – compare this equation to equation (3.2b)). The selection function F is obtained from the individual growth rates as

$$F = \frac{1}{N_T}\left(\frac{N_2}{N_T}G_1 - \frac{N_1}{N_T}G_2\right),$$

but this shall not be of importance here.

3.5.2 Existence of cline solutions

We will study properties of cline solutions to equation (3.11), though mathematically their existence has not yet been established. We consider cline solutions $\tilde{p}(x,t) = P(x - c\,t) = P(z)$ that connect $P(-\infty) = 1$ with $P(+\infty) = 0$ and move with speed c (positive c means movement to the right, negative c to the left). The analysis of the inverse case, $P(-\infty) = 0$ and $P(+\infty) = 1$, follows by symmetry.

If the selection function F fulfills $F(0) = F(1) = 0$, $F'(0) \neq 0$ and $F'(1) \neq 0$, and changes sign at most once on $(0,1)$, it is possible to prove that cline solutions to equation (3.11) exist. This, in particular, encompasses the case of Fisher waves, where F is a quadratic polynomial, and bistable waves with cubic selection function F. In the latter case, which we discuss in more detail in Section 3.5.5, cline solutions are even unique (modulo the above-mentioned symmetry). More complicated selection functions may or may not permit cline solutions, depending on F itself, and on $M(p)$ and $V(p)$. We do not go into technical details here; a proof of these statements will be presented elsewhere. For the purpose of the following, we may simply assume the existence of cline solutions to equation (3.11).

3.5.3 The speed of a cline

Given a cline solution to equation (3.11), we may study its speed more closely. For an easier interpretation of the following results, it is convenient to define $\Delta_M = M_1 - M_2$, and write $V_1 = V + \Delta_V$ and $V = V_2$. Hence, the two types differ in their mean

displacement by a constant $\Delta_M \in \mathbb{R}$, and in their variance of dispersal by a constant $\Delta_V > -V$. With this notation, equation (3.11) can be written as

$$\partial_t p = \frac{V + \Delta_V(1-p)}{2}\,\partial_{xx} p - \left(\frac{M_1 + M_2}{2} + \frac{\Delta_M}{2}(1-2p)\right)\partial_x p + F(p). \qquad (3.11')$$

Assume that $P(z) = P(x - ct)$ is a travelling wave solution to equation (3.11') that moves with wave speed c. Inserting P into (3.11') produces

$$-c\,P' = \frac{V + \Delta_V(1-P)}{2}\,P'' - \left(\frac{M_1 + M_2}{2} + \frac{\Delta_M}{2}(1-2P)\right)P' + F(P).$$

Multiply this equation by $P' = dP/dz$ and integrate over $z \in (-\infty, \infty)$. We assume that the admissible solutions P have vanishing derivatives for $z \to \pm\infty$. Then, we obtain upon integration by parts

$$\begin{aligned} c\int_{-\infty}^{\infty}(P')^2 dz = &-\frac{\Delta_V}{4}\int_{-\infty}^{\infty}(P')^3 dz + \frac{M_1+M_2}{2}\int_{-\infty}^{\infty}(P')^2 dz + \\ &+\frac{\Delta_M}{2}\int_{-\infty}^{\infty}(1-2P)(P')^2 dz - \int_{-\infty}^{\infty}F(P)P'dz. \end{aligned}$$

If $P(-\infty) = 1$ and $P(+\infty) = 0$, the rightmost integral is transformed into $-\int_0^1 F(P)dP$. Thus, we write the speed of the cline as

$$c = c_S + c_V + c_M, \qquad (3.12)$$

where the three components of this expression are given by

$$c_S = \frac{\int_0^1 F(P)dP}{\int_{-\infty}^{\infty}(P')^2 dz}, \qquad c_V = -\frac{\Delta_V}{4}\frac{\int_{-\infty}^{\infty}(P')^3 dz}{\int_{-\infty}^{\infty}(P')^2 dz}, \qquad \text{and}$$

$$c_M = \frac{M_1 + M_2}{2} + \frac{\Delta_M}{2}\frac{\int_{-\infty}^{\infty}(P')^2(1-2P)dz}{\int_{-\infty}^{\infty}(P')^2 dz}.$$

This formula is implicit in the solution P, hence the contributions of selection, mean displacement, and variance of dispersal are not purely additive as suggested by the decomposition of c into c_S, c_V, and c_M. Rather, this representation is chosen such that the respective summand disappears if any of these characteristics – selection, variance of dispersal, or mean displacement – is neutral with respect to the genotypes.

The contribution of selection, c_S. If the two genotypes have different fitnesses, selective pressure acts on them. The term c_S is already known (Fife, 1979) and can be made explicit, e.g., in the case of disruptive selection (see below). In the absence of type-dependent dispersal, the direction of movement of the cline is determined by the sign of the average selection $\int_0^1 F(P)dP$.

The contribution of the variance of dispersal, $\mathbf{c_V}$. If the two genotypes have different variances of dispersal, only their difference Δ_V has an effect on the speed of the cline. Since P' does not change its sign (see Section 3.5.2), the cline shifts towards the genotype with smaller variance of dispersal, i.e., more mobile individuals gradually push back less mobile ones.

The contribution of the mean displacement, $\mathbf{c_M}$. The mean displacements enter c_M in two ways, first via the arithmetic mean $(M_1 + M_2)/2$. This expression already appears in the type-independent case ($M_1 = M_2$) and can be scaled away by shifting the coordinate system accordingly. Second, there is a term proportional to the difference $M_1 - M_2 = \Delta_M$ that is difficult to interpret. If the cline solution P is symmetric to the point $(z_o, P(z_o))$, where z_o is the position of the half-height of the cline defined by $P(z_o) = 1/2$, the term evaluates to zero. This applies, for example, if the cline has a sigmoid shape, i.e., is of the form $(1 + \exp[\gamma(x - ct)])^{-1})$, as is the case for type-independent dispersal and disruptive selection (see below). However, the sigmoid shape of the cline can be perturbed by breaking the symmetry of forces maintaining it, e.g., by type-dependent variance of dispersal.

3.5.4 Clines maintained by dispersal

Assume that the two genotypes are selectively neutral, i.e. $F(p) \equiv 0$, and have identical variance of dispersal, $\Delta_V = 0$. Then, type-dependent mean displacements $M_1 \neq M_2$ may lead to the existence of a cline solution for the dynamics (3.11). It is straightforward to check that

$$\tilde{p}(x,t) = \left(1 + \exp\left[-\frac{\Delta_M}{V}(x - ct)\right]\right)^{-1}, \tag{3.13}$$

satisfies equation (3.11). This cline solution has a sigmoid shape and moves with speed $c = c_M = (M_1 + M_2)/2$. Hence, it is a standing wave if the mean displacements of the two genotypes are of equal size but have opposite signs. The width of a cline $\tilde{p}$ can be defined as $\mathcal{L} = (\max|\partial_x \tilde{p}|)^{-1}$, see Endler (1977). It determines a characteristic length scale and evaluates to $\mathcal{L} = 4V/|\Delta_M|$ for $\tilde{p}$ in equation (3.13). Overall, this example shows that spatial clines can be maintained without selection, just by the

presence of type-dependent dispersal. This is not surprising; for example, if both genotypes have a movement bias in the direction of the half plane where they are predominantly present, then they only mix to a certain degree in the area where they meet.

3.5.5 Type-dependent dispersal in hybrid zones

Consider two alleles subject to selection against heterozygotes, such that common alleles have an advantage over rare alleles. Call the first allele the A allele with frequency p, and the second allele the a allele. Assume that selection is homogeneous in space and that the fitness values of the three possible genotypes AA, Aa, and aa are $1+2\alpha s$, $1-s(1-\alpha)$, and 1, respectively. With this notation, $s>0$ measures the strength of selection and $\alpha \in (-1,1)$ scales the fitness asymmetry between the two homozygotes. It follows that there is a threshold frequency $\hat{p}=(1-\alpha)/2$ such that selection increases the frequency of the A allele if it is above $\hat{p}$, and reduces it from below that value. If we assume that fitness differences are small ($s \ll 1$), we may reformulate the local selection terms and obtain $F(p)=2sp(1-p)(p-\hat{p})$. As mentioned in Section 3.5.2, equation (3.11) has a unique cline solution $\tilde{p}(x,t)=P(x-ct)$ with $P(-\infty)=1$ and $P(+\infty)=0$ under this specification of F . Clearly, there is another unique cline solution with the opposite configuration, $P(-\infty)=0$ and $P(+\infty)=1$, and a generally different wave speed.

Type-dependent mean displacement. Let $\Delta_V = 0$. With type-dependent mean displacements $M_1 \neq M_2$, equation (3.11) has two sigmoidal cline solutions given by

$$\tilde{p}^{\pm}(x,t)=\left(1+\exp\left[\zeta^{\pm}s(x-c^{\pm}t)\right]\right)^{-1}, \tag{3.14}$$

where

$$\zeta^{\pm}=4\left(\Delta_M \pm \sqrt{\Delta_M^2+8Vs}\right)^{-1},$$

and the speed of the cline is

$$c^{\pm}=\frac{1-2\hat{p}}{\zeta^{\pm}}+\frac{M_1+M_2}{2}.$$

For each set of parameters (i.e. V, s, M_1, and M_2), $\tilde{p}^{+}$ is monotonically increasing and connects $\tilde{p}^{+}(-\infty)=0$ with $\tilde{p}^{+}(+\infty)=1$. Conversely, $\tilde{p}^{-}$ is monotonically decreasing,

$\tilde{p}^-(-\infty) = 1$ and $\tilde{p}^-(+\infty) = 0$. These solutions hence correspond to the two possible configurations of either genotype being absent on one and fixed on the other end of the habitat. As discussed above in Section 3.5.2, these two solutions are the only cline solutions.

The two components of the wave speed of the solutions (3.14) have been identified in equation (3.12). The first summand, $(1 - 2\hat{p})/\zeta^{\pm}$, brings in the effect of selection. It is scaled relative to dispersal by the parameter $\zeta^{\pm}$, which leads to a non-additive dependence of the speed of the cline on selection and dispersal. If dispersal is type-independent ($\Delta_M = 0$), the term $(M_1 + M_2)/2$ becomes a shift of the cline due to the displacement of the population as a whole. Then, the second summand can be disposed of by the rescaling described above, $x \mapsto x - Mt$, such that we recover known results (Barton, 1979; Bazykin, 1969).

Type-dependent variance of dispersal. Let $\Delta_M = 0$. If the variance of dispersal is different for the two genotypes, the cline solution becomes asymmetric which impedes an explicit solution of equation (3.11). However, if the values of V_1 and V_2 are sufficiently similar, $|\Delta_V| \ll 1$, we may assume that the shape of the cline does not differ from the cline solution under type-independent dispersal. Then, from (3.12) we find that the contribution to the speed of the cline of the type-dependence variance of dispersal is

$$c_V = -\frac{\Delta_V}{4}\frac{\int_{-\infty}^{\infty}(P')^3 dz}{\int_{-\infty}^{\infty}(P')^2 dz} \approx \frac{\Delta_V}{10}\sqrt{\frac{s}{2V}}. \tag{3.15}$$

Thus, the cline moves to the right towards the genotype with smaller variance of dispersal ($P(-\infty) = 1$ and $P(+\infty) = 0$). In Figure 3.1, the accuracy of the approximation leading to equation (3.15) is confirmed numerically. If Δ_V is small relative to V, simulated wave speeds are very precisely predicted by equation (3.15). For higher values of Δ_V, the induced wave speed increases slower than predicted. However, the fit is very close up to considerable deviations in the variances of dispersal; prediction and simulation start to diverge by more than 5% only around $d_V \approx 0.1\,V$ for the parameters studied here.

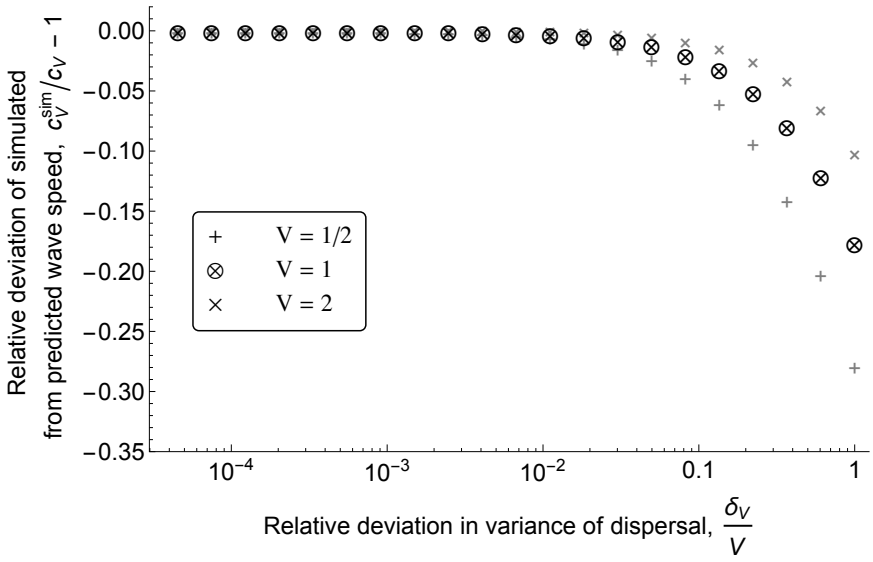

Figure 3.1: Wave speed induced by deviations in the variance of dispersal. Equation (3.11) was simulated with $M_1 = M_2 = \Delta_M = 0$, $s = 1$, and $\hat{p} = 1/2$. The simulation was initialized at $t = 0$ with the solution of equation (3.11) for type-independent dispersal, i.e., by $\tilde{p}(x, 0)$ as in equation (3.14) for $\Delta_M = 0$, and stopped at $t = 60$. Assuming that the solution closely approaches a stable wave form within the first 50 time units (confirmed numerically), the displacement of the solution in the last ten time units (between $t = 50$ and $t = 60$) was used to calculate its wave speed c_V induced by positive Δ_V. The relative deviation of the simulated wave speed c_V^{sim} from the predicted c_V in equation (3.15) is evaluated for various values of Δ_V/V. This is done for $V = 1$ ($\otimes$), $V = 1/2$ ($+$), and $V = 2$ ($\times$). Clearly, small values of Δ_V/V lead to a good fit between the simulation and the analytic prediction.

3.5.6 Discussion

In nature, dispersal properties can vary between individuals even of the same population. There are documented cases in which either the capacity to disperse is variable itself, or systematic differences in dispersal direction are observable (Edelaar and Bolnick, 2012). Classical mathematical models of evolution in spatially extended populations however predominantly assume homogeneous dispersal properties (we refer to classical work by Fisher (1937); Bazykin (1969); Slatkin (1973); Nagylaki (1975); Barton (1979) for the type of models treated in this chapter).

Here, we consider a population with two different dispersal types that may also differ in fitness. The assumption of complete linkage is justified if either a single locus pleiotropically determines fitness and dispersal at the same time, or if recombination between the fitness and the dispersal genes is sufficiently unlikely. The other extreme, a dispersal trait that is completely unlinked from any fitness-related genes, is typically studied in the context of dispersal evolution (Ronce, 2007). Here, we employed a continuous diffusion model, equation (3.11), to investigate the effect of type-dependent dispersal on gene frequency clines. We considered two genotypes that may differ in their fitness, their variance of dispersal (dispersal propensity), and in their mean displacement (directional dispersal bias).

If there is a cline solution to our model, equation (3.11), we derived a general formula for the wave speed, equation (3.12), given implicitly in terms of the cline solution. It allows us to decompose the total speed of the cline (c) into individual components due to selection (c_S), differences in the variance of dispersal (c_V), and differences in the mean displacement (c_M). While c_S is a well-known result, the components c_V and c_M are new and quantify the relative contributions of selection, variance of dispersal, and mean displacement to the speed of a cline.

Type-dependent mean displacement alone (i.e., $V_1 - V_2 = \Delta_V = 0$) as introduced in this model does not break the asymmetry in the solutions of the model equations (3.11). Thus, the equations can still be solved relatively easily whenever the choice of the local selection function F permits. Notably, even without selection, there may be cline solutions that are maintained solely by type-dependent dispersal (see Section 3.5.4). Intuitively, if the two genotypes have a tendency to move away from

each other, i.e., their directional dispersal bias points in the direction of the half-plane where they are predominantly present, complete mixing between the types is prevented.

In hybrid zones, selection against heterozygotes is known to maintain genotype frequency clines (Bazykin, 1969). These clines can – at least in the simplest cases – be calculated analytically and have proven to be of practical importance in biocontrol to predict rates of spatial spread, local introduction numbers necessary to initialize spatial spread, and sufficient environmental conditions that interrupt spatial spread (Barton and Turelli, 2011). For the case that only the mean displacement is type-dependent, we generalized the known cline solution to type-dependent dispersal (equation (3.14)).

Type-dependent variance of dispersal disrupts the symmetry in the solutions of the selection-dispersal model (3.11) and consequently makes analytic solutions intractable. Thus, we employed a perturbation argument assuming that the difference in the variance of dispersal values (Δ_V) is small. This allows us to derive a prediction for the wave speed induced by Δ_V, equation (3.15), that should be accurate at least for small values of $|\Delta_V|$. Numerical simulations, however, show that the validity of the approximation is surprisingly broad; for the studied parameter ranges, noticeable deviations from the predicted wave speed only start to appear if Δ_V/V exceeds 10%, see Figure 3.1.

The variance of dispersal can be interpreted as the mobility of a genotype. Thus, the result above – and more generally the formula for c_V in equation (3.12) – shows that more mobile types push back less mobile ones. It is interesting to interpret this in the light of the evolution of dispersal strategies, as we have a case in which increased dispersal spreads through the population even in the absence of the classic factors of dispersal evolution, i.e., any kind of spatio-temporal habitat variability, explicit relatedness structure, or inbreeding effect. Instead, selection maintains heterogeneities in the spatial genotype frequency profile, which has been shown to be sufficient to create selection for elevated dispersal, see Section 3.3.3. According to equation (3.7), the rate of increase of a dispersal type with elevated variance of dispersal is $\Delta_V/2 \times \int_{\mathbb{R}} (\partial_x p)^2 dx$. Inserting the unperturbed cline solution for type-independent dispersal yields $c_V \approx \Delta_V \sqrt{s/2V}/6$. Hence, the order of magnitude of c_V and its dependence on the parameters s and V agree with our equation (3.15), even though the

two models are different.

Throughout this section, we assumed that population density is spatially and temporally constant. This is a common assumption in population genetics, but in the case of type-dependent dispersal it is even more of an abstraction. Areas in which more mobile types are located will experience an excess of emigration and hence will be underpopulated relative to areas where slow dispersers are abundant. Hence, population density is bound to fluctuate in time, heterogeneously over space, as a consequence of type-dependent dispersal. However, constant population densities can be justified if the differences in dispersal strategies between genotypes are small (see Section 3.2), or if there is an external population regulation mechanism, for example, a limited number of nesting places available to a large progeny each generation. To incorporate a dynamic response of population density to the heterogeneities in dispersal strategies of the population, one has to include an ecological layer into the model, i.e., consider equation (3.2a). Moving clines are known to speed up when moving down population density gradients and thus can be trapped in population sinks (Barton and Turelli, 2011). However, since population density itself changes with the changing genetic composition of the population with type-dependent dispersal, even such simple qualitative predictions will be hard to establish for a joint ecological-evolutionary selection-dispersal model.

4 Multivariate Quantitative Genetics

The goal of my work on multivariate quantitative genetics is understanding the evolution of genetic variation in phenotypic traits in natural (haploid) populations, which entails the consideration of multiple traits and variable selection. This task is challenging and requires a solid understanding of multiple traits under constant selection first. As such, much of the content of this chapter does not consider fluctuating selection explicitly. In Section 4.4, however, I explain how to extend our model to fluctuating selection, and how it may provide a basic framework to include temporal variation in selection.

4.1 Why multivariate stabilizing selection?

4.1.1 Quantitative traits and genetic variance

Quantitative genetics is concerned with the inheritance of genetically complex traits, i.e., characteristics that are influenced by many genes. We consider quantitative traits that can, in principle, assume a continuum of values. Examples may be the milk yield of cows, expression levels of genes, migratory behaviour of birds, or individual body size. Even if only a moderate number of genes are involved in determining the quantitative trait, the much larger number of possible gene combinations typically gives rise to a seemingly continuous distribution of possible trait values.

The phenotype of an individual is determined by genetic and non-genetic contributions, see Falconer and Mackay (1995). Accordingly, one partitions the phenotypic

value P into two independent components: the genetic component G, and the environmental component E, i.e., $P = G + E$. The environmental component can be seen as the extent to which genetically identical individuals differ from each other; it should not be confused with the effects of changing environments that are the theme of this thesis. The genetic component G can be further broken up as $G = A + D + I$. The first contribution, A, is the breeding value, defined as the sum of (additive) contributions of each gene to the trait. The second, D, contains contributions due to dominance between homologous alleles in diploids, and I comprises epistatic interactions between genes at different loci. These components are defined so that they are statistically independent. Accordingly, the variance of the trait can be partitioned into the contributions of the different components as $V_P = V_A + V_D + V_I + V_E$ In principle, all these variance components can be measured by comparing the phenotypic values of relatives (Barton *et al.* (2007), Ch.14); in practice, they are difficult to estimate.

The proportion of the phenotypic variance that is due to additive genetic effects is called the (narrow-sense) heritability $h^2 = V_A/V_P$ (Falconer and Mackay, 1995). This dimensionless quantity can be interpreted as the slope of the regression of trait values from parent to offspring. Therefore, it can be quantified relatively easily, which makes it a convenient measure of the genetic variance in natural populations.

On a population level, quantitative traits very often exhibit abundant heritable variation. This can be seen directly, because close relatives are more similar than more distantly related individuals. More indirect evidence comes from the sustained response of trait means to artificial selection (Barton and Keightley, 2002). Estimates of the heritabilities h^2 over a wide range of traits indicate that h^2 typically takes values between 0.2 and 0.6 (Lynch and Walsh, 1998).

The genetic variance of quantitative traits is a fundamental concept for the evolution of quantitative traits. Crucially, the response to selection, i.e., the change in the trait mean between generations, is proportional to the genetic variance of the trait (the breeder's equation, Lush, 1937). Sustained selection fixes allelic variants and thereby depletes genetic variation; hence, the (additive) genetic variance can be seen as the fuel of adaptation. Genetic variation thus plays a central role for the evolvability of phenotypic traits, and its evolution is tightly linked to changes in the strength, direction,

and pattern of natural selection. For most traits, the genetic variance can mainly be ascribed to the additive effects of separate genes (Hill *et al.*, 2008), such that V_D and V_I are typically neglected in theoretical investigations. Therefore, V_G and V_A are used interchangeably in this chapter.

4.1.2 Mutations, genetic drift, and stabilizing selection

Mutations are the ultimate source of genetic variation. The increase of the heritability h^2 due to mutation is typically measured in terms of the mutational heritability $h^2_M = V_M/V_E$, where V_M is simply the sum of the square of effects of all mutations that occurred in one generation. Similarly to h^2, the values of h^2_M are also remarkably consistent across many traits and organisms, approximately between 0.001 and 0.01 (Lynch and Walsh (1998), Ch.II.12). In comparison, mutation rates μ_i per gene or per locus are relatively low ($\sim 10^{-5}$ and $\sim 10^{-9}$, respectively). Therefore, to obtain the observed values for h^2_M, mutations must either have large effects, or very many loci must influence the trait such that the overall mutation rate U on the trait (i.e., the expected number of mutations affecting the trait per generation) is high (Turelli, 1984).

Random genetic drift is known to decrease variation within populations. According to the Wright-Fisher model of a finite population of N haploid individuals, the genetic variance is reduced by a factor of $(1 - 1/N)$ each generation (see Barton *et al.*, 2007, Ch.15, Box 15.1). Under the influence of mutation and genetic drift, the additive genetic variance in the next generation, V_A^{t+1}, can thus be calculated from its value in the previous generation V_A^t as

$$V_A^{t+1} = V_A^t \left(1 - \frac{1}{N}\right) + V_M.$$

At equilibrium, when $V_A^{t+1} = V_A^t = \hat{V}_A$, we then have

$$\hat{V}_A = NV_M = NU\,\mathbb{E}[\alpha^2], \tag{4.1}$$

(c.f. Lynch and Hill, 1986) where U is the number of mutations per generation that affect the trait (as above), and $\mathbb{E}[\alpha^2]$ denotes the mean square effect of a mutation on the trait (i.e., the expected contribution to the trait variance per mutation). This

formula represents our expectation of the genetic variance in the balance of mutation and genetic drift when the system is in a stationary state. Since (constant) selection reduces genetic variation in the long run (c.f. Section 1.3 and Appendix A3), it sets an upper limit to the long-term genetic variation in the presence of selection.

Selection is believed to be stabilizing for most traits, i.e., there is an optimal trait value conferring highest fitness, and fitness is reduced for individuals deviating from that optimum. Heuristic evidence for the prevalence of stabilizing selection comes from the apparent long-term stasis of many phenotypic characters (e.g. Gould and Eldredge, 1977; Jackson and Cheetham, 1999), and from the observation that extreme phenotypes typically have reduced fitness. Actually determining the mode of selection on particular traits, let alone measuring its strength, is challenging. Regressing phenotype on fitness, one may measure linear gradients of directional selection (typically denoted by β, see also Section 4.4), and quadratic selection gradients indicating whether selection prefers intermediates (stabilizing selection, negative quadratic selection gradient) or extremes (disruptive selection, positive quadratic selection gradient). The most well-known survey of selection gradients in the published literature, Kingsolver *et al.* (2001), indicates that stabilizing selection of reasonable strength is at least not uncommon in nature. Such data, however, have to be regarded with suspicion, since constraints in adaptation, selection on trait combinations, or fluctuating selection may mask the true mode of selection on quantitative traits. The apparent discrepancy between stabilizing selection being widely anticipated, yet empirically underrepresented, is still subject to debate (Kingsolver *et al.*, 2012).

The strength of stabilizing selection is described by the selection variance V_S that scales the fitness reduction when deviating from the optimum, see Barton *et al.* (2007), Ch.18. A typical choice for V_S was proposed by Turelli (1984) as $V_S/V_E \approx 20$, which is still widely used for reference. In mathematical models of (quadratic) stabilizing selection, the strength of stabilizing selection is given by the selection intensity S, which is the curvature of fitness as a function of trait value at the trait optimum. It relates to the selection variance as $S = 1/V_S$.

Ignoring random genetic drift (i.e., considering a sufficiently large population), Turelli (1984) showed that the genetic variance V_G in the balance between mutation and sta-

bilizing selection is given by twice the product of mutation rate times the selection variance,

$$\hat{V}_A = 2UV_S = \frac{2U}{S}. \tag{4.2}$$

(This assumes a certain model of mutation, the house-of-cards model, but I do not go into details here.) Note that we consider haploid organisms here, hence equation (4.2) differs from the classical expression by a factor of two. Furthermore, it is interesting that the prediction is independent of the actual effects of mutations on the trait. These cancel out, because larger effects influence the genetic variance more, yet also cause larger deviations from the optimum and thus are eliminated by selection more readily. This is consistent with the load argument by Haldane (1937).

4.1.3 The relevance of pleiotropy

We may apply the above parameter estimates to a rough back-of-the-envelope calculation. Take a reasonable heritability of $h^2 = 0.5$, so that $V_E = V_A (= V_G)$, and assume stabilizing selection with intensity $V_S = 20V_E$. Inserting into equation (4.2), we require a total mutation rate of $U = 0.025$ to reconcile these values. With our current estimates of mutation rates per gene (around 10^{-5}), we may thus conclude that the trait is determined by at least a few thousand genes (Johnson and Barton, 2005). While this is no reason for discomposure by itself, it raises the question of how many traits may be encoded independently on any finite genome. For example, the human genome is currently estimated to contain merely around $20,000$ genes. However, as noted by Johnson and Barton (2005), any living organism is made up of a myriad of traits, hence there is simply not enough space to put all traits on the genome separately. As a consequence, individual genes affect multiple traits and thus also experience stronger selective pressures; under simple mathematical models (c.f. Johnson and Barton, 2005), this reduces the genetic variance of each trait. Thus, it is hard to explain observed levels of genetic variance due to a balance of mutation and stabilizing selection on many traits.

Our observations allow for two conclusions: quantitative traits will typically overlap in their genetic basis, and other factors not considered in our simple models increase genetic variation and thus distort our estimates. As argued in Section 1.3, spatio-

temporal variation increases genetic variation, thus perturbing our simple estimate. However, even if our predictions were off by one or two orders of magnitude, the problem would persist: Assuming that determining a trait takes only a few tens or hundreds of genes still does not seem to allow for an independent genetic encoding of all traits necessary to describe a functional organism. Hence, pleiotropy – i.e., individual genes affecting multiple traits simultaneously – must be pervasive.

Phenotypic traits are thus connected via the genes that pleiotropically determine them. The size and structure of such trait clusters, however, remains unknown. How big are they, how strongly are they linked, and how does selection on the individual traits combine to selection on the underlying genes? More concretely, we may ask: How is the genetic variance of a given (focal) trait influenced by selection acting independently on pleiotropically connected background traits? The answers to those questions depend on the correlation structure between traits that may be due to correlations in the effects of genes on the traits (pleiotropic structure; correlations in allelic effects), and due to selection acting on combinations of traits rather than on traits individually (trade-off; correlations in selection). Understanding these basic structural problems are a first step towards an understanding of the dynamic processes of multivariate quantitative genetics, which may then be extended by temporally fluctuating and spatially heterogeneous selection.

4.2 Multivariate QG as a fluctuating selection process

4.2.1 Notation and setting

Multivariate quantitative genetic models were introduced by Lande (1980) in a statistical (macroscopic) model assuming Gaussian allelic effects. The multivariate house-of-cards model by Turelli (1985) takes into account genetic (microscopic) details of the trait architecture and leads to different conclusions. These classical models can be seen as two extreme cases with other quantitative genetic models in between (Slatkin and Frank, 1990). The model presented here is similar to a more recent approach by Zhang and Hill (2003) and allows to determine the variances of allele frequencies underlying the traits. Integrating the allele frequency variances over their allelic effect

distribution, we obtain an expression for the expected genetic variances of any number of traits themselves. Even though we assume selection and the trait distributions to be Gaussian, we need to overcome two main difficulties: First, the distribution of allele frequencies is complicated and hard to determine explicitly. Second, the integrals emerging in the expression for the expected genetic variances are intricate and can be resolved only numerically in most cases.

Consider a randomly mating population of N haploid individuals. We study the dynamics of K quantitative traits that are determined pleiotropically by (effectively infinitely) many loci, $n \gg 1$. The allelic effects on the traits are assumed to be additive, i.e., the contributions of two genes to any trait simply add up; there are no epistatic interactions between loci. Furthermore, we assume that recombination is strong relative to the other processes, so that the loci are in linkage equilibrium and it suffices to consider the allele frequencies at each locus to describe the microscopic dynamics underlying the traits.

We consider the regime of very low per-locus mutation rates (the weak-mutation limit, $\mu \ll 1$) so that we may assume that every locus is affected by mutation at most once in the time scale of interest. With very many loci, but very rare mutations, we assume that the actual number of new mutations occurring in a generation is Poisson distributed. To obtain the mean of this distribution, fix the genome-wide mutation rate $U = n\mu$ and let $n \to \infty$; consequently, $\mu \to 0$. Thus, each generation, U loci become polymorphic on average, which is eventually balanced by polymorphic loci fixing for either of the two alleles (the population is finite). Consequently, only finitely many loci are polymorphic at any point in time.

In this section, we scale the system so that the ancestral states (Q_i) of each locus has zero contribution to all traits; once a locus is affected by mutation, we draw the effects on the K traits of the new allele (P_i) from a K-variate distribution, which is the same for all loci. We denote the allelic effect of allele i on trait γ by $\alpha_{i\gamma}$, and collect the allelic effect of a given allele i on all K traits in the vector $\boldsymbol{\alpha}_i = (\alpha_{i1}, ..., \alpha_{iK})$. Between different mutations, allelic effects are drawn independently from each other (thus cov$(\alpha_{i\gamma}, \alpha_{j\gamma}) = 0$ for $i \neq j$). There may, however, be correlations between the effects on different traits (i.e., cov$(\alpha_{i\gamma}, \alpha_{i\lambda}) \neq 0$ for $\gamma \neq \lambda$). These correlations in allelic

effects describe the genetic structure of pleiotropy.

We further assume that the effects on each trait are distributed symmetrically around zero, i.e., $\mathbb{E}^{(i)}[\alpha_{i\gamma}] = 0$ for every trait $\gamma = 1, ..., K$, where the expectation $\mathbb{E}^{(i)}$ is taken across loci. The pleiotropic structure may be represented by the variance-covariance matrix of allelic effects $\boldsymbol{M}$ given by $M_{\gamma\lambda} = \mathbb{E}^{(i)}[\alpha_{i\gamma}\alpha_{i\lambda}]$. The mean contribution of mutation to the genetic variance of trait γ each generation is then $V_{M,\gamma} = U\,\mathbb{E}^{(i)}[\alpha_{i\gamma}^2] = U\,\sigma_{M,\gamma}^2$, so that the expectation of the square of effects $\mathbb{E}^{(i)}[\alpha_{i\gamma}^2]$ equals the variance of allelic effects $\sigma_{M,\gamma}^2$ on the trait.

With at most two alleles per locus, the ancestral state Q_i and the derived (mutated) allele P_i, we denote the frequency of allele P_i by p_i, and the frequency of allele Q_i by $q_i = 1 - p_i$. For a given genotype, let X_i be the indicators for the alleles P_i, i.e., $X_i = 1$ if locus i carries allele P_i and $X_i = 0$ if it carries the allele Q_i. Clearly, $\mathbb{E}[X_i] = p_i$ and Var$[X_i] = p_i q_i$, and for different loci $i \neq j$, the indicators X_i and X_j are independent since the loci are in linkage equilibrium. As a consequence, the value of trait γ of the genotype is given by $Z_\gamma = \sum_i \alpha_{i\gamma} X_i$, and hence the means and variances of the trait distributions are given in terms of allele frequencies and allelic effects as

$$\bar{z}_\gamma = \sum_i \alpha_{i\gamma} p_i \qquad \text{and} \qquad V_\gamma = \sum_i \alpha_{i\gamma}^2 p_i q_i \qquad \text{for } \gamma = 1, ..., K, \tag{4.3}$$

and the covariances between traits values are $V_{\gamma\lambda} = \sum_i \alpha_{i\gamma}\alpha_{i\lambda} p_i q_i$. We collect these values in a vector $\bar{\boldsymbol{z}}$ of trait means, and a variance-covariance matrix $\boldsymbol{V}$ between traits. If sufficiently many alleles are contributing to the traits, we may assume that the joint distribution of the K traits is a multivariate normal distribution, $\boldsymbol{Z} \sim \mathcal{N}(\bar{\boldsymbol{z}}, \boldsymbol{V})$.

Assume that every trait γ has an optimal value θ_γ, and write $\boldsymbol{\theta} = (\theta_1, ..., \theta_K)$. To generalize models of Gaussian stabilizing selection on a single trait to multiple traits, we consider a symmetric and positive definite selection matrix $\boldsymbol{S}$ and define the fitness of an individual with trait values given by $\boldsymbol{Z} = (Z_1, ..., Z_K)$ by

$$\begin{aligned} w(\boldsymbol{Z}) &= \exp\left[-\frac{1}{2}\,(\boldsymbol{Z}-\boldsymbol{\theta})\,.\boldsymbol{S}.\,(\boldsymbol{Z}-\boldsymbol{\theta})\right] \\ &= \exp\left[-\frac{1}{2}\sum_{\gamma,\lambda=1}^{K} S_{\gamma\lambda}\,(Z_\gamma-\theta_\gamma)\,(Z_\lambda-\theta_\lambda)\right]. \end{aligned} \tag{4.4}$$

Thus, selection may act on pairs of traits via $S_{\gamma\lambda} \neq 0$, i.e., there may be correlations in selection. If $\boldsymbol{S}$ is a diagonal matrix, the fitness reduction due to the deviations from

the trait optima is multiplicative across traits. Integrating the individual fitness (4.4) over the normal distribution of trait values, $\mathcal{N}(\bar{\boldsymbol{z}}, \boldsymbol{V})$, we obtain the mean fitness of the population,

$$\bar{w} = \exp\left[-\frac{1}{2}\big((\boldsymbol{Z}-\boldsymbol{\theta}).(\boldsymbol{I}+\boldsymbol{SV})^{-1}\boldsymbol{S}.(\boldsymbol{Z}-\boldsymbol{\theta}) + \log[\det(\boldsymbol{I}+\boldsymbol{SV})]\big)\right],$$

where $\boldsymbol{I}$ is the K-dimensional unit matrix. Provided that selection is weak (i.e., all entries of $\boldsymbol{S}$ are sufficiently close to zero), we may approximate $(\boldsymbol{I}+\boldsymbol{SV})^{-1}\boldsymbol{S} \approx \boldsymbol{S}$ and $\log[\det(\boldsymbol{I}+\boldsymbol{SV})] \approx \mathrm{tr}(\boldsymbol{SV})$, where $\mathrm{tr}(\boldsymbol{SV})$ is the sum of the diagonal entries (the trace) of the matrix $\boldsymbol{SV}$. We thus obtain a general expression for the mean fitness of the population,

$$\bar{w} = \exp\left[-\frac{1}{2}\big((\bar{\boldsymbol{z}}-\boldsymbol{\theta}).\boldsymbol{S}.(\bar{\boldsymbol{z}}-\boldsymbol{\theta}) + \mathrm{tr}(\boldsymbol{SV})\big)\right]. \tag{4.5}$$

Mutations and stabilizing selection can be seen as two opposing forces acting on the distribution of traits in the K-dimensional trait space. The directions in which they most strongly inflate or depress the genetic variances is encoded in their variance-covariance matrices $\boldsymbol{M}$ and $\boldsymbol{S}$, respectively. Applying a linear transformation on the trait space, however, we may greatly simplify the problem, see also Zhang and Hill (2003): There is always a (non-singular) matrix $\boldsymbol{T}$ so that $\boldsymbol{T}^T\boldsymbol{MT} = \boldsymbol{I}$ and $\boldsymbol{T}^T\boldsymbol{ST} = \boldsymbol{D}$, where $\boldsymbol{D}$ is a diagonal matrix and $\boldsymbol{T}^T$ denotes the transpose of $\boldsymbol{T}$. Hence, a linear change of variables transforms a system of correlated selection and mutation into an uncorrelated one.

Without loss of generality, we may thus assume that selection acts only on single traits (no correlations in selection, $S_{\gamma\lambda} = 0$ for $\gamma \neq \lambda$), and that the distribution of allelic effects is spherically symmetric (no correlations in allelic effects, $\boldsymbol{M} \propto \boldsymbol{I}$). The latter implies that, to determine the allelic effects of a new mutation, $\boldsymbol{\alpha}_i$, we may first choose the direction of the effect vector by taking a vector uniformly from the K-dimensional unit sphere, and then draw the length of the vector, $|\boldsymbol{\alpha}_i|$, from some given distribution. The vector of allelic effects thus effectively depends just on a single random variable, the total allelic effect $\rho_i = |\boldsymbol{\alpha}_i| = \sqrt{\sum_{\gamma=1}^{K} \alpha_{i\gamma}^2}$ of the mutation. Any specific system with correlations in selection and mutation may be analysed by studying the uncorrelated system and applying the corresponding reverse transformation.

This observation greatly simplifies our problem, in particular since correlations between traits, $V_{\gamma\lambda}$ for $\gamma \neq \lambda$, do not play a role in the new scaling: Writing $S_\gamma = S_{\gamma\gamma}$, the mean fitness of the population, equation (4.5), is given by

$$\bar{w} = \exp\left[-\frac{1}{2}\sum_{\gamma=1}^{K} S_\gamma \left((\bar{z}_\gamma - \theta_\gamma)^2 + V_\gamma\right)\right]. \tag{4.6}$$

4.2.2 Fluctuating selection on individual genes

The ensemble of all genes determines the set of phenotypic traits, and selection on these traits translates into selection on the individual genes. At the level of a single gene P_i, selection is described exclusively by its selection coefficient s_i that depends on the genetic background of the gene (i.e., the allele frequencies at the other loci), and on how they interact with the traits. Given the great complexity of the dynamics of many alleles and multiple traits, it is hopeless to gather all the data needed to predict the dynamics of selection on any gene; the detailed process will remain obscure, with an essentially random appearance. We may, however, obtain a statistical description of the selection coefficients s_i in terms of macroscopic observables, replacing its explicit dynamics by a stochastic process of fluctuating selection. To understand the properties of the process causing the fluctuations, we first consider stabilizing selection for fixed trait optima with fixed selection intensities. For the rest of this Section 4.2, and throughout the following Section 4.3, we thus assume that the trait optima $\boldsymbol{\theta}$ and the selection intensities $\boldsymbol{S}$ are constant.

As explained in the previous section, we wish to follow the dynamics of newly arising mutations under the joint influence of weak selection and random genetic drift. Each mutation eventually either goes to fixation or is lost. Considering the collection of a class of mutations (e.g., of a given allelic effect size), we may analyse the properties of their allele frequency distributions. Then, averaging over the distributions of their allelic effects allows to calculate characteristics of the trait distributions, e.g., the genetic variances. We consider stochastic allele frequency dynamics of the form

$$dp_i = s_i\, p_i\,(1-p_i)\, dt + \sqrt{\frac{p_i\,(1-p_i)}{N}}\, dW, \tag{4.7}$$

where W is a standard Wiener process, hence the rightmost term describes the action of genetic drift. The selection coefficient of allele P_i is $s_i = \partial \log(\bar{w})/\partial p_i$. Inserting

the expressions for the trait means and variances, equation (4.3), into the mean fitness (4.6), and taking the corresponding derivative, we obtain

$$s_i = \frac{\partial \log(\bar{w})}{\partial p_i} = -\sum_{\gamma=1}^{K} S_\gamma \left[\alpha_{i\gamma} \left(\bar{z}_\gamma - \theta_\gamma \right) + \alpha_{i\gamma}^2 \left(\frac{1}{2} - p_i \right) \right]. \tag{4.8}$$

Selection on the frequency on an allele P_i thus has two components. The term $-\sum_\gamma S_\gamma \alpha_{i\gamma}^2 \left(1/2 - p_i\right)$ describes selection against variance, i.e., disruptive selection on the allelic level. It only depends on the allele frequency p_i, being negative for $p_i < 1/2$ and positive for $p_i > 1/2$. Thus, it always favours the more common allele on locus i, reducing variation at the locus. The remaining term, $-\sum_\gamma S_\gamma \alpha_{i\gamma} \left(\bar{z}_\gamma - \theta_\gamma \right)$, describes directional selection due to deviations between the trait means and their optimal values. For example, if the mean of trait γ is above its optimum, $\bar{z}_\gamma > \theta_\gamma$, there is a negative contribution to the selection coefficient on an allele with positive effect $\alpha_{i\gamma} > 0$ on the trait. The directional selection component contains the allele frequencies at all loci within the trait means $\bar{z}_\gamma$ and thus couples the dynamics of allele frequencies at the different loci.

In the classical quantitative genetics of a single trait, selection efficiently maintains the trait mean close to its optimum such that the directional selection component can be neglected (Bulmer, 1972; Barton, 1989). As a consequence, the equations for the allele frequencies decouple and the system becomes analytically tractable. With multiple traits involved, the situation is less clear; in principle, the joint action of stabilizing selection on many traits might prevent all trait means to adjust to their optima simultaneously, or at least may require relatively strong selection intensities for doing so. If the latter is the case, one could speculate that the effects of selection per trait add up to a perceivably high directional selection component. Furthermore, when the trait optima change over time, there must be a lag between trait means and optima, giving rise to noticeable directional selection. These considerations motivate a more detailed study of the directional component of stabilizing selection.

4.2.3 The directional selection component as a random process

Since we consider constant trait optima, we may rescale $\boldsymbol{\theta} \equiv 0$ without loss of generality. Furthermore, assume for simplicity that the intensity of selection is the same

on all traits, i.e., $S_\gamma \equiv S$ for all $\gamma = 1, ..., K$. The directional selection component of stabilizing selection is a linear combination of the mean trait values $\bar{z}_\gamma$ ($\gamma = 1, ..., K$), whose coefficients are given by S times the effects of the allele under consideration, $\boldsymbol{\alpha}_i$.

For the moment, consider a single trait with trait mean $\bar{z}$ and a genetic variance of V_G. Averaging over the genetic details, the dynamics of the trait mean are well-described by an Ornstein-Uhlenbeck process (Lande, 1976), i.e., they satisfy a process of the form

$$d\bar{z} = -\vartheta\, \bar{z}\, dt + \sigma\, dW, \tag{4.9}$$

where W is a standard Wiener process. The rate of return of $\bar{z}$ to its long-term mean $\theta = 0$ is given by $\vartheta = S\, V_G$. This is just the rate of response of a trait under directional selection (c.f. the breeder's equation, Lush, 1937). The random fluctuations in the trait mean have a variance of $\sigma^2 = V_G/N$. The stationary distribution of such an Ornstein-Uhlenbeck process is a Gaussian distribution centred around $\theta = 0$ with variance $\sigma^2/(2\vartheta) = 1/(2NS)$.

If there are multiple traits with $S_\gamma \equiv S$ and no correlations between traits, we may heuristically extrapolate from the behaviour of a single trait. Dropping the index i denoting the locus, and writing $\zeta = S \sum_\gamma \alpha_\gamma \bar{z}_\gamma$ for the directional selection component, ζ is a linear combination of Ornstein-Uhlenbeck processes. Assuming their random components to be uncorrelated, ζ itself satisfies an Ornstein-Uhlenbeck process,

$$d\zeta = -\vartheta\, \zeta\, dt + \sigma S \rho_i\, dW, \tag{4.10}$$

where $\rho_i = \sqrt{\sum_\gamma \alpha_{i\gamma}^2}$ is the total allelic effect of the allele P_i under consideration (see also Section 4.2.1). The long-term variance of ζ at stationarity is given by

$$\sigma_\zeta^2 = \frac{(\sigma S \rho_i)^2}{2\vartheta} = \frac{S\rho_i^2}{2N}. \tag{4.11}$$

We numerically tested the Ornstein-Uhlenbeck description of the directional selection component ζ, simulating $K = 10$ traits under stabilizing selection ($S = 0.01$). In the simulation, mutations create segregating alleles that evolve under selection and genetic drift (with $N = 100$ individuals) as described above in Section 4.2.1. Figure 4.1a shows a simulated trajectory of ζ for an allelic effect vector of length $\rho_i = 1$ over 10^5

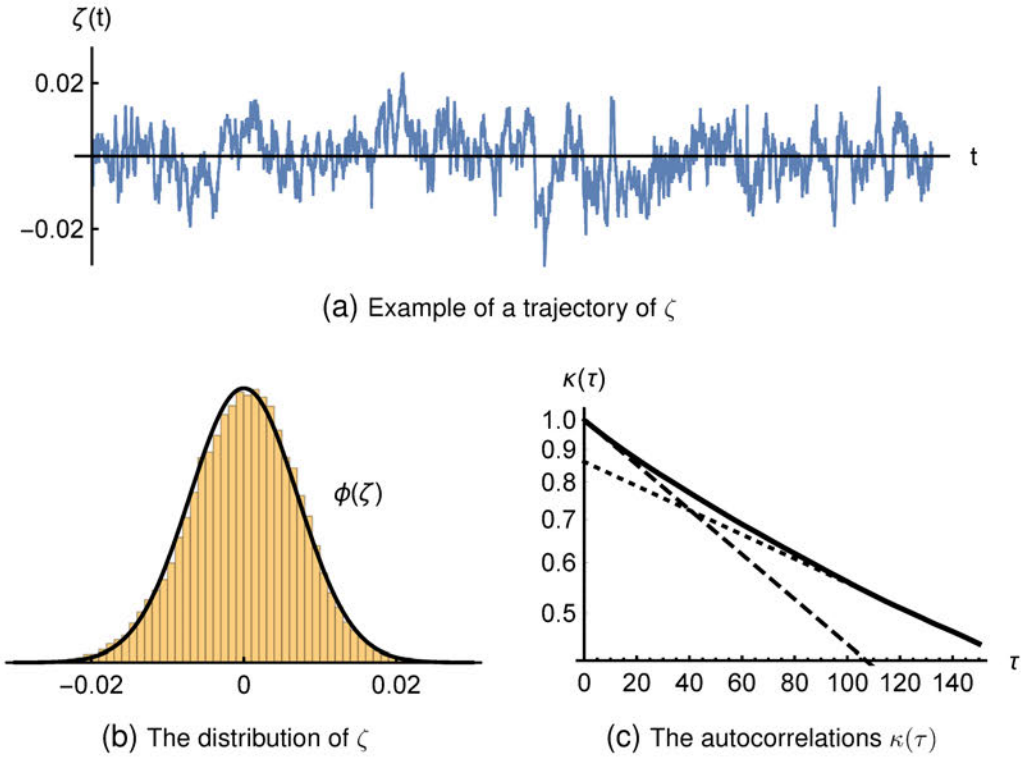

(a) Example of a trajectory of ζ

(b) The distribution of ζ

(c) The autocorrelations $\kappa(\tau)$

Figure 4.1: Dynamics of the directional selection component ζ. We simulated $K = 10$ quantitative traits under stabilizing selection ($S_\gamma \equiv 0.01$) in a finite population ($N = 100$ individuals). The number of mutations in each generation is drawn randomly with mean $NU = 10$. Each mutation occurs on a locus that has not been affected by mutation before, and the new allele evolves under selection and random drift. The allelic effect of the new allele is chosen randomly from a spherically symmetric distribution with exponentially distributed radius ρ with mean $\mathbb{E}[\rho] = 1$. For a given allele with allelic effects $\boldsymbol{\alpha} = 1/7 \times (3, -3, 2, 1, -2, 3, 1, -2, -2, 2)$, we calculate the directional selection component $\zeta = S\,\boldsymbol{\alpha}.\bar{\boldsymbol{z}}$ for each generation. As the underlying allele frequencies change dynamically over time, the trait means evolve and ζ fluctuates as depicted in panel (a). Its stationary distribution $\phi(\zeta)$ is well approximated by a normal distribution with zero mean and variance $S\rho^2/(2N) = 5 \times 10^{-5}$, see panel (b). The temporal autocorrelation function $\kappa(\tau) = \mathrm{corr}[\zeta(t), \zeta(t+\tau)]$ is shown in panel (c). Its initial slope is well predicted by $\vartheta = SV_G \approx 0.008$ (dashed line), where we estimated V_G from the simulation data by averaging over the genetic variances of all traits. For larger τ, however, the autocorrelations decay more slowly, approaching a rate of decay of about 0.004 (dotted line).

generations (c.f. the figure caption for parameter details). The distribution of these values, shown in Figure 4.1b, closely matches a normal distribution with zero mean and variance $\sigma_\zeta^2 = 5 \times 10^{-5}$, as predicted from the stationary state of the Ornstein-Uhlenbeck characterisation (4.10).

Nevertheless, describing the directional selection component ζ by an Ornstein-Uhlenbeck process is an approximation, which becomes evident from looking at temporal autocorrelations, $\kappa(\tau) = \mathrm{corr}[\zeta(t), \zeta(t+\tau)]$. For an Ornstein-Uhlenbeck process, these autocorrelations decay exponentially at rate ϑ. Measuring the mean genetic variance through all $K = 10$ simulated traits leads to an accurate estimate of the initial slope in the autocorrelation function of the simulated values of ζ, compare the solid and dashed lines in Figure 4.1c. However, the decay of the autocorrelations in the simulated process is slower, i.e., the actual process has a longer memory than predicted; in the long run, the decay of the autocorrelation function $\kappa(\tau)$ tends to a different exponential at a considerably lower rate, shown by the dotted line in Figure 4.1c. Numerical analyses indicate that this is partially due to fluctuations in the genetic variances. Their dynamics typically exhibit pronounced spikes as alleles of major effect rise to intermediate frequencies; hence, their mean might be higher than "typical" values, which leads to an overestimate in the initial rate of decay of the autocorrelations in ζ. Furthermore, the random components of the Ornstein-Uhlenbeck processes for the individual trait means, see equation (4.9), are not uncorrelated since they are ascribed to the dynamics of alleles that pleiotropically affect multiple traits. Thus, pleiotropy itself leads to deviations between simulated realizations of ζ and their statistical description by equation (4.10).

Given that the stationary distribution of ζ is well approximated by a Gaussian with variance σ_ζ^2 (see equation (4.11)), characteristic magnitudes of the directional selection component are given by its standard deviation $\sigma_\zeta = \sqrt{S\rho_i/(2N)}$ (since $\mathbb{E}[|\zeta|] = \sqrt{2/\pi}\,\sigma_\zeta \approx \sigma_\zeta$). From the selection coefficient of allele P_i, equation (4.8), we see that the strength of selection against variance is about $S\rho_i^2/2$, at least at low allele frequencies. Furthermore, the strength of genetic drift is $1/N$ in haploid populations. Putting these three forces into relation gives

$$\begin{bmatrix} \text{directional} \\ \text{selection} \end{bmatrix} : \begin{bmatrix} \text{sel. against} \\ \text{variance} \end{bmatrix} : \begin{bmatrix} \text{random} \\ \text{drift} \end{bmatrix} = \sqrt{\frac{NS\rho_i^2}{2}} : \frac{NS\rho_i^2}{2} : 1.$$

If selection on the allele is weak, $NS\rho_i^2/2 \ll 1$, then $\frac{NS\rho_i^2}{2} \ll \sqrt{\frac{NS\rho_i^2}{2}} \ll 1$ and genetic drift dominates the dynamics of allele frequencies. If, conversely, selection on the allele is strong, $NS\rho_i^2/2 \gg 1$, then $1 \ll \sqrt{\frac{NS\rho_i^2}{2}} \ll \frac{NS\rho_i^2}{2}$ and selection against variance is the driving force of the dynamics. In both cases, the directional selection component only plays a subordinate role.

If $NS\rho_i^2/2 \approx 1$, the factors genetic drift, directional selection, and selection against variance can be expected to contribute equally to the dynamics of allele frequencies. In this case, statistics of single allele frequency trajectories, e.g., fixation probabilities or sojourn times, can be very different compared to the extreme cases when directional selection can be ignored. When considering the expected genetic variance of quantitative traits, however, simulations show that the directional selection component does not have an impact. Intuitively, this is because averages are taken across time and allelic effect distributions, such that the effect of directional selection balances out. We study this in more detail in the following Section 4.3. Fluctuating stabilizing selection, i.e., trait optima changing in time, may systematically introduce considerable directional selection. This goes beyond the analysis of the next section and remains to be studied in detail; the next steps in this endeavour are outlined in Section 4.4.

4.3 The stationary distribution approach

4.3.1 Adjusting the model framework

In this section, we derive a formula for the expected genetic variances of multiple phenotypic traits, each being under stabilizing selection and being determined pleiotropically by the underlying genes. The procedure is analogous to the traditional approach demonstrated by Keightley and Hill (1989) that calculates the expected genetic variance assuming that the dynamics has reached a stationary state (the statistical balance between mutation, selection, and drift), using the stationary distribution of allele

frequencies. To do the same, we slightly adjust the framework of our model, thereby obtaining a symmetric distribution of allele frequencies.

More precisely, we modify the notation introduced in Section 4.2.1 as follows. We assume that there is a fixed number of n loci that pleiotropically determine the K traits. Each trait γ is under stabilizing selection with selection intensity $S_\gamma > 0$ for the optimal value $\theta_\gamma = 0$ (without loss of generality). There are two alleles per locus i that have allelic effects $\pm\alpha_{i\gamma}/2$ on trait $\gamma \in \{1, ..., K\}$. These are chosen independently between loci and traits. Furthermore, we assume symmetric mutation from one allele to the other at rate μ.

In analogy to the previous section, we think of very many loci, $n \gg 1$, with very low per-locus mutation rate, $\mu \ll 1$, and a given genome-wide mutation rate $n\mu = U$. The new scaling of the allelic effects maintains the difference in the effects of the two alleles at each locus. Thus, it shifts the trait means, yet leaves the trait variances the same, i.e.,

$$\bar{z}_\gamma = \sum_i \alpha_{i\gamma}\left(p_i - \frac{1}{2}\right) \qquad \text{and} \qquad V_\gamma = \sum_i \alpha_{i\gamma}^2 p_i q_i \qquad \text{for } \gamma = 1, ..., K, \tag{4.12}$$

compare equation (4.3). Going through the procedure outlined in Section 4.2.2 to calculate the selection coefficient s_i for the allele P_i shows that the dynamics of allele frequencies remain unchanged in the modified framework.

Our modifications represent a different way of looking the same problem. They simply correspond to shifting the scale of allelic effects or, equivalently, exchanging the labels of the two alleles at every other locus (hence dropping the notion of ancestral and derived alleles). As a consequence, the stationary distribution of allele frequencies at every locus becomes symmetric. In the framework of the previous section, mutations only create P alleles from Q alleles, hence the distribution of allele frequencies in the balance of mutation, selection, and genetic drift is asymmetric, approximately inversely proportional to the P-allele frequency, $\sim p^{-1}$, see Figure 4.2a. With the new setting, the distribution is symmetric, since about half of the loci will mostly carry the P allele, and the other half the Q allele, with occasional flips between those states, see Figure 4.2b.

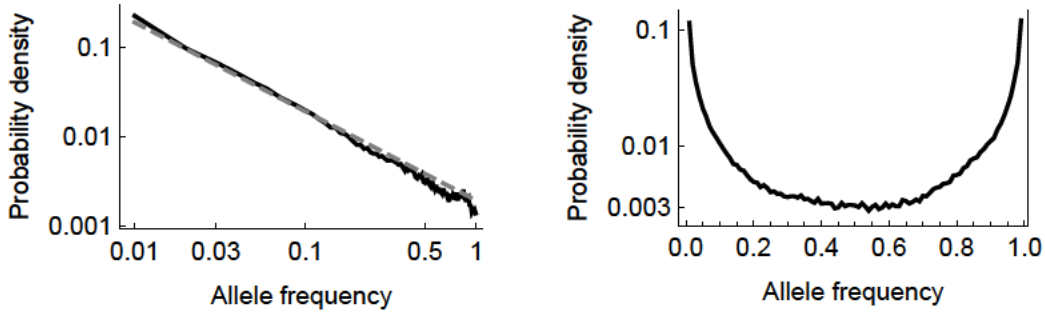

(a) Asymmetric case (b) Symmetric case

Figure 4.2: Allele frequency distributions in the asymmetric and the symmetric case. Panel (a) shows the distribution of allele frequencies in our simulations of the model described in Section 4.2; the data is the same as in Figure 4.1. New alleles are always generated at low frequency and only very few of them reach high frequencies and fix, such that their distribution is shaped approximately as p^{-1} (grey dashed line). (b) Symmetrizing the system as described in this section leads to a U-shaped distribution, because P and Q alleles are created by mutation at the same rate and thus probability mass is generated at both boundaries of the state space, $p = 0$ and $p = 1$.

4.3.2 Genetic variances at the stationary distribution

Stationary distributions. According to the classical diffusion approach, the joint stationary distribution of allele frequencies in the balance of mutation, selection, and drift in a haploid population is given by

$$\Phi(p_1, ..., p_n) = \frac{1}{Z}\, \bar{w}^{2N} \prod_{i=1}^{n} (p_i q_i)^{2N\mu - 1}, \tag{4.13}$$

where Z normalizes Φ to a probability distribution (Kimura, 1955, 1964). Inserting the mean fitness $\bar{w}$ from equation (4.6) with $\boldsymbol{\theta} \equiv 0$, and the trait means and variances from equation (4.12), we obtain

$$\Phi(p_1, ..., p_n) \propto \exp\left[-\sum_{\gamma} NS_\gamma \left(\left(\sum_i \alpha_{i\gamma} \left(p_i - \frac{1}{2} \right) \right)^2 + \sum_i \alpha_{i\gamma}^2 p_i q_i \right) \right] \prod_i (p_i q_i)^{2N\mu - 1}. \tag{4.14}$$

Using this stationary distribution, the genetic variance of trait γ is given by

$$\mathbb{E}[V_\gamma] = \mathbb{E}\left[\sum_{i=1}^{n} \alpha_{i\gamma}^2 p_i q_i \right] = \sum_{i=1}^{n} \alpha_{i\gamma}^2 \int_0^1 p_i q_i\, \Phi(p_1, ..., p_n)\, dp_1 \cdots dp_n.$$

Evaluating this integral without further assumptions is challenging (see Barton (1989) for the case of a single trait and equal allelic effects). However, following Bulmer

(1972), we argue that with many loci ($n \gg 1$) the expected genetic variance of trait γ is well approximated by

$$\mathbb{E}[V_\gamma] = \sum_{i=1}^{n} \alpha_{i\gamma}^2 \int_0^1 p_i q_i \, \phi_i(p_i) \, dp_i, \tag{4.15}$$

with the distributions

$$\phi_i(p_i) \propto \exp\left[-\sum_\gamma N S_\gamma \alpha_{i\gamma}^2 \, p_i q_i \right] (p_i q_i)^{2N\mu - 1}. \tag{4.16}$$

To see this, define

$$X_\gamma = \sum_i \alpha_{i\gamma} \left(p_i - \frac{1}{2} \right) \qquad \text{and} \qquad Y_\gamma = \sum_i \alpha_{i\gamma}^2 p_i q_i,$$

and assume that the allele frequencies p_i are independently distributed with density ϕ_i, equation (4.16). Because this distribution is symmetric in p_i, the random variables p_i and $p_i q_i$ are uncorrelated. Hence, also every two random variables Y_γ and X_λ are uncorrelated. Furthermore, if the number of loci is large, $n \gg 1$, the X_γ and Y_γ are approximately normally distributed (central limit theorem). Since uncorrelated normal random variables are automatically independent, every two random variables Y_γ and X_λ are independent from each other – asymptotically in the limit $n \to \infty$.

The expression (4.15) can be rewritten as an expectation of Y_γ over a joint distribution $\prod_i \phi_i(p_i)$ of independent random variables,

$$\sum_{i=1}^{n} \alpha_{i\gamma}^2 \int_0^1 p_i q_i \, \phi_i(p_i) \, dp_i = \int_0^1 \left(\sum_{i=1}^{n} \alpha_{i\gamma}^2 p_i q_i \right) \prod_{j=1}^{n} \phi_j(p_j) \, dp_1 \cdots dp_n.$$

However, since Y_γ is independent from every X_λ, the distribution of Y_γ does not change if we multiply it by a function that only depends on $X_1, ..., X_K$. Therefore, the above integral remains unchanged if we replace $\prod_j \phi_j(p_j)$ by $\Phi(p_1, ..., p_n)$. Overall, this shows that

$$\sum_{i=1}^{n} \alpha_{i\gamma}^2 \int_0^1 p_i q_i \, \phi_i(p_i) \, dp_i \approx \sum_{i=1}^{n} \alpha_{i\gamma}^2 \int_0^1 p_i q_i \, \Phi(p_1, ..., p_n) \, dp_1 \cdots dp_n = \mathbb{E}[V_\gamma]$$

if the number of loci contributing to the trait is large.

Calculating the expected genetic variance. To obtain a general expression for the expected genetic variances, we need to evaluate equation (4.15). Thus, it is necessary to calculate integrals of the form

$$\mathcal{I}(A,B) = \int_0^1 e^{-Ap\,(1-p)}\,(p\,(1-p))^{B-1}\,dp = \int_0^{1/4} e^{-Ay} y^{B-1} \left(\frac{1}{4}-y\right)^{-1/2} dy.$$

In the limit of small per-locus mutation rate ($N\mu \ll 1$), we may calculate explicitly

$$\int_0^1 p_i q_i\,\phi_i(p_i)\,dp_i = \frac{\mathcal{I}\left[\sum_\gamma NS_\gamma\alpha_{i\gamma}^2,\,2N\mu+1\right]}{\mathcal{I}\left[\sum_\gamma NS_\gamma\alpha_{i\gamma}^2,\,2N\mu\right]} \approx N\mu\,H\left[\sum_\gamma NS_\gamma\alpha_{i\gamma}^2\right],$$

where

$$H(x) = e^{-x/4}\sum_{j=0}^{\infty}\frac{(x/4)^j}{(2j+1)j!}. \tag{4.17}$$

This is accurate for $\mu \to 0$. To keep the genome-wide mutation rate $U = n\mu$ constant, we simultaneously let $n \to \infty$. Then, we may replace the sum over the individual loci $i = 1, ..., n$ in equation (4.15) by an integral over the distribution of allelic effects, i.e.,

$$\sum_{i=1}^{n}\alpha_{i\gamma}^2\int_0^1 p_i q_i\,\phi_i(p_i)\,dp_i = n\int_{\mathbb{R}^K}\alpha_{i\gamma}^2\left(\int_0^1 p_i q_i\,\phi_i(p_i)\,dp_i\right) f_\alpha(\boldsymbol{\alpha})\,d\boldsymbol{\alpha},$$

where f_α is the probability density of the (K-dimensional) distribution of allelic effects. Since this distribution is the same for all loci i, we may drop the index i. In other words, instead of a given set of loci with given allelic effects, we think of a distribution over a huge number of loci, whose effect vectors have the K-variate density f_α. Inserting our approximation for the inner integral, we obtain for the expected genetic variances

$$\mathbb{E}[V_\gamma] = NU\int_{\mathbb{R}^K}\alpha_\gamma^2\,H\left[\sum_\lambda NS_\lambda\alpha_\lambda^2\right] f_\alpha(\boldsymbol{\alpha})\,d\boldsymbol{\alpha} \qquad (\gamma = 1, ..., K), \tag{4.18}$$

where the function H is defined above in equation (4.17). This formula generalizes the expected genetic variance of a single trait under stabilizing selection, see Keightley and Hill (1989), to multiple pleiotropically connected traits. To accommodate correlations in selection and mutation (non-diagonal selection matrix $\boldsymbol{S}$ and mutational effects matrix $\boldsymbol{M}$), apply a linear transformation as described in Section 4.2.1 to obtain a non-diagonal genetic variance-covariance matrix $\boldsymbol{V}$.

4.3.3 Limit cases: Neutrality, weak and strong selection

The cases of no selection and strong selection can be analysed by investigating the limiting behaviour of the function $H(x)$. It is easy to see that $H(0) = 1$, and that $H(x) \approx 2/x$ for large x. A Taylor series approximation for small x furthermore shows that $H(x) = 1 - x/6 + \mathcal{O}(x^2)$ as $x \to 0$.

Consequently, if none of the traits are under selection ($S_\gamma = 0$ for all γ), the expected genetic variances become

$$\mathbb{E}[V_\gamma] = NU\,\mathbb{E}[\alpha_\gamma^2]. \tag{4.19}$$

This is just the expected genetic variance under the balance of mutation and random genetic drift, which we derived above by a simple back-of-the-envelope calculation, see equation (4.1).

Note that, generally, stabilizing selection couples the genetic variances of the different traits via the S_γ. Neutral traits however do not affect the dynamics of pleiotropically connected traits – the neutral genetic variance above can be calculated without knowledge of background traits. Conversely, traits under selection modify the genetic variance of pleiotropically connected traits. This will be discussed in Section 4.3.4.

If the overall selection on the K traits is sufficiently weak relative to random genetic drift, i.e., $\sum_\gamma NS_\gamma\alpha_\gamma^2 \ll 1$, we approximate

$$H\left[\sum_\gamma NS_\gamma\alpha_\gamma^2\right] \approx 1 - \frac{1}{6}\sum_\gamma NS_\gamma\alpha_\gamma^2.$$

Assuming that we may exchange the order of limit and integration, we obtain

$$\mathbb{E}[V_\gamma] \approx NU\,\mathbb{E}[\alpha_\gamma^2] - \frac{1}{6}\sum_\lambda NS_\lambda\,\mathbb{E}[\alpha_\gamma^2\alpha_\lambda^2]. \tag{4.20}$$

Thus, to a first approximation, the reduction of the neutral genetic variance by selection is proportional to the covariances of the squares of the allelic effects between different traits. Conversely, if selection is strong relative to genetic drift, so that $\sum_\gamma NS_\gamma\alpha_\gamma^2 \gg 1$, we approximate

$$H\left[\sum_\gamma NS_\gamma\alpha_\gamma^2\right] \approx \frac{2}{\sum_\gamma NS_\gamma\alpha_\gamma^2}$$

to obtain

$$\mathbb{E}[V_\gamma] \approx 2U\int_{\mathbb{R}^K} \frac{\alpha_\gamma^2 f_\alpha(\boldsymbol{\alpha})}{\sum_\lambda S_\lambda\alpha_\lambda^2}\,d\boldsymbol{\alpha}. \tag{4.21}$$

Thus, calculating the total expected genetic variance weighted by the selection coefficients, we arrive at the simple identity

$$\sum_{\gamma} S_\gamma \mathbb{E}[V_\gamma] = 2U. \tag{4.22}$$

For a single trait, this becomes equation (4.2). Notably, also in the multivariate case, equation (4.22) is independent of the allelic effects and can be interpreted as a load argument. Mutations introduce deleterious variation at rate U per generation that has to be purged by selection. Alleles of small effects do not exert a high load, yet are not removed by selection as easily as alleles of large effect. These two opposing effects of the allelic effect size cancel out, and the mutational load only depends on the rate at which new mutations occur (Haldane, 1937).

4.3.4 Selection on pleiotropically connected traits

Spherical symmetry of allelic effects. The effect of selection on pleiotropically connected traits on the genetic variance of a given focal trait is mediated by the pleiotropic structure of how the individual alleles influence the set of traits. As described in Section 4.2.1 above, we may rescale the system to spherically symmetric distributions of allelic effects, i.e., no correlations between the allelic effects on different traits (cov$(\alpha_\gamma, \alpha_\lambda) = 0$ for $\gamma \neq \lambda$). In this section, we show how using spherically symmetric distributions of allelic effects allows us to say more about the impact of selection on pleiotropically connected traits.

A distribution is called spherically symmetric if it remains unchanged under rotations. Any spherically symmetric random variable $\boldsymbol{\alpha}$ in $\mathbb{R}^K$ can be written as the product of two independent random variables ρ and $\tilde{\boldsymbol{\xi}}$, where $\tilde{\boldsymbol{\xi}}$ is a uniform distribution on the unit sphere in $\mathbb{R}^K$ determining the direction of $\boldsymbol{\alpha}$, and $\rho = |\boldsymbol{\alpha}|$ is the length of $\boldsymbol{\alpha}$, i.e., the total allelic effect. To obtain a uniform distribution on the unit sphere in $\mathbb{R}^K$, we may draw a vector $\boldsymbol{\xi}$ from a K-variate normal distribution, and normalize the result to modulus one, i.e., $\tilde{\boldsymbol{\xi}} = \boldsymbol{\xi}/|\boldsymbol{\xi}|$. Hence, substituting $\boldsymbol{\alpha} = \rho\,\boldsymbol{\xi}/|\boldsymbol{\xi}|$ and $f_\alpha(\boldsymbol{\alpha}) = f_\rho(\rho)\, f_\xi(\boldsymbol{\xi})$, where $f_\xi(\boldsymbol{\xi}) = (2\pi)^{-K/2}\exp[-|\xi|^2/2]$, we obtain from equation (4.18)

$$\mathbb{E}[V_\gamma] = NU \int_0^\infty \int_{\mathbb{R}^K} \rho^2 \, \frac{\xi_\gamma^2}{|\boldsymbol{\xi}|^2} \, H\left[\sum_\lambda N S_\lambda \, \rho^2 \, \frac{\xi_\lambda^2}{|\boldsymbol{\xi}|^2}\right] f_\rho(\rho)\, (2\pi)^{-K/2}\, e^{-|\boldsymbol{\xi}|^2/2}\, d\boldsymbol{\xi}\, d\rho.$$

The substitution $\boldsymbol{\alpha} = \rho\,\boldsymbol{\xi}/|\boldsymbol{\xi}|$ describes the vector of allelic effects by a direction in trait space and a total allelic effect ρ. To quantify the expected increase in genetic variation of each trait due to mutation, the mutational variance V_M (see Section 4.1.2), it is necessary to retrieve information about the $\mathbb{E}[\alpha_\gamma^2]$ from the new variables. Clearly, $\sum_\lambda \mathbb{E}[\xi_\lambda^2/|\boldsymbol{\xi}|] = 1$, hence due to symmetry $\mathbb{E}[\xi_\gamma^2/|\boldsymbol{\xi}|] = 1/K$ for every $\gamma \in \{1, ..., K\}$. Therefore, we obtain the identity

$$\mathbb{E}[\alpha_\gamma^2] = \mathbb{E}[\rho^2]\,\mathbb{E}\left[\frac{\xi_\gamma^2}{|\boldsymbol{\xi}|^2}\right] = \frac{\mathbb{E}[\rho^2]}{K}. \tag{4.23}$$

The genetic variance in polar coordinates. In the following, we relabel the traits so that the focal trait has index 1. This is convenient for casting $\boldsymbol{\xi}$ into polar coordinates, where the ordering of the angles matters. We thus substitute

$$\begin{aligned}
\xi_1 &= |\boldsymbol{\xi}|\,\cos(\varphi_1),\\
\xi_\lambda &= |\boldsymbol{\xi}|\,\cos(\varphi_\lambda)\prod_{i=1}^{\lambda-1}\sin(\varphi_i) \qquad \text{for } \lambda = 2, ..., K-1,\\
\xi_K &= |\boldsymbol{\xi}|\,\prod_{i=1}^{K-1}\sin(\varphi_i).
\end{aligned}$$

Then, the genetic variance of the focal trait can be written as

$$\mathbb{E}[V_1] = NU\,\frac{\Gamma[k/2]}{2\pi^{k/2}}\int_0^\infty \rho^2 f_\rho(\rho)\int_0^{2\pi}\int_0^\pi\cdots\int_0^\pi \cos^2(\varphi_1)\,H\big[\rho^2 X\big]\,d\Omega_K\,d\rho, \tag{4.24}$$

where

$$\begin{aligned}
X &= \sum_{\gamma=1}^K NS_\gamma\xi_\gamma^2 = \left(\sum_{\lambda=1}^{K-1} NS_\lambda\cos^2(\varphi_\lambda)\prod_{i=1}^{\lambda-1}\sin^2(\varphi_i)\right) + NS_K\prod_{i=1}^{K-1}\sin^2(\varphi_i),\\
d\Omega_K &= \sin^{K-2}(\varphi_1)\sin^{K-1}(\varphi_2)\cdots\sin(\varphi_{K-2})\,d\varphi_1\cdots d\varphi_{K-1},
\end{aligned}$$

and Γ is the gamma function generalizing factorials. In general, this integral can only evaluated numerically. If the focal trait is neutral, it may be written in terms of hypergeometric functions, yet these expressions do not provide further insight.

To investigate how selection on a background trait is reflected in the genetic variance of the focal trait, we from now on focus on $K = 2$ traits. Reducing the above formula, equation (4.24), to two traits produces

$$\mathbb{E}[V_1] = \frac{NU}{2\pi}\int_0^\infty \rho^2 f_\rho(\rho)\int_0^{2\pi}\cos^2(\varphi)\,H\big[\rho^2\left(NS_1\cos^2(\varphi) + NS_2\sin^2(\varphi)\right)\big]\,d\varphi\,d\rho. \tag{4.25}$$

Indirect selection on a neutral trait. Consider a neutral focal trait ($S_1 = 0$) and a second trait under stabilizing selection, $S_2 = S$. Then, the inner integral of equation (4.25) can be evaluated analytically to produce

$$\mathbb{E}[V_1] = \frac{2U}{S} \int_0^\infty \left[\sqrt{\pi\, NS\rho^2}\, \mathrm{Erf}\left[\sqrt{\frac{NS\rho^2}{4}} \right] + e^{-\frac{NS\rho^2}{4}} - 1 \right] f_\rho(\rho)\, d\rho, \tag{4.26}$$

where Erf is the error function given by $\mathrm{Erf}(x) = 2/\sqrt{\pi}\, \int_0^x e^{-y^2}\, dy$.

Keeping NU/NS constant and letting $NS \to \infty$, we find (assuming that we may exchange the order of integration and taking the limit)

$$\frac{\mathbb{E}[V_1]}{\sqrt{NS\rho^2}} \longrightarrow \frac{NU}{NS} \times \frac{\sqrt{\pi}}{2} > 0. \tag{4.27}$$

Thus, with spherically symmetric mutational effects, the expected genetic variance of a neutral trait decays with the square root of the selection intensity on the background trait. In contrast, the genetic variance of the selected trait decays linearly with selection, i.e., one can show that

$$\mathbb{E}[V_2] \longrightarrow \frac{2NU}{NS}$$

in the same limit. As a consequence, the classical limit of strong selection is inconsistent with indirect selection on a neutral trait: Letting $NS \to \infty$ with fixed NU/NS, we have $\mathbb{E}[V_2] = 2U/S$ for the selected trait, but the genetic variance of a pleiotropically connected neutral trait diverges.

In general, equation (4.26) shows that the effect of indirect selection on the focal trait depends on the distribution of allelic effects. For example, assume that ρ is drawn from a normal distribution that is cut off for negative values, i.e.,

$$f_\rho(\rho) = \sqrt{\frac{2}{\pi\sigma_\rho^2}}\, e^{-\frac{\rho^2}{2\sigma_\rho^2}},$$

where $\sigma_\rho^2 = \mathbb{E}[\rho^2]$. Then, equation (4.26) can be integrated explicitly and yields

$$\mathbb{E}[V_1] = \frac{NU\sigma_\rho^2}{1 + \sqrt{1 + \frac{NS\sigma_\rho^2}{2}}}. \tag{4.28}$$

Note that due to the identity (4.23), $\sigma_\rho^2/2 = \mathbb{E}[\alpha_1^2]$. Hence, stabilizing selection on the background trait reduces the genetic variance expected under neutrality for the focal

trait ($NU\mathbb{E}[\alpha_1^2]$) by a factor depending on $\sqrt{NS\,\mathbb{E}[\alpha_1^2]}$. Calculating the expected genetic variance of the selected trait, $\mathbb{E}[V_2]$, we furthermore find that

$$\frac{\mathbb{E}[V_1]}{\mathbb{E}[V_2]} = \sqrt{1 + \frac{NS\sigma_\rho^2}{2}}. \tag{4.29}$$

Two traits under strong selection. Assume two traits under strong stabilizing selection with selection intensities S_1 and S_2. Since we may approximate $H(x) \approx 2/x$ for large x (c.f. Section 4.3.3), equation (4.25) can be approximated by

$$\begin{aligned}\mathbb{E}[V_1] &= \frac{NU}{2\pi}\int_0^\infty \rho^2 f_\rho(\rho)\int_0^{2\pi} \frac{2\cos^2(\varphi)}{\rho^2\left[NS_1\cos^2(\varphi) + NS_2\sin^2(\varphi)\right]}\,d\varphi\,d\rho \\ &= \frac{2U}{S_1 + \sqrt{S_1S_2}}.\end{aligned} \tag{4.30}$$

This confirms that the effect of selection on the background trait affects the genetic variance of the focal trait by the square root of its intensity, $\sqrt{S_2}$. By symmetry, we have $\mathbb{E}[V_2] = 2U/(S_2 + \sqrt{S_1S_2})$ and thus

$$\frac{\mathbb{E}[V_1]}{\mathbb{E}[V_2]} = \sqrt{\frac{S_2}{S_1}}. \tag{4.31}$$

Hence, the ratio between the expected genetic variances of two traits under strong stabilizing selection is inversely proportional to the square root of the ratio of their selection intensities.

Using polar coordinates, it is easy to see that the genetic variances under strong selection in general do not depend on the distribution of allelic effects if it is spherically symmetric. For intermediate to low selection strengths, however, this is not the case. Figure 4.3 shows the ratio $\mathbb{E}[V_1]/\mathbb{E}[V_2]$ of two pleiotropically connected traits as a function of the strength of selection on the first trait by the example of normal (circles) and exponential (crosses) distributions for the total allelic effect ρ, and for two different values of $\mathbb{E}[\rho^2]$, $\mathbb{E}[\rho^2] = 1$ (blue) and $\mathbb{E}[\rho^2] = 2$ (orange). Clearly, different distributions produce different outcomes even with identical $\mathbb{E}[\rho^2]$, although the patterns are very similar. Increasing the value of $\mathbb{E}[\rho^2]$ for a given distribution increases the rate of convergence towards the limit of strong selection, equation (4.31) (dashed line) approximately proportionally.

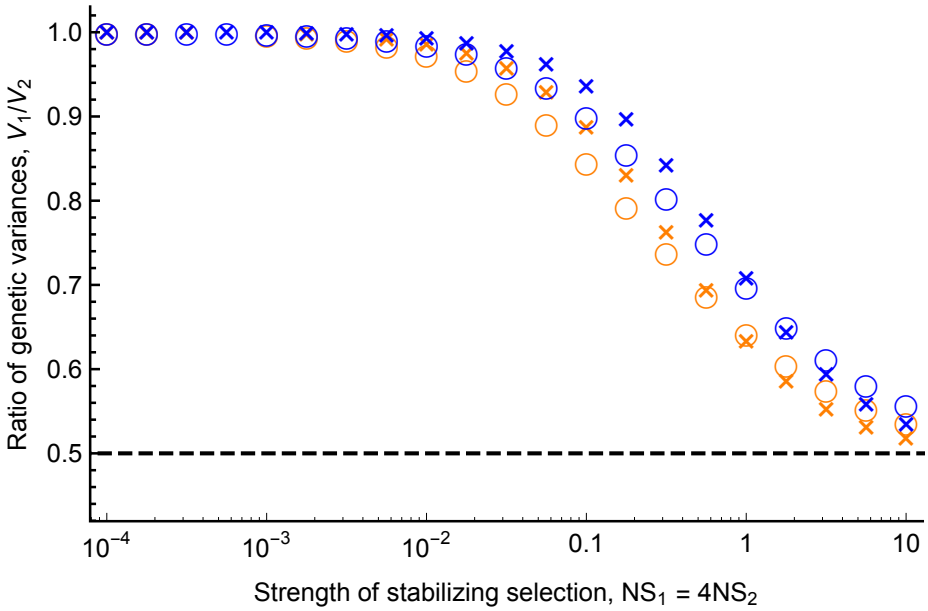

Figure 4.3: Ratio of the expected genetic variances of two traits. For two traits under stabilizing selection ($NS_1 = 4NS_2$), we calculated $\mathbb{E}[V_1]/\mathbb{E}[V_2]$ by numerical integration of equation (4.25) for normal (circles) and exponential (crosses) total allelic effect distributions with $\mathbb{E}[\rho^2] = 1$ (blue) and $\mathbb{E}[\rho^2] = 2$ (orange). Larger allelic effects lead to an approximately proportionally quicker convergence towards the limit of strong selection, equation (4.31) (dashed line). The choice of the allelic effect distribution influences the ratio of genetic variances $\mathbb{E}[V_1]/\mathbb{E}[V_2]$ in a non-trivial way.

4.4 Discussion and outlook

4.4.1 Constant selection

In the previous two sections, we investigated multivariate stabilizing selection with fixed intensities and optima. As argued above, the complexity of interactions between traits and the genetic loci causes selection on the individual alleles to essentially appear stochastic, even in the case of constant selection. The more complicated the genetic details are, the better can we expect the fluctuating selection process described in Section 4.2 to capture the features of the explicit dynamics of allele frequencies. Using this description, one may investigate the characteristics of allele frequency trajectories, e.g., fixation probabilities and expected times to fixation or loss. In particular, the approach of describing the system by a fluctuating selection process on individual alleles may provide an alternative way to calculating the stationary distribution of allele frequencies, and hence the expected genetic variances of multiple quantitative traits.

However, there are two major challenges to overcome. First, the dynamics of the focal allele influences the trait means and hence its selection coefficient in practice. In Section 4.2.3, we assumed that the pattern of fluctuations is determined by an independent process. However, there is a feedback between the stochastic processes describing the frequency of an allele and its directional selection component, since the focal allele influences the dynamics of the trait means. This feedback can be modelled explicitly, but greatly complicates an analytical treatment. There are scenarios when the feedback between allele frequency and selection coefficient may be neglected, for instance, if the allelic effects of the focal allele are sufficiently small, or if a great number of alleles are segregating such that the contribution of the focal allele is irrelevant.

Second, the time scale of fluctuations in the trait means, and hence in the directional selection components, depend on the genetic variances (c.f. Section 4.2.3): both the returning force and the volatility of the trait means are linear in V_G, see equation (4.9). On a short time scale of a few generations, Figure 4.1c indicates that that the process is well-described by substituting the mean genetic variance for V_G. However, if the allele frequency trajectories are determined by changes of the trait means over longer periods of time, a deeper understanding of the macroscopic dynamics of

the genetic variances is required. This adds an additional layer of complexity to the model, since the dynamics of allele frequencies and the directional selection components are coupled to the dynamics of the genetic variances.

It may seem paradoxical that our model of fluctuating directional selection components requires information about the very quantity that is subject of our investigations. Similarly to the dynamics of the trait means, equation (4.9), the dynamical process of the genetic variance has been described on a macroscopic level (Bürger, 2000). It should thus be possible to apply this process and obtain the directional selection components of segregating alleles, their stationary frequency distributions, and the moments of the trait distributions, as functions of its characteristics. These may be inverted to produce, e.g., the expected genetic variances we are interested in.

The challenges mentioned above are worth tackling and our method provides ample opportunity for future work and an alternative method to calculating the stationary distribution of allele frequencies under constant selection. The problem in principle remains unchanged if we allow the trait optima to fluctuate stochastically in time. Deviations between mean and optimal trait value, and thus the directional selection components of the alleles, are still due to a stochastic process. In this case, however, this process is additionally influenced by the fluctuation patterns of the trait optima. Thus, our stochastic description of multivariate stabilizing selection may lend itself to investigating genetic variances under fluctuating stabilizing selection – more so than the traditional approach exercised in Section (4.3).

Applying Kimura's stationary distribution of allele frequencies, equation (4.13), to calculate the expected genetic variances of multiple traits sheds light on the effect of pleiotropic interactions between traits in the presence of constant stabilizing selection. Section 4.3.2 shows that known formulae can be generalized to the multivariate case (equation (4.18)). In the limit of strong selection, we further recover a classical mutation load argument, equation (4.22), that relates the rate of (deleterious) mutations with the reduction in fitness due to variation of the traits around their optimal values.

One important interest in studying multiple traits is identifying the effect of pleiotropically connected traits under stabilizing selection on the genetic variance of a focal trait. In Section 4.3.4, we showed that stabilizing selection with strength S on a back-

ground trait reduces the genetic variance of the focal trait by a factor that scales with the square root of S. In particular, we find that the ratio of the genetic variances of two traits under strong selection is inversely proportional to the square roots of their selection intensities, see equation (4.31).

Our results were derived under the assumption that selection acts on the traits separately (no correlations in selection; the matrix $\boldsymbol{S}$ containing the selection intensities is diagonal), and that there is no pleiotropic structure in the allelic effects on different traits (no correlations in mutation; the distribution of $\boldsymbol{\alpha}$ is spherically symmetric). However, any correlation structure in selection and mutation may be obtained by a linear transformation of the uncorrelated case (Section 4.2.1). It will be interesting to study the admissible transformations to compare expected genetic variances under perceived strengths of stabilizing selection in the presence of a correlation structure between allelic effects. It is to be expected that measuring stabilizing selection and mutational effects on a single trait alone can lead to misleading predictions about its genetic variance if it is part of a group of traits that evolve together under correlated selection and mutation (Lande and Arnold, 1983).

4.4.2 Fluctuating selection

Fluctuations in a trait optimum have been shown numerically to have great potential to increase the genetic variance, e.g., Kondrashov and Yampolsky (1996); Bürger and Gimelfarb (2002). In their simulations, a fluctuating trait optimum was found to amplify genetic variances by up to an order of magnitude or more. Because fluctuating trait optima add a great deal of complexity to the dynamics of quantitative trait evolution, analytical models have mostly looked at simple patterns of fluctuations, e.g., a linearly moving optimum (Lynch and Lande, 1993; Bürger and Lynch, 1995; Matuszewski *et al.*, 2015) or an abrupt change of the optimum to a new value (Gomulkiewicz and Holt, 1995; Chevin, 2013). Generally, however, the analytic results of these studies are concerned more with the dynamics of the trait mean rather than the genetic variance, which is typically analysed numerically (Jones *et al.*, 2004). In this final section of Chapter 4, I describe ideas to extend our framework of multivariate stabilizing selection to fluctuating trait optima. It is not meant to present any results, but deliver some

detailed insight into possible next steps of the project.

If the trait optima fluctuate in time, they give rise to systematic differences between the trait means and optima. Hence, directional selection components emerge that we may not neglect as we did in the stationary distribution approach for constant selection, Section 4.3. Depending on the pattern of fluctuations, however, there are different modelling techniques of approaching the problem. In the following, I first cover linearly moving trait optima and abrupt shifts in the optimal trait values. These can be seen as building blocks from which to assemble more complicated patterns of fluctuating selection. I conclude by discussing how fluctuating trait optima may translate into fluctuating selection on individual alleles, using our modelling approach from Section 4.2.

Linearly moving optima. For simplicity, consider a single trait under stabilizing selection for the optimum θ with intensity S with equal allelic effects ($\alpha_i \equiv \alpha$), and assume that $\theta = \theta(t)$ changes linearly in time at some given velocity. The trait mean will then lag behind its optimum; given that the velocity of the trait optimum is not too high (such that the trait mean is able to keep up), the lag between trait mean and optimum eventually reaches a stable value $\theta - \bar{z} = \Delta$ (Lynch and Lande, 1993). Assuming weak allelic effects, $\alpha \ll 1$, we find from equation (4.8) that the selection coefficient for the alleles contributing to the trait is approximately $s = \alpha S \Delta$. Hence, if we aim at understanding the genetic variance under linearly moving trait optima, we first have to understand the genetic variance under directional selection with (linear) selection gradient $\beta = S\Delta$ (c.f. Section 4.1.2).

As in the previous sections, we consider the limit of many loci at low per-locus mutation rate ($n \to \infty$, $\mu \to 0$, and $n\mu = U$). Each of the loci has two possible allelic variants with allelic effects $\pm\alpha/2$; let a fraction $\mathcal{P}$ of the loci be fixed for the $+$ allele, and a fraction $\mathcal{Q} = 1 - \mathcal{P}$ be fixed for the $-$ allele. Assuming that the trait optimum moves with positive velocity, $\Delta > 0$, we call a mutation beneficial if it occurs on a locus fixed for the $-$ allele, and deleterious if it occurs on a locus fixed for the $+$ allele.

Our aim is to calculate the distribution $t_{avg}(p)$ of times a single mutation spends at frequency $p = 1/N, ..., (N-1)/N$ before it hits either $p = 0$ or $p = 1$, because this distribution allows us to determine the steady-state distribution of allele frequencies in the balance of new mutations occurring and segregating alleles being fixed or lost.

Conditioning on the corresponding distributions of times for beneficial and deleterious mutations, t_b and t_d, respectively, we may write

$$t_{avg}(p) = \mathcal{Q}\, t_b(p) + \mathcal{P}\, t_d(p). \tag{4.32}$$

To obtain an expression for t_b, we condition on whether the mutation is fixed or lost eventually. Let $t_b^{loss}(p)$ and $t_b^{fix}(p)$ denote the distribution of times a beneficial allele spends at frequency $p = 1/N, ..., (N-1)/N$ before it hits either $p = 0$ or $p = 1$, respectively. Approximating the fixation probability of a beneficial allele by $2s/(1 - e^{-2Ns})$ (Kimura, 1962) and the probability of losing the allele by 1, we obtain

$$t_b(p) = \frac{2s}{1 - e^{-2Ns}}\, t_b^{fix}(p) + t_b^{loss}(p). \tag{4.33}$$

Analogously, we find an expression for t_d in terms of t_d^{fix} and t_d^{loss}. The required distributions t_b^{fix}, t_b^{loss}, t_d^{fix}, and t_d^{loss} can be calculated, see Ewens (1979), Ch.4.6. Applying these formulae to our case yields

$$t_{avg}(p) \propto \frac{\mathcal{P}\left(1 - e^{2Nsp}\right) + \mathcal{Q}\left(e^{2Nsp} - e^{2Ns}\right)}{\left(1 - e^{2Ns}\right) p\,(1-p)}. \tag{4.34}$$

If $\mathcal{P}$ and $\mathcal{Q}$ emerged from a simple balance of transitions between $+$ and $-$ alleles, i.e.,

$$\mu\, \mathcal{P}\, \frac{-2s}{1 - e^{2Ns}} = \mu\, \mathcal{Q}\, \frac{2s}{1 - e^{-2Ns}},$$

we would obtain $\mathcal{P}/\mathcal{Q} = e^{2Ns}$. Inserting this into equation (4.34) yields

$$\mathcal{Q}\, t_b(p) + \mathcal{P}\, t_d(p) \propto \frac{e^{2Nsp}}{p\,(1-p)}. \tag{4.35}$$

This has the form of a stationary distribution of a population with mean fitness e^{sp}, in the limit of small mutation rates ($\mu \to 0$). However, the actual distribution of allele frequencies in this model is different, see Figure 4.4: We simulated $n = 10^6$ loci in a population of 100 haploid individuals with $\mu = 10^{-6}$ and $s = \alpha\beta = 0.02$. The steady state distribution of allele frequencies (orange) is different from the distribution (4.35) (dashed line) and the stationary distribution under neutrality (dotted line).

Using the data from our simulation, we may simply count the number of loci being fixed for the $+$ and $-$ alleles to estimate $\mathcal{P}$ and $\mathcal{Q}$. Inserting these values into equation (4.34) gives rise to a distribution that fits the simulation very well (Figure 4.4, solid

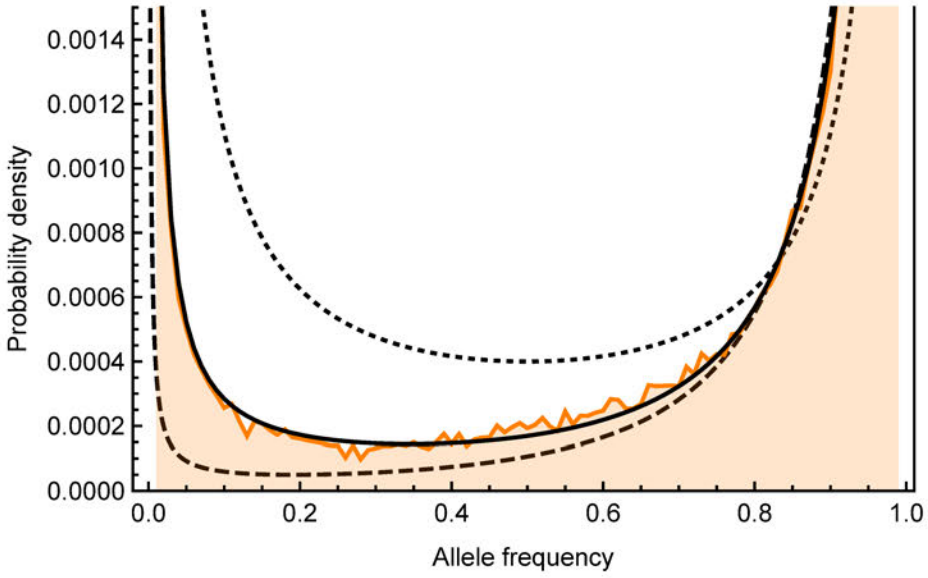

Figure 4.4: The steady state distribution of allele frequencies under directional selection. We considered a haploid population of $N = 100$ individuals and a trait under directional selection that is determined by $n = 10^6$ loci in linkage equilibrium with (bi-directional) mutation rates $\mu = 10^{-6}$. The allelic effect α was chosen such that the selection coefficient for the $+$ allele is $s = \alpha\beta = 0.02$. Upon numerically iteration under selection, mutation, and genetic drift, the distribution of allele frequencies equilibrates at its steady state distribution (orange). This distribution is well described by equation (4.34) if we estimate $\mathcal{P}$ and $\mathcal{Q}$ from the simulation data (solid line). However, it is different from the stationary distributions under neutrality (dotted line) and under directional selection with $\bar{w} = e^{sp}$, distribution (4.35) (dashed line).

line). Unfortunately, this numeric approach to finding $\mathcal{P}$ and $\mathcal{Q}$ does not provide insight into how they can be calculated from the model parameters. To be able to predict the expected genetic variance under directional selection, we require analytic expressions for the boundary masses $\mathcal{P}$ and $\mathcal{Q}$ of the steady state distribution, i.e., the probabilities of being fixed for the $+$ and $-$ states. These could be obtained using the transition rates between those states in combination with the expected sojourn times of new mutations. We halt the discussion at this point, and leave the problem open as one of the prospective lines of research in this project.

Abruptly shifting optima. Assume that the optimum of a trait switches abruptly to a different value. How does the genetic variance evolve as the trait adjusts to its new optimum, and how are pleiotropically connected traits affected? We exemplify this by looking at $K = 10$ traits under stabilizing selection with $NS_\gamma \equiv 1$ for all $\gamma = 1, ..., 10$. We set $NU = 10$ and consider spherically symmetric mutational effects with exponential radius with mean 1, i.e., $f_\rho(\rho) = e^{-\rho}$. Numerical simulations show that, initially, the trait means remain around their original optima given by $\boldsymbol{\theta} = \mathbf{0}$, and the genetic variances settle to fluctuations around their expectation of about $\mathbb{E}[V_\gamma] \approx 0.8$, see Figure 4.5. This value for $\mathbb{E}[V_\gamma]$ can be predicted from equation (4.18) and agrees well with our simulations – see Figure 4.5b, dashed line.

At some point in time, indicated by the vertical dot-dashed lines in Figure 4.5, we change the optimum for the first trait to $\theta_1 = 10$. While the trait mean of the first trait adjusts to the new optimum (Figure 4.5a, blue trajectory), the remaining traits seem to remain unaffected; since there is no pleiotropic structure, the trait means evolve approximately independently. The genetic variances, however, all show a significant increase following the shift of θ_1. Nevertheless, while the impact on the genetic variance of the adapting trait is highest (Figure 4.5b, blue trajectory), the other traits also experience a moderate increase of their genetic variances as alleles with positive effect on the adapting trait rise in frequency.

Figure 4.6 shows the difference between the mean of the first trait and its new optimum, $\Delta = 10 - \bar{z}_1$, for the first $1,000$ generations following the shift. The numerical trajectory of Δ (orange line) is very close to exponential at a rate that can be estimated from the data as $\Delta(t+1)/\Delta(t) \approx 0.991$ (dotted black line). The response $\mathcal{R}$ of a trait

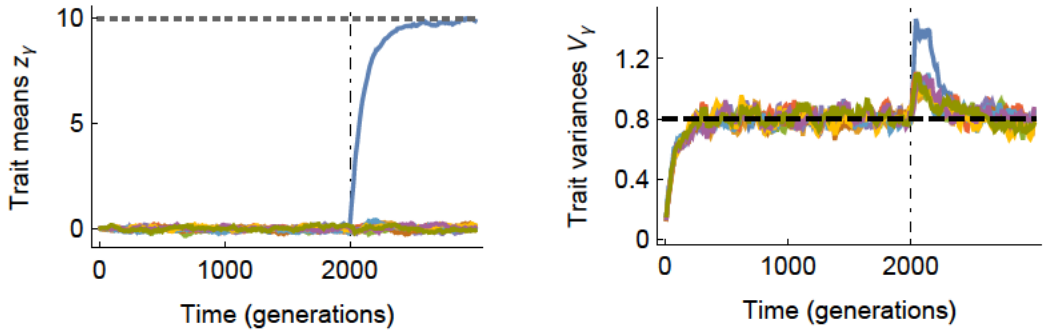

(a) Dynamics of trait means over time

(b) Dynamics of trait variances over time

Figure 4.5: Trait dynamics following a shift of the optimum. The set-up and parameters of the presented numerical data are the same as in Figure 4.1; the shown trajectories are averages over 50 simulation replicates. Initially, the trait means of the ten traits fluctuate around their optimal values $\theta_\gamma = 0$, and their genetic variances equilibrate around $\mathbb{E}[V_\gamma] = 0.8$. After $2,000$ generations, the optimum of the first trait abruptly shifts to $\theta_1 = 10$, forcing the first trait to adapt (panel (a), blue trajectory). As a consequence, also the genetic variances are temporarily increased: panel (b) shows that there is a significant rise in the genetic variances of all traits, though not as pronounced as of the first trait (blue trajectory). When the first trait reaches its new optimum, the genetic variances settle back at their equilibrium values.

to directional selection is defined as the change in trait mean per generation, and is given by the genetic variance of the trait times the selection gradient $\beta = S\Delta$ (see also the previous paragraph on linearly moving optima and Section 4.1.2). Estimating the genetic variance from equation (4.18), we may calculate

$$\mathcal{R} = \beta\,\mathbb{E}[V_1] = S\,\mathbb{E}[V_1]\,\Delta \approx 0.008\,\Delta.$$

Since $\Delta(t+1) = \Delta(t)\,(1-\mathcal{R})$, we find $\Delta(t+1)/\Delta(t) \approx 0.992$, which closely matches our inference from the simulation data above.

This example indicates that the response of a trait to a shift in its optimal value may be approximated very well by a deterministic process, whose parameters can be estimated from the model parameters. The directional component of stabilizing selection, and hence the selection coefficients of segregating alleles, follow an approximately deterministic pattern. Thus, to describe the dynamics of the genetic variances following a shift of the optimal trait values, we may iterate the distribution of allele frequencies in time by applying a transition matrix that depends on the strength of genetic drift and a given sequence of (time-varying) selection coefficients. We have not yet arrived at tackling this problem, but will do so as this project progresses.

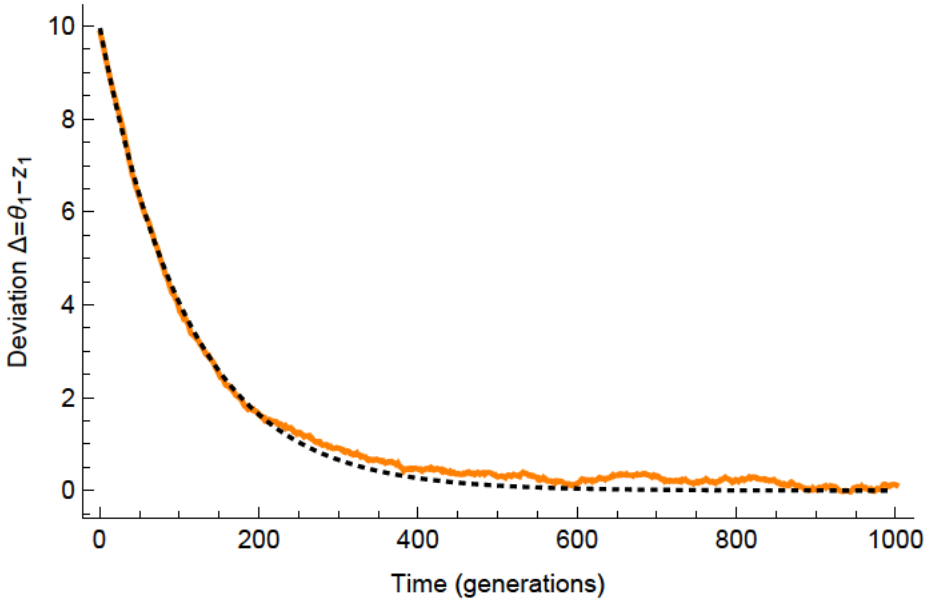

Figure 4.6: The difference between the trait mean and optimum over time. The simulated data are the same as in Figure 4.5; the orange trajectory shows the mean of $\Delta = \theta_1 - z_1$ over 50 simulation replicates for the first $1,000$ generations following the shift of the trait optimum to $\theta_1 = 10$. The predicted reduction (black) of Δ is 0.8% per generation, see main text, and closely fits the numerical results for most of the adaptation process.

Randomly fluctuating optima. As mentioned above in Section 4.4.1, our description of multivariate stabilizing selection by fluctuating selection on single alleles may lend itself to including trait optima that obey some given random process. Recall that the dynamics of trait means can be described by Ornstein-Uhlenbeck processes, see Section 4.2.3. If the trait optima are different from zero, the dynamics of $\bar{z}_\gamma$ satisfy

$$d\bar{z}_\gamma = -\vartheta_\gamma \left(\bar{z}_\gamma - \theta_\gamma\right) dt + \sigma_\gamma \, dW,$$

generalizing equation (4.9). Our method proposed in Section 4.2.3 combines the values of $\bar{z}_\gamma$ $(\gamma = 1, ..., K)$ to obtain the directional component of the selection coefficient on the alleles, given by $\zeta = \sum_\gamma \alpha_\gamma S_\gamma \left(\bar{z}_\gamma - \theta_\gamma\right)$.

Now let the trait optima θ_γ follow stochastic processes themselves. Then, the process for the $\bar{z}_\gamma$ becomes a generalization of the Ornstein-Uhlenbeck process, which is of conceptual interest. Characterizations of generalized Ornstein-Uhlenbeck processes of similar forms can be found in the literature, e.g., Cáceres and Budini (1997) consider stochastic noise σ_γ, and Benth and Khedher (2016) discuss stochastic speed

of mean reversion ϑ_γ. Hence, there is also a purely mathematical motivation for investigating the effect of stochastic θ_γ.

Furthermore, the application of tools from stochastic analysis to our problem opens up a set of mathematical techniques that have so far rarely been used in the context of quantitative genetics; thus, they may provide new alternatives for studying the distribution of allele frequencies under fluctuating trait optima. Clearly, this is not a simple task. A great simplification will be to consider the limit of large populations first, so that random fluctuations in the trait means can be neglected and the process of the $\bar{z}_\gamma$ depends on the dynamics of θ_γ in a deterministic manner. Thus, the trait optima $\boldsymbol{\theta}$ are the single source of stochasticity, which may allow to investigate the evolution of allele frequency distribution in the balance of mutation and stabilizing selection for fluctuating optima. This, however, will be subject to future work.

4.4.3 Conclusion

In summary, I presented the current status of my work on multivariate stabilizing selection on a set of quantitative traits. The shown results constitute first steps to a better understanding of how coupled traits interact and how selection on background traits influences the genetic variance of a focal trait. There are several ways to extend the project, which I indicated in this section. First, concerning the fluctuating selection approach of Section 4.2, the feedback between the two processes for the frequency of the focal allele and its directional selection component is unclear. Furthermore, the impact of fluctuations of the genetic variance on the Ornstein-Uhlenbeck description of the trait means $\bar{z}_\gamma$ should be investigated more closely. Second, it will be interesting to quantify the effect of correlations in selection (trade-off) and mutation (pleiotropic structure) on the expected genetic variances. This can be achieved by studying linear transformations of the uncorrelated case that we are focussing on here. Third, temporally fluctuating selection on quantitative traits remains virtually unexplored analytically. I described several possibilities to tackle this shortcoming. These are (i) linearly moving trait optima, which may be approximated by a constant lag between trait mean and optimum and hence constant directional selection; (ii) an abrupt change of the trait optimum, which is followed by a phase of exponential adaptation and hence

a pre-determined sequence of directional selection components; and (iii) fluctuating trait optima according to some stochastic process, which may be integrated into the Ornstein-Uhlenbeck description of the trait means to obtain a randomly fluctuating selection coefficient.

Each of the above-mentioned extensions are challenging and may be tackled relatively independently. Yet, putting together the presented results with prospective lines of research, my project will contribute to a deeper understanding of the evolution of quantitative traits under multivariate stabilizing selection that is necessary to comprehend the dynamics of genetic variation in complex functional organisms evolving in realistic environments.

5 Conclusion

In this thesis, I present three seemingly unrelated topics that are connected by the common theme of changing environments. Environmental change in space and time is ubiquitous in natural populations and may either give rise to or strongly interfere with evolutionary phenomena. The former is the case in Chapter 2 and Chapter 3, where temporally fluctuating or spatially heterogeneous external conditions induce selective forces on a mutation or dispersal modifier. The latter is discussed in the context of quantitative genetics, see Chapter 4, where spatio-temporal variation in selection is known to have the potential to greatly inflate the genetic variances of phenotypic traits.

Stress-induced mutagenesis. In clinical applications, humans deliberately force extreme environmental fluctuations on bacterial populations and other pathogenic organisms by devising drug treatment regimes to eradicate target populations (Bollenbach, 2015). In the resulting biological arms race, species evolve mechanisms to deal with the imposed challenges, which necessitates the development of treatment strategies that inhibit resistance evolution. One possibility, for instance, is the cyclical application of a set of drugs that attack different vital pathways in the target organism (Bonhoeffer *et al.*, 1997).

However, under repeated challenges of different kinds, there may be selection pressure for evolvability, i.e., the capability of adapting to unforseen situations. Increasing mutation rates under unfavourable conditions (stress-induced mutagenesis, SIM) can be an effective mechanism to enhance evolvability, which I discuss in Chapter 2. The model studied there indicates that the diversity of applied challenges is a crucial factor

for positive second-order selection on SIM alleles. This may have implications for antibiotic treatment plans to come up with strategies to both inhibit resistance evolution and evolvability. In the face of the current antibiotic resistance crisis, such considerations may be of critical relevance. The main challenges will be to theoretically quantify the strength of second-order selection in terms of clinically relevant variables, and to experimentally confirm that stress-induced mutagenesis actually plays an active role in recovering population growth rates under environmental challenges.

Evolution of dispersal. Heterogeneous environments may feature habitats of different quality levels, capable of sustaining populations of variable size. As I explain in Chapter 3, random dispersal in such situations leads to a net flow of individuals from good-quality into bad-quality habitat such that dispersal is disfavoured on average (Hastings, 1983). There are other costs to dispersal due to, e.g., the expenditure of time and energy, the risk of predation, and maladaptation due to migration into foreign habitat (Bonte *et al.*, 2012). Consequently, dispersal must entail significant benefits to be maintained. Two main drivers of the evolution of positive dispersal are known to be temporal environmental fluctuations – in the extreme case, to spatially bet-hedge against catastrophic events (Van Valen, 1971) – and effects of relatedness between individuals to avoid competition with relatives (Hamilton and May, 1977).

In Chapter 3, I present a model of dispersal evolution, which indicates that spatial changes in dispersal type frequencies cause selection for increased dispersal. This is an abstract, yet very general formulation of a force promoting dispersal that contains selection for dispersal due to relatedness and allows to quantify its strength. Heterogeneities in dispersal type frequencies, however, may be generated and maintained by various processes. For example, the direction of movement of clines maintained by selection is biased towards slower-diffusing types, which may be interpreted as a selective advantage of increased dispersal, c.f. Section 3.5. Another process that may interact with dispersal may be genetic draft, i.e., the spatial sweep of beneficial alleles through the population, which may perturb the frequencies of dispersal modifiers that are linked to the sweeping allele. My result indicates that there may be yet unnoticed factors of dispersal evolution to be explored, and it enables us to put them on a single scale by the amount they perturb dispersal type frequencies.

Multivariate quantitative genetics. Constant selection on quantitative traits is generally believed to erode genetic variation in the long run. This is more an empirical observation than an affirmed result, because selection on a trait leads to complicated epistatic interactions in fitness between the underlying alleles. This makes it difficult to arrive at simple conclusions, since it may be conceivable to devise a fitness function such that the evolutionary dynamics maintain a positive level of genetic variance even without mutations generating variation. From the proof I present in Appendix A3, however, it follows that this is impossible in haploid populations. The novelty of this result lies in the fact that my argument allows for arbitrary epistasis between alleles, and hence is applicable to selection on quantitative traits. In models of (constant) selection and mutation, it is thus justified to think of the genetic variance of traits as emerging from a balance between mutation generating variation, and selection eroding it.

In Chapter 4, I argue for generalizing relatively simple models of a single trait under constant stabilizing selection to sets of multiple traits and fluctuating selection. The results I present in this chapter come from ongoing work and contribute to our understanding of how the presence of and selection on pleiotropically connected traits influence the expected genetic variance of a focal trait. The full dynamics of the process is highly intricate, yet the approach outlined in Section 4.2 may take advantage of its complexity and describe it statistically in terms of stochastic processes.

In the light of genetic loads, the results from Chapter 4 provide interesting insight. The mean fitness, equation (4.6), is reduced below its maximal value of $\bar{w} = 1$ by two factors, the deviation of the mean from the optimum giving rise to “drift load”, and the genetic variance leading to “mutation load” (Crow, 1970). Our simulations show that the stationary distribution of the deviation of the mean of a given trait from its optimum is independent of the number of pleiotropically connected traits. Consistently with the Ornstein-Uhlenbeck description of the dynamics of trait means, c.f. Section 4.2.3, the stationary distribution is close to a Gaussian with variance $1/(2NS)$. Due to the sum over all traits in the expression for $\bar{w}$, equation (4.6), it follows that the drift load is proportional to the number of traits. In contrast, the mutation load is independent of the number of traits, at least in the limit of strong selection (infinite population), due to equation (4.22). Our formula for the expected genetic variance, equation (4.18),

may be used to study the mutation load in finite populations (c.f. Kimura *et al.*, 1963) to investigate the dependence of the mutation load on the number of traits and the population size.

Our results on selection on pleiotropically connected traits show a square-root dependence of the genetic variance of the focal trait on selection on the background trait. This is likely due to the spherical symmetry of mutational effects assumed in our model, since we average over a uniformly distributed angle between the effects on different traits. With stronger correlations in mutational effects between traits, we may expect stronger dependence of the focal trait on background traits. However, note that selection on pleiotropically connected traits influences the genetic variance of the focal trait even though there are no genetic covariances between the traits ($V_{\gamma\lambda} = 0$). In particular, we saw in Section 4.3.4 that selection on pleiotropically connected traits reduces the genetic variance of a neutral trait below its expected value of $NU\mathbb{E}[\alpha_\gamma^2]$. This is reminiscent of apparent stabilizing selection (c.f. Barton, 1990), i.e., the false appearance of stabilizing selection on the trait itself. Making the analogy precise may be a fruitful way towards a better understanding of the effect of selection on pleiotropically connected traits.

In Section 4.4, I discuss several ways of advancing my project. The task is challenging, but will lead to a deeper understanding of how pleiotropy interferes with the ability of populations to adapt to changing environments, which undoubtedly has gained acute urgency. Furthermore, it may help us investigate structural properties of sets of phenotypic traits that shape complex living organisms. Is the pleiotropic network between traits subdivided into clusters, and if it is, do the traits of a given cluster have some functional relationship (modularity)? How many such clusters can there be, and how are the correlation structures between traits in each cluster? How many degrees of freedom does the underlying genetic basis afford for exploring the phenotypic space? How strongly does selection act on each trait, and how many traits may be maintained at an optimum efficiently? These are few of the many questions that may be asked, yet will be hard to answer. Chapter 4 constitutes a small contribution towards understanding the big picture, and there is ample opportunity for pushing my research further beyond the steps indicated here.

Bibliography

A. F. Agrawal and A. D. Wang, Increased transmission of mutations by low-condition females: evidence for condition-dependent DNA repair, *PLoS Biology*, 6(2):e30, 2008.

M. K. Alam, A. Alhhazmi, J. F. DeCoteau, Y. Luo, and C. R. Geyer, RecA inhibitors potentiate antibiotic activity and block evolution of antibiotic resistance, *Cell Chemical Biology*, 23(3):381–391, 2016.

L. A. Bach, J. Ripa, and P. Lundberg, On the evolution of conditional dispersal under environmental and demographic stochasticity, *Evolutionary Ecology Research*, 9(4):663, 2007.

B. J. Balkau and M. W. Feldman, Selection for migration modification, *Genetics*, 74(1):171–174, 1973.

N. H. Barton, The dynamics of hybrid zones, *Heredity*, 43(3):341–359, 1979.

N. H. Barton, The divergence of a polygenic system subject to stabilizing selection, mutation and drift, *Genetical Research*, 54(1):59–78, 1989.

N. H. Barton, Pleiotropic models of quantitative variation, *Genetics*, 124(3):773–782, 1990.

N. H. Barton, Clines in polygenic traits, *Genetical Research*, 74(03):223–236, 1999.

N. H. Barton, Genetic hitchhiking, *Phil. Trans. R. Soc. Lond. B*, 355(1403):1553–1562, 2000.

N. H. Barton, D. E. G. Briggs, J. A. Eisen, D. B. Goldstein, and N. H. Patel, *Evolution*, Cold Spring Harbor Laboratory Press, NY, 2007.

N. H. Barton and B. Charlesworth, Why sex and recombination?, *Science*, 281(5385):1986–1990, 1998.

N. H. Barton and A. Clark, Population structure and processes in evolution, In *Population Biology*, pages 115–173. Springer, 1990.

N. H. Barton and P. D. Keightley, Understanding quantitative genetic variation, *Nature Reviews Genetics*, 3(1):11–21, 2002.

N. H. Barton and M. Turelli, Spatial waves of advance with bistable dynamics: Cytoplasmic and genetic analogues of Allee effects, *The American Naturalist*, 178(3):E48–E75, 2011.

L. E. Baum and J. A. Eagon, An inequality with applications to statistical estimation for probabilistic functions of Markov processes and to a model for ecology, *Bull. Amer. Math. Soc*, 73(3):360–363, 1967.

M. Baym, L. K. Stone, and R. Kishony, Multidrug evolutionary strategies to reverse antibiotic resistance, *Science*, 351(6268):aad3292, 2016.

A. D. Bazykin, Hypothetical mechanism of speciation, *Evolution*, 23(4):685–687, 1969.

G. Bell and A. Gonzalez, Evolutionary rescue can prevent extinction following environmental change, *Ecology Letters*, 12(9):942–948, 2009.

F. E. Benth and A. Khedher, Weak stationarity of Ornstein-Uhlenbeck processes with stochastic speed of mean reversion, In *The Fascination of Probability, Statistics and their Applications*, pages 153–189. Springer, 2016.

C. T. Bergstrom, M. Lo, and M. Lipsitch, Ecological theory suggests that antimicrobial cycling will not reduce antimicrobial resistance in hospitals, *Proceedings of the National Academy of Sciences*, 101(36):13285–13290, 2004.

A. T. Bharucha-Reid, *Elements of the theory of Markov processes and their applications*, McGraw-Hill Series in Probability and Statistics. McGraw-Hill Book Co., Inc., New York, 1960.

S. Billiard and T. Lenormand, Evolution of migration under kin selection and local adaptation, *Evolution*, 59(1):13–23, 2005.

I. Bjedov, O. Tenaillon, B. Gérard, V. Souza, E. Denamur, M. Radman, F. Taddei, and I. Matic, Stress-induced mutagenesis in bacteria, *Science*, 300(5624):1404–1409, 2003.

F. Blanquart and S. Gandon, Evolution of migration in a periodically changing environment, *The American Naturalist*, 177(2):188–201, 2011.

F. Blanquart and S. Gandon, On the evolution of migration in heterogeneous environments, *Evolution*, 68(6):1617–1628, 2014.

T. Bollenbach, Antimicrobial interactions: mechanisms and implications for drug discovery and resistance evolution, *Current Opinion in Microbiology*, 27:1–9, 2015.

D. I. Bolnick, L. K. Snowberg, C. Patenia, W. E. Stutz, T. Ingram, and O. L. Lau, Phenotype-dependent native habitat preference facilitates divergence between parapatric lake and stream stickleback, *Evolution*, 63(8):2004–2016, 2009.

S. Bonhoeffer, M. Lipsitch, and B. R. Levin, Evaluating treatment protocols to prevent antibiotic resistance, *Proceedings of the National Academy of Sciences*, 94(22):12106–12111, 1997.

D. Bonte, H. Van Dyck, J. M. Bullock, A. Coulon, M. Delgado, M. Gibbs, V. Lehouck, E. Matthysen, K. Mustin, M. Saastamoinen, N. Schtickzelle, V. M. Stevens, S. Vandewoestijne, M. Baguette, K. Barton, T. G. Benton, A. Chaput-Bardy, J. Clobert, C. Dytham, T. Hovestadt, C. M. Meier, S. C. F. Palmer, C. Turlure, and J. M. J. Travis, Costs of dispersal, *Biological Reviews*, 87(2):290–312, 2012.

D. E. Bowler and T. G. Benton, Causes and consequences of animal dispersal strategies: relating individual behaviour to spatial dynamics, *Biological Reviews*, 80(2):205–225, 2005.

J. R. Bridle, S. J. E. Baird, and R. K. Butlin, Spatial structure and habitat variation in a grasshopper hybrid zone, *Evolution*, 55(9):1832–1843, 2001.

M. G. Bulmer, The genetic variability of polygenic characters under optimizing selection, mutation and drift, *Genetical Research*, 19(1):17–25, 1972.

R. Bürger, *The mathematical theory of selection, recombination, and mutation*, volume 228, Wiley Chichester, 2000.

R. Bürger and A. Gimelfarb, Fluctuating environments and the role of mutation in maintaining quantitative genetic variation, *Genetical Research*, 80(1):31–46, 2002.

R. Bürger and M. Lynch, Evolution and extinction in a changing environment: a quantitative-genetic analysis, *Evolution*, 49(1):151–163, 1995.

M. O. Cáceres and A. A. Budini, The generalized Ornstein-Uhlenbeck process, *Journal of Physics A: Mathematical and General*, 30(24):8427–8444, 1997.

C. Cadet, R. Ferrière, J. A. J. Metz, and M. van Baalen, The evolution of dispersal under demographic stochasticity, *The American Naturalist*, 162(4):427–441, 2003.

R. S. Cantrell, C. Cosner, D. L. Deangelis, and V. Padron, The ideal free distribution as an evolutionarily stable strategy, *Journal of Biological Dynamics*, 1(3):249–271, 2007.

R. S. Cantrell, C. Cosner, and Y. Lou, Evolution of dispersal and the ideal free distribution., *Mathematical Biosciences and Engineering*, 7(1):17–36, 2010.

R. Chait, A. Craney, and R. Kishony, Antibiotic interactions that select against resistance, *Nature*, 446(7136):668–671, 2007.

P. L. Chesson and R. R. Warner, Environmental variability promotes coexistence in lottery competitive systems, *The American Naturalist*, 117(6):923–943, 1981.

L.-M. Chevin, Genetic constraints on adaptation to a changing environment, *Evolution*, 67(3):708–721, 2013.

R. T. Cirz, J. K. Chin, D. R. Andes, V. de Crécy-Lagard, W. A. Craig, and F. E. Romesberg, Inhibition of mutation and combating the evolution of antibiotic resistance, *PLoS Biology*, 3(6):e176, 2005.

R. Courant and D. Hilbert, *Methods of Mathematical Physics, Vol. I*, Interscience, New York, 1954.

R. Cressman and V. Křivan, Migration dynamics for the ideal free distribution, *The American Naturalist*, 168(3):384–397, 2006.

J. F. Crow, Genetic loads and the cost of natural selection, In *Mathematical Topics in Population Genetics*, pages 128–177. Springer, 1970.

E. M. C. D'Agata, M. Dupont-Rouzeyrol, P. Magal, D. Olivier, and S. Ruan, The impact of different antibiotic regimens on the emergence of antimicrobial-resistant bacteria, *PLoS One*, 3(12):e4036, 2008.

E. R. Dempster, Maintenance of genetic heterogeneity, In *Cold Spring Harbor Symposia on Quantitative Biology*, volume 20, pages 25–32. Cold Spring Harbor Laboratory Press, 1955.

U. Dieckmann, B. O'Hara, and W. Weisser, The evolutionary ecology of dispersal, *Trends in Ecology and Evolution*, 14(3):88–90, 1999.

J. E. Diffendorfer, Testing models of source-sink dynamics and balanced dispersal, *Oikos*, 81(3):417–433, 1998.

J. Dockery, V. Hutson, K. Mischaikow, and M. Pernarowski, The evolution of slow dispersal rates: a reaction diffusion model, *Journal of Mathematical Biology*, 37(1):61–83, 1998.

M. J. Donahue, M. Holyoak, and C. Feng, Patterns of dispersal and dynamics among habitat patches varying in quality, *The American Naturalist*, 162(3):302–317, 2003.

C. P. Doncaster, J. Clobert, B. Doligez, E. Danchin, and L. Gustafsson, Balanced dispersal between spatially varying local populations: an alternative to the source-sink model, *The American Naturalist*, 150(4):425–445, 1997.

C. Dytham, Evolved dispersal strategies at range margins, *Proc. R. Soc. Lond. B*, 276(1661):1407–1413, 2009.

P. Edelaar and D. I. Bolnick, Non-random gene flow: an underappreciated force in evolution and ecology, *Trends in Ecology & Evolution*, 27(12):659–665, 2012.

J. A. Endler, *Genetic Variation, Speciation and Clines. (MPB-10)*, Princeton University Press, 1977.

W. J. Ewens, *Mathematical population genetics*, Springer, Berlin, 1979.

D. S. Falconer and T. F. C. Mackay, *Introduction to Quantitative Genetics*, Longman, London, 1995.

J. Felsenstein, Genetic drift in clines which are maintained by migration and natural selection, *Genetics*, 81(1):191–207, 1975.

P. C. Fife, *Mathematical aspects of reacting and diffusing systems*, volume 28 of *Lecture Notes in Biomathematics*, Springer, Berlin, 1979.

R.A. Fisher, The wave of advance of advantageous genes, *Annals of Human Genetics*, 7(4):355–369, 1937.

W. H. Fleming and C.-H. Su, Some one-dimensional migration models in population genetics theory, *Theoretical Population Biology*, 5(3):431–449, 1974.

S. Gandon, Kin competition, the cost of inbreeding and the evolution of dispersal, *Journal of Theoretical Biology*, 200(4):345–364, 1999.

S. Gandon and Y. Michalakis, Evolutionarily stable dispersal rate in a metapopulation with extinctions and kin competition, *Journal of Theoretical Biology*, 199(3):275–290, 1999.

S. Gandon and F. Rousset, Evolution of stepping-stone dispersal rates, *Proc. R. Soc. Lond. B*, 266(1437):2507–2513, 1999.

J. H. Gillespie, Is the population size of a species relevant to its evolution?, *Evolution*, 55(11):2161–2169, 2001.

R. Gomulkiewicz and R. D. Holt, When does evolution by natural selection prevent extinction?, *Evolution*, 49(1):201–207, 1995.

S. J. Gould and N. Eldredge, Punctuated equilibria: the tempo and mode of evolution reconsidered, *Paleobiology*, 3(02):115–151, 1977.

A. Gros, H. J. Poethke, and T. Hovestadt, Evolution of local adaptations in dispersal strategies, *Oikos*, 114(3):544–552, 2006.

C. R. Haag, M. Saastamoinen, J. H. Marden, and I. Hanski, A candidate locus for variation in dispersal rate in a butterfly metapopulation, *Proc. R. Soc. Lond. B*, 272(1580):2449–2456, 2005.

J. B. S. Haldane, The effect of variation on fitness, *The American Naturalist*, 71(735):337–349, 1937.

J. B. S. Haldane, The theory of a cline, *Journal of Genetics*, 48(3):277–284, 1948.

J. B. S. Haldane and S. D. Jayakar, Polymorphism due to selection depending on the composition of a population, *Journal of Genetics*, 58(3):318–323, 1963.

W. D. Hamilton and R. M. May, Dispersal in stable habitats, *Nature*, 269:578–581, 1977.

A. Hastings, Can spatial variation alone lead to selection for dispersal?, *Theoretical Population Biology*, 24(3):244–251, 1983.

A. Hastings and C. L. Hom, Pleiotropic stabilizing selection limits the number of polymorphic loci to at most the number of characters., *Genetics*, 122(2):459–463, 1989.

M. Hegreness, N. Shoresh, D. Hartl, and R. Kishony, An equivalence principle for the incorporation of favorable mutations in asexual populations, *Science*, 311(5767):1615–1617, 2006.

E. Heidenreich, Adaptive mutation in *Saccharomyces cerevisiae*, *Critical Reviews in Biochemistry and Molecular Biology*, 42(4):285–311, 2007.

W. G. Hill, M. E. Goddard, and P. M. Visscher, Data and theory point to mainly additive genetic variance for complex traits, *PLoS Genetics*, 4(2):e1000008, 2008.

R. D. Holt, Population dynamics in two-patch environments: some anomalous consequences of an optimal habitat distribution, *Theoretical Population Biology*, 28(2):181–208, 1985.

T. Hovestadt, S. Messner, and H. J. Poethke, Evolution of reduced dispersal mortality and fat-tailed dispersal kernels in autocorrelated landscapes, *Proc. R. Soc. Lond. B*, 268(1465):385–391, 2001.

J. B. C. Jackson and A. H. Cheetham, Tempo and mode of speciation in the sea, *Trends in Ecology & Evolution*, 14(2):72–77, 1999.

V. A. A. Jansen and R. Vitalis, The evolution of dispersal in a Levins' type metapopulation model, *Evolution*, 61(10):2386–2397, 2007.

M. L. Johnson and M. S. Gaines, Evolution of dispersal: theoretical models and empirical tests using birds and mammals, *Annual Review of Ecology and Systematics*, 21:449–480, 1990.

T. Johnson and N. H. Barton, Theoretical models of selection and mutation on quantitative traits, *Phil. Trans. R. Soc. Lond. B*, 360(1459):1411–1425, 2005.

A. G. Jones, S. J. Arnold, R. Burger, and J. Fry, Evolution and stability of the G-matrix on a landscape with a moving optimum, *Evolution*, 58(8):1639–1654, 2004.

A. Kacelnik, J. R. Krebs, and C. Bernstein, The ideal free distribution and predator-prey populations, *Trends in Ecology & Evolution*, 7(2):50–55, 1992.

T. J. Kawecki and D. Ebert, Conceptual issues in local adaptation, *Ecology Letters*, 7(12):1225–1241, 2004.

P. D. Keightley and W. G. Hill, Quantitative genetic variability maintained by mutation-stabilizing selection balance: sampling variation and response to subsequent directional selection, *Genetical Research*, 54(1):45–58, 1989.

S. Kim, T. D. Lieberman, and R. Kishony, Alternating antibiotic treatments constrain evolutionary paths to multidrug resistance, *Proceedings of the National Academy of Sciences*, 111(40):14494–14499, 2014.

M. Kimura, Stochastic processes and distribution of gene frequencies under natural selection, In *Cold Spring Harbor Symposia on Quantitative Biology*, volume 20, pages 33–53. Cold Spring Harbor Laboratory Press, 1955.

M. Kimura, On the probability of fixation of mutant genes in a population, *Genetics*, 47(6):713, 1962.

M. Kimura, Diffusion models in population genetics, *Journal of Applied Probability*, 1(2):177–232, 1964.

M. Kimura, On the evolutionary adjustment of spontaneous mutation rates, *Genetical Research*, 9(1):23–34, 1967.

M. Kimura, T. Maruyama, and J. F. Crow, The mutation load in small populations, *Genetics*, 48(10):1303–1312, 1963.

M. Kimura and G. H. Weiss, The stepping stone model of population structure and the decrease of genetic correlation with distance, *Genetics*, 49(4):561, 1964.

J. G. Kingsolver, S. E. Diamond, A. M. Siepielski, and S. M. Carlson, Synthetic analyses of phenotypic selection in natural populations: lessons, limitations and future directions, *Evolutionary Ecology*, 26(5):1101–1118, 2012.

J. G. Kingsolver, H. E. Hoekstra, J. M. Hoekstra, D. Berrigan, S. N. Vignieri, C. E. Hill, A. Hoang, P. Gibert, and P. Beerli, The strength of phenotypic selection in natural populations, *The American Naturalist*, 157(3):245–261, 2001.

M. Kirkpatrick and N. H. Barton, Evolution of a species' range, *The American Naturalist*, 150(1):1–23, 1997.

V. Kirzhner and Y. Lyubich, Multilocus dynamics under haploid selection, *Journal of Mathematical Biology*, 35(4):391–408, 1997.

A. S. Kondrashov and L. Y. Yampolsky, High genetic variability under the balance between symmetric mutation and fluctuating stabilizing selection, *Genetical Research*, 68(2):157–164, 1996.

R. Lande, Natural selection and random genetic drift in phenotypic evolution, *Evolution*, 30(2):314–334, 1976.

R. Lande, The genetic covariance between characters maintained by pleiotropic mutations, *Genetics*, 94(1):203–215, 1980.

R. Lande and S. J. Arnold, The measurement of selection on correlated characters, *Evolution*, 37(6):1210–1226, 1983.

T. Lenormand, D. Roze, and F. Rousset, Stochasticity in evolution, *Trends in Ecology & Evolution*, 24(3):157–165, 2009.

H. Leturque and F. Rousset, Dispersal, kin competition, and the ideal free distribution in a spatially heterogeneous population, *Theoretical Population Biology*, 62(2):169–180, 2002.

H. Levene, Genetic equilibrium when more than one ecological niche is available, *The American Naturalist*, 87(836):331–333, 1953.

J. L. Lush, *Animal Breeding Plans*, Iowa State Press, Ames, Iowa, 1937.

F. Lutscher, E. McCauley, and M. A. Lewis, Spatial patterns and coexistence mechanisms in systems with unidirectional flow, *Theoretical Population Biology*, 71(3):267–277, 2007.

M. Lynch and W. G. Hill, Phenotypic evolution by neutral mutation, *Evolution*, 40(5):915–935, 1986.

M. Lynch and J. B. Walsh, *Genetics and analysis of quantitative traits*, Sinauer Press, Sunderland, MA, 1998.

Michael Lynch and Russell Lande, Evolution and extinction in response to environmental change, *Biotic Interactions and Global Change*, pages 234–250, 1993.

K. A. Lythgoe, Consequences of gene flow in spatially structured populations, *Genetical Research*, 69(01):49–60, 1997.

Y. I. Lyubich, *Mathematical Structures in Population Genetics*, Springer, Berlin, Heidelberg, New York, 1992.

R. C. MacLean, C. Torres-Barceló, and R. Moxon, Evaluating evolutionary models of stress-induced mutagenesis in bacteria, *Nature Reviews Genetics*, 14(3):221–227, 2013.

J. Masel, O. D. King, and H. Maughan, The loss of adaptive plasticity during long periods of environmental stasis, *The American Naturalist*, 169(1):38, 2007.

A. Mathias, E. Kisdi, and I. Olivieri, Divergent evolution of dispersal in a heterogeneous landscape, *Evolution*, 55(2):246–259, 2001.

S. Matuszewski, J. Hermisson, and M. Kopp, Catch me if you can: Adaptation from standing genetic variation to a moving phenotypic optimum, *Genetics*, 200(4):1255–1274, 2015.

M. A. McPeek and R. D. Holt, The evolution of dispersal in spatially and temporally varying environments, *The American Naturalist*, 140(6):1010–1027, 1992.

D. W. Morris, P. Lundberg, and J. Ripa, Hamilton's rule confronts ideal free habitat selection, *Proc. R. Soc. Lond. B*, 268(1470):921–924, 2001.

D. J. Murrell, J. M. J. Travis, and C. Dytham, The evolution of dispersal distance in spatially-structured populations, *Oikos*, 97(2):229–236, 2002.

T. Nagylaki, Conditions for the existence of clines, *Genetics*, 80(3):595, 1975.

T. Nagylaki, Random genetic drift in a cline, *Proceedings of the National Academy of Sciences*, 75(1):423–426, 1978.

T. Nagylaki and M. Moody, Diffusion model for genotype-dependent migration, *Proceedings of the National Academy of Sciences*, 77(8):4842–4846, 1980.

D. Nichol, P. Jeavons, A. G. Fletcher, R. A. Bonomo, P. K. Maini, J. L. Paul, R. A. Gatenby, A. R. A. Anderson, and J. G. Scott, Steering evolution with sequential therapy to prevent the emergence of bacterial antibiotic resistance, *PLoS Computational Biology*, 11(9):e1004493, 2015.

S. Novak, The number of equilibria in the diallelic Levene model with multiple demes, *Theoretical Population Biology*, 79(3):97–101, 2011.

S. Novak, Habitat heterogeneities versus spatial type frequency variances as driving forces of dispersal evolution, *Ecology and Evolution*, 4(24):4589–4597, 2014.

K. Parvinen, A. Seppänen, and J. D. Nagy, Evolution of complex density-dependent dispersal strategies, *Bulletin of Mathematical Biology*, 74:2622–2649, 2012.

N. Perrin and J. Goudet, Inbreeding, kinship, and the evolution of natal dispersal, In *Dispersal*, pages 123–142. Oxford University Press, 2001.

G. G. Perron, S. Kryazhimskiy, D. P. Rice, and A. Buckling, Multidrug therapy and evolution of antibiotic resistance: when order matters, *Applied and Environmental Microbiology*, 78(17):6137–6142, 2012.

S. Pigolotti and R. Benzi, Selective Advantage of Diffusing Faster, *Physical Review Letters*, 112(18):188102, 2014.

A. R. Pitman, R. W. Jackson, J. W. Mansfield, V. Kaitell, R. Thwaites, and D. L. Arnold, Exposure to host resistance mechanisms drives evolution of bacterial virulence in plants, *Current Biology*, 15(24):2230–2235, 2005.

M. Prudhomme, L. Attaiech, G. Sanchez, B. Martin, and J.-P. Claverys, Antibiotic stress induces genetic transformability in the human pathogen *Streptococcus pneumoniae*, *Science*, 313(5783):89–92, 2006.

H. R. Pulliam, Sources, sinks, and population regulation, *The American Naturalist*, 132(5):652–661, 1988.

Y. Ram and L. Hadany, The evolution of stress-induced hypermutation in asexual populations, *Evolution*, 66(7):2315–2328, 2012.

C. Reading and M. Cole, Clavulanic acid: a beta-lactamase-inhibiting beta-lactam from *Streptomyces clavuligerus*, *Antimicrobial Agents and Chemotherapy*, 11(5):852–857, 1977.

R. Roemhild, C. Barbosa, R. E. Beardmore, G. Jansen, and H. Schulenburg, Temporal variation in antibiotic environments slows down resistance evolution in pathogenic *Pseudomonas aeruginosa*, *Evolutionary Applications*, 8(10):945–955, 2015.

O. Ronce, How does it feel to be like a rolling stone? Ten questions about dispersal evolution, *Annu. Rev. Ecol. Evol. Syst.*, 38:231–253, 2007.

S. M. Rosenberg, Evolving responsively: adaptive mutation, *Nature Reviews Genetics*, 2(7):504–515, 2001.

F. Rousset and S. Gandon, Evolution of the distribution of dispersal distance under distance-dependent cost of dispersal, *Journal of Evolutionary Biology*, 15(4):515–523, 2002.

D. Roze and F. Rousset, Inbreeding depression and the evolution of dispersal rates: a multilocus model, *The American Naturalist*, 166(6):708–721, 2005.

D. Sellis, B. J. Callahan, D. A. Petrov, and P. W. Messer, Heterozygote advantage as a natural consequence of adaptation in diploids, *Proceedings of the National Academy of Sciences*, 108(51):20666–20671, 2011.

M. Slatkin, Gene flow and selection in a cline, *Genetics*, 75(4):733, 1973.

M. Slatkin, Gene flow in natural populations, *Annual Review of Ecology and Systematics*, 16:393–430, 1985.

M. Slatkin and S. A. Frank, The quantitative genetic consequences of pleiotropy under stabilizing and directional selection, *Genetics*, 125(1):207–213, 1990.

P. D. Sniegowski, P. J. Gerrish, T. Johnson, and A. Shaver, The evolution of mutation rates: separating causes from consequences, *BioEssays*, 22(12):1057–1066, 2000.

M. L. Stanton, Reproductive biology of petal color variants in wild populations of Raphanus sativus: I. Pollinator response to color morphs, *American Journal of Botany*, 74(2):178–187, 1987.

M. Szulkin and B. C. Sheldon, Dispersal as a means of inbreeding avoidance in a wild bird population, *Proc. R. Soc. Lond. B*, 275(1635):703–711, 2008.

J. M. Szymura and N. H. Barton, Genetic analysis of a hybrid zone between the fire-bellied toads, *Bombina bombina* and *B. variegata*, near Cracow in southern Poland, *Evolution*, 40(6):1141–1159, 1986.

F. Taddei, M. Radman, J. Maynard-Smith, B. Toupance, P. H. Gouyon, and B. Godelle, Role of mutator alleles in adaptive evolution, *Nature*, 387(6634):700–702, 1997.

P. D. Taylor, An inclusive fitness model for dispersal of offspring, *Journal of Theoretical Biology*, 130(3):363–378, 1988.

K. C. Teeter, B. A. Payseur, L. W. Harris, M. A. Bakewell, L. M. Thibodeau, J. E. O'Brien, J. G. Krenz, M. A. Sans-Fuentes, M. W. Nachman, and P. K. Tucker, Genome-wide patterns of gene flow across a house mouse hybrid zone, *Genome Research*, 18(1):67–76, 2008.

C. Torres-Barceló, M. Kojadinovic, R. Moxon, and R. C. MacLean, The SOS response increases bacterial fitness, but not evolvability, under a sublethal dose of antibiotic, *Proc. R. Soc. Lond. B*, 282(1816):20150885, 2015.

J. M. J. Travis and E. R. Travis, Mutator dynamics in fluctuating environments, *Proc. R. Soc. Lond. B*, 269(1491):591–597, 2002.

M. Turelli, Heritable genetic variation via mutation-selection balance: Lerch's zeta meets the abdominal bristle, *Theoretical Population Biology*, 25(2):138–193, 1984.

M. Turelli, Effects of pleiotropy on predictions concerning mutation-selection balance for polygenic traits, *Genetics*, 111(1):165–195, 1985.

M. Turelli and N. H. Barton, Polygenic variation maintained by balancing selection: pleiotropy, sex-dependent allelic effects and G$\times$E interactions, *Genetics*, 166(2):1053–1079, 2004.

L. Van Valen, Group selection and the evolution of dispersal, *Evolution*, 25(4):591–598, 1971.

J. N. Waddell, L. M. Sander, and C. R. Doering, Demographic stochasticity versus spatial variation in the competition between fast and slow dispersers, *Theoretical Population Biology*, 77(4):279–286, 2010.

R. Weinstock, *Calculus of Variations*, Dover, New York, 1974.

G. H. Weiss and M. Kimura, A mathematical analysis of the stepping stone model of genetic correlation, *Journal of Applied Probability*, 2(1):129–149, 1965.

A. C. Whibley, N. B. Langlade, C. Andalo, A. I. Hanna, A. Bangham, C. Thébaud, and E. Coen, Evolutionary paths underlying flower color variation in *Antirrhinum*, *Science*, 313(5789):963–966, 2006.

R. J. Woods, J. E. Barrick, T. F. Cooper, U. Shrestha, M. R. Kauth, and R. E. Lenski, Second-order selection for evolvability in a large *Escherichia coli* population, *Science*, 331(6023):1433–1436, 2011.

S. Wright, Isolation by distance, *Genetics*, 28(2):114, 1943.

X.-S. Zhang and W. G. Hill, Multivariate stabilizing selection and pleiotropy in the maintenance of quantitative genetic variation, *Evolution*, 57(8):1761–1775, 2003.

Appendix

A1 Modelling SIM alleles

A1.1 Dynamics of SIM allele frequencies

We start by casting the schematic dynamics of Figure 2.1 into differential equations of the form (2.1) and analysing their behaviour. The aim of this section is to analyse the dynamics of the SIM allele frequency in the stress and the no-stress environments.

The normal environment. In the normal (i.e., no-stress) environment, the genotype frequencies evolve according to,

$$\begin{cases} \dot{p}_{mr} &= \mu_M\, p_{Mr} + \mu_R\, p_{mR} - \nu_R\, p_{mr} \\ \dot{p}_{Mr} &= \mu_R\, p_{MR} - (\mu_M + \nu_R)\, p_{Mr} \\ \dot{p}_{mR} &= \nu_R\, p_{mr} + \mu_M\, p_{MR} - \mu_R\, p_{mR} \\ \dot{p}_{MR} &= \nu_R\, p_{Mr} - (\mu_M + \mu_R)\, p_{MR} \end{cases}, \tag{A1.1}$$

where the dot indicates a derivative with respect to time, $\dot{p} = dp/dt$. In terms of the the frequency of the SIM allele, $p_M = p_{Mr} + p_{MR}$, the frequency of resistant genotypes, $p_R = p_{mR} + p_{MR}$, and the frequency of resistant genotypes among those that carry the SIM allele, $q = p_{MR}/p_M$, we may rewrite equations (A1.1) as

$$\begin{cases} \dot{p}_M &= -\mu_M\, p_M \\ \dot{p}_R &= \nu_R\,(1 - p_R) - \mu_R\, p_R \\ \dot{q} &= \nu_R\,(1 - q) - \mu_R\, q \end{cases}. \tag{A1.2}$$

Remarkably, these equations are independent from each other. Furthermore, the equations for p_R and q are identical; given the same initial conditions $p_R(0)$ and $q(0)$, these two variables thus remain the same. The solution to the equations (A1.2) are

$$\begin{cases} p_M(t) &= p_M(0)\, e^{-\mu_M\, t} \\ p_R(t) &= \left(1 - e^{-(\mu_R+\nu_R)t}\right) \frac{\nu_R}{\mu_R+\nu_R} + p_R(0)\, e^{-(\mu_R+\nu_R)t} \\ q(t) &= \left(1 - e^{-(\mu_R+\nu_R)t}\right) \frac{\nu_R}{\mu_R+\nu_R} + q(0)\, e^{-(\mu_R+\nu_R)t} \end{cases} . \tag{A1.3}$$

The stress environment. To obtain tractable equations for the stress environment, we assume that s and σ are large, and that the duration of stress is short relative to the duration of no stress. More precisely, we take the full set of equations,

$$\begin{cases} \dot{p}_{mr} &= -s\, p_{mr}\, (p_{mR} + p_{MR}) + \sigma \mu_M\, p_{Mr} - \nu_R\, p_{Mr} + \mu_R\, p_{mR} \\ \dot{p}_{Mr} &= -s\, p_{Mr}\, (p_{mR} + p_{MR}) - \sigma\, (\mu_M + \nu_R)\, p_{Mr} + \mu_R\, p_{MR} \\ \dot{p}_{mR} &= s\, p_{mR}\, (1 - p_{mR} - p_{MR}) + \nu_R\, p_{mr} - \mu_R\, p_{mR} + \mu_M\, p_{MR} \\ \dot{p}_{MR} &= s\, p_{MR}\, (1 - p_{mR} - p_{MR}) + \sigma \nu_R\, p_{Mr} - (\mu_R + \mu_M)\, p_{MR} \end{cases} , \tag{A1.4}$$

replace $s \mapsto \alpha s$, $\sigma \mapsto \alpha\sigma$, and rescale time $dt \mapsto dt/\alpha$. Then, dividing by α and letting $\alpha \to \infty$, we may neglect the rightmost terms of the above equations. We thus obtain

$$\begin{cases} \dot{p}_{mr} &= -s\, p_{mr}\, (p_{mR} + p_{MR}) + \sigma \mu_M\, p_{Mr} \\ \dot{p}_{Mr} &= -s\, p_{Mr}\, (p_{mR} + p_{MR}) - \sigma\, (\mu_M + \nu_R)\, p_{Mr} \\ \dot{p}_{mR} &= s\, p_{mR}\, (1 - p_{mR} - p_{MR}) \\ \dot{p}_{MR} &= s\, p_{MR}\, (1 - p_{mR} - p_{MR}) + \sigma \nu_R\, p_{Mr} \end{cases} . \tag{A1.5}$$

This approximation corresponds to neglecting all mutational transitions that are not multiplied by σ in Figure 2.1b. Evidently, this dynamics converges to a unique equilibrium where all genotypes are resistant, and some fraction of genotypes containing the SIM allele. In terms of the variables introduced above, this corresponds to $p_R(t) \to 1$, $q(t) \to 1$, and $p_M(t) \to p_M^*$ for $t \to \infty$.

To calculate an expression for p_M^* analytically, we recast the system (A1.5) using the variables $p_R = p_{mR} + p_{MR}$, $y = p_{Mr}/p_R$, and $z = p_{mR}/p_R$:

$$\begin{cases} \dot{p}_R &= s\, p_R\, (1 - p_R) + \sigma\, \nu_R\, p_R\, y \\ \dot{y} &= -y\, [s + \sigma\, (\mu_M + \nu_R\, (1 + y))] \\ \dot{z} &= -\sigma \nu_R\, y\, z \end{cases} . \tag{A1.6}$$

For given initial conditions ($p_R(0)$, $y(0)$, $z(0)$) and $t \to \infty$, this system converges to $p_R(t) \to 1$, $y(t) \to 0$, and

$$z(t) \to z_\infty = z(0)\,\frac{s + \sigma\,(\mu_M + \nu_R)}{s + \sigma\,(\mu_M + \nu_R\,(1 + y(0)))}. \tag{A1.7}$$

The expression for p_M^* is then calculated as $p_M^* = (1 - z_\infty)$.

A1.2 Recursions for the SIM allele frequencies

Here, we set up recursions for the SIM allele frequency in the two limiting cases discussed in the main text, Section 2.3.1, the (R) and (NR) regimes. In both cases, we measure the genotype frequencies directly before each stress to obtain the SIM allele frequency p'_M after one cycle of stress and no stress by

$$p'_M = (\mathcal{G} \circ \mathcal{F})\,(p_M), \tag{A1.8}$$

where $\mathcal{F}$ and $\mathcal{G}$ are two mappings describing the stress and no-stress phases, respectively.

Throughout, we use the approximation of the stress dynamics from the previous section, describing it by an instantaneous jump in the SIM allele frequency, $p_M \to \mathcal{F}(p_M) = p_M^*$. Thus, selection is assumed to be strong enough to fix the resistance allele practically immediately. Furthermore, if the stress does not persist for long, mutations from p_{MR} to p_{mR} can be neglected, and $p_M^* = (1 - z_\infty)$ (with z_∞ from equation (A1.7)) can be expected to approximate the full dynamics (A1.4) (Figure 2.1b) well.

We assume that one iteration of stress and no stress takes τ time units. In the main text (Section 2), we denoted the duration of the stress and no-stress environments by τ_S and τ_{NS}, respectively. In our analytical approach here, stress is approximated by an instantaneous jump in allele frequencies, hence $\tau_S = 0$, and we apply the no-stress environment for $\tau_{NS} = \tau$ time units. Thus, the mapping $\mathcal{G} = \mathcal{G}_\tau$ depends explicitly on τ; due to equation (A1.3), we have

$$\mathcal{G}(P) = \mathcal{G}_\tau(P) = P\,e^{-\mu_P\,\tau}. \tag{A1.9}$$

The mappings of the jumps for the two stress regimes, $\mathcal{F}^{(R)}$ and $\mathcal{F}^{(NR)}$, will be defined below.

In contrast to the approximation described here, numerical simulations of the full dynamics, i.e., iterating the equations (A1.4) for the stress environment and equations (A1.1) for the no-stress environment, naturally require $\tau_S > 0$ and $\tau_{NS} = \tau - \tau_S$. However, a comparison between our analytical results (see below) and simulations of the full dynamics for identical values of τ demonstrates a good fit between the two approaches, indicating that the approximations made here are justified (see also Figure 2.3).

The recurrent stress regime. Suppose that the same stress occurs every $\tau > 0$ time units. Since we assume that each stress phase leads to the fixation of the resistance allele, we have that $p_R = q = 1$ at the beginning of each no-stress phase. Hence, because the equations of these two variables are identical, see equation (A1.2), we have $p_R(t) = q(t)$ for all times after the first occurrence of stress. At the end of each no-stress period, we thus have

$$p_R(\tau) = q(\tau) = \frac{\nu_R}{\mu_R + \nu_R} + e^{-(\mu_R+\nu_R)\tau}\left(1 - \frac{\nu_R}{\mu_R + \nu_R}\right) \tag{A1.10}$$

due to equation (A1.3). Inserting these values to obtain new initial frequencies for the next stress phase required for equation (A1.7) allows us to calculate z_∞ and thus

$$\begin{aligned}\mathcal{F}^{(R)}(P) &= 1 - z_\infty = \\ &= 1 - \frac{(p_R(\tau) - P\,q(\tau))\,(s + \sigma\,(\mu_P + \nu_R))}{s\,p_R(\tau) + \sigma\,[p_R(\tau)\,(\mu_P + \nu_R) + \nu_R\,P\,(1 - q(\tau))]}.\end{aligned} \tag{A1.11}$$

Inserting this expression and the identity (A1.9) into the general recursion (A1.8), and solving for equilibria fulfilling $\hat{p}_M^{(R)} = \left(\mathcal{G} \circ \mathcal{F}^{(R)}\right)(\hat{p}_M^{(R)})$, provides the long-term prevalence of the SIM allele in the recurrent stress regime, $\hat{p}_M^{(R)}$, as given in equation (2.3a).

The non-recurrent stress regime. Suppose that the population does not experience the same stress twice. As a consequence, we may neglect any resistance gained from previous stress occurrences. Instead, we assume that the fraction of genotypes that initially are resistant against an upcoming stress is in mutation balance, i.e., determined by the relative rates of gaining and losing resistance by mutation. Hence, we may use $p_R = q = \nu_R/\,(\mu_R + \nu_R)$ to determine the initial conditions for the stress phase leading to z_∞ in equation (A1.7). Analogously to the above, this yields an expression

for $\mathcal{F}^{(NR)}$. Solving $\hat{p}_M^{(NR)} = \left(\mathcal{G} \circ \mathcal{F}^{(NR)}\right)(\hat{p}_M^{(NR)})$, we obtain the long-term prevalence of the SIM allele in the non-recurrent stress regime, $\hat{p}_M^{(NR)}$, as given in equation (2.3b).

A1.3 Comparison between stress regimes

We assign the following names to the non-trivial terms on the right hand sides of equation (2.3):

$$\mathcal{P}_\tau^{(R)} = e^{-\mu_M \tau} - \aleph\left(1 - e^{-\mu_M \tau}\right)\left(1 + \frac{\mu_R + \nu_R}{\nu_R}\left(e^{(\mu_R+\nu_R)\tau} - 1\right)^{-1}\right), \tag{A1.12a}$$

$$\mathcal{P}_\tau^{(NR)} = e^{-\mu_M \tau} - \aleph\left(1 - e^{-\mu_M \tau}\right), \tag{A1.12b}$$

where $\aleph > 0$ is defined in equation (2.4). Since

$$\Delta = \mathcal{P}_\tau^{(NR)} - \mathcal{P}_\tau^{(R)} = \frac{1 - e^{-\mu_P \tau}}{e^{(\mu_R+\nu_R)\tau} - 1}\,\frac{\mu_R + \nu_R}{\nu_R}\,\aleph > 0, \tag{A1.13}$$

the long-term SIM allele prevalence under non-recurrent stresses is never lower than in the recurrent stress regime ($\hat{p}_M^{(NR)} \geq \hat{p}_M^{(R)}$). In particular, for $\tau = \tau_c$ the value of Δ, and hence of $\mathcal{P}_{\tau_c}^{(R)}$, is already negative.

We may argue that the SIM allele cannot be maintained in the population in the recurrent stress regime if ν_R is sufficiently small compared to μ_R. To this end, we rewrite equation (A1.13) as

$$\Delta = \frac{1}{\varepsilon}\,\frac{1 - e^{-\mu_P \tau}}{e^{(\mu_R+\nu_R)\tau} - 1}\,\aleph. \tag{A1.14}$$

Then, $\nu_R \ll \mu_R$ corresponds to $\varepsilon \ll 1$. Furthermore, on the closed interval $[0, \tau_c]$, the function

$$\frac{1 - e^{-\mu_P \tau}}{e^{(\mu_R+\nu_R)\tau} - 1}\,\aleph$$

is bounded away from zero, i.e., it has a positive minimum. Therefore, if ν_R is small, $1/\varepsilon$ is large, and hence Δ is large on $[0, \tau_c]$. Thus, by choosing ν_R sufficiently small, we may push $\mathcal{P}_\tau^{(R)}$ arbitrarily far below zero, thus $\hat{p}_M^{(R)} \equiv 0$ for all $\tau \geq 0$.

A2 Technical details of dispersal evolution

A2.1 Derivation of the model equations

Here, I derive the model equations (3.2) for a population consisting of n types that occupy a habitat $\Omega \subseteq \mathbb{R}$. In addition to the main text, I consider variable growth rates between types to illustrate how, e.g., explicit cost of dispersal or selection could be incorporated into the model. Let $r_i = r_i(x, N_T)$ denote the per-capita growth rate of type i.

Local reproduction changes the type densities N_i to N_i^*. We assume that this change is small, namely proportional to the (infinitesimal) time interval under consideration, Δt, and neglect all weaker effects, $o(\Delta t)$. Then, we may write

$$N_i^*(x,t) = N_i(x,t)(1 + r_i(x,t)\Delta t) + o(\Delta t). \tag{A2.1}$$

Second, we model dispersal. For each individual of type i that is located at position y at time t, the probability to migrate into an interval around x of length Δx within Δt time units is expressed via the dispersal kernels μ_i by $\mu_i(y,t;x,t+\Delta t)\Delta x$. Using the dispersal kernels μ_i, which naturally fulfil $\int_\Omega \mu_i(y,t;x,s)dx = 1$, we obtain the next generation by

$$N_i(x,t+\Delta t) = \int_\Omega N_i^*(y,t)\mu_i(y,t;x,t+\Delta t)dy. \tag{A2.2}$$

If the dispersal kernels fulfil the assumptions (3.1) and are sufficiently smooth, they satisfy a Kolmogorov forward equation (see, e.g., Bharucha-Reid (1960), pp.130–136)

$$\begin{aligned}\partial_s \mu_i(y,t;x,s) =& \frac{1}{2}\partial_{xx}\left(V_i(x,t)\mu_i(y,t;x,s)\right) - \\ &- \partial_x\left(M_i(x,t)\mu_i(y,t;x,s)\right).\end{aligned} \tag{A2.3}$$

Using equations (A2.1) and (A2.2), and dividing by Δt, we find

$$\begin{aligned}&\frac{N_i(x,t+\Delta t) - N_i(x,t)}{\Delta t} = \\ &= \int_\Omega N_i(y,t)\,\frac{\mu_i(y,t;x,t+\Delta t) - \mu_i(y,t;x,t)}{\Delta t}\,dy + \\ &+ \int_\Omega \left(N_i(y,t)r_i(y,t) + \frac{o(\Delta t)}{\Delta t}\right)\mu_i(y,t;x,t+\Delta t)\,dy.\end{aligned} \tag{A2.4}$$

For $\Delta t \to 0$, (A2.3) can be inserted into (A2.4) to obtain

$$\begin{aligned}\partial_t N_i(x,t) = \frac{1}{2}\partial_{xx}\left(V_i(x,t)\int_\Omega N_i(y,t)\mu_i(y,t;x,t)dy\right) - \\ - \partial_x\left(M_i(x,t)\int_\Omega N_i(y,t)\mu_i(y,t;x,t)dy\right) + \\ + \int_\Omega N_i(y,t)r_i(y,t)\mu_i(y,t;x,t)dy. \qquad \text{(A2.5)}\end{aligned}$$

Since $\mu_i(y,t;x,t)$ is a point mass, the integrals resolve to

$$\partial_t N_i = -\partial_x J_i + N_i r_i, \qquad \text{(A2.6)}$$

where $J_i = M_i N_i - \frac{1}{2}\partial_x(V_i N_i)$ is the flux of individuals of type i as in the main text.

With $N_T(x,t) = \sum_i N_i(x,t)$ and $p_i(x,t) = \frac{N_i(x,t)}{N_T(x,t)}$, a short calculation shows that N_T evolves according to

$$\begin{aligned}\partial_t N_T &= -\partial_x\left(\bar{M}N_T - \frac{1}{2}\partial_x\left(\bar{V}N_T\right)\right) + \sum_{j=1}^n N_j r_j \\ &= -\partial_x J_T + N_T\bar{r}, \qquad \text{(A2.7a)}\end{aligned}$$

where $\bar{r} = \sum_{j=1}^n p_j r_j$, $\bar{M} = \sum_{j=1}^n M_j p_j$ and $\bar{V} = \sum_{j=1}^n V_j p_j$, and $J_T = \sum_i J_i$ is the overall flux of individuals. Applying the quotient rule to $\partial_t p_i = \partial_t(N_i/N_T)$ furthermore gives

$$\begin{aligned}\partial_t p_i &= \frac{1}{N_T}\left(-\partial_x J_i + p_i\partial_x J_T + N_i r_i - p_i\sum_{j=1}^n N_j r_j\right) \\ &= \frac{1}{N_T}\left(-\partial_x J_i + p_i\partial_x J_T\right) + p_i(r_i - \bar{r}). \qquad \text{(A2.7b)}\end{aligned}$$

Compare (A2.7b) to the model by Nagylaki and Moody (1980). With $r_i = r$ for all i, the equations (A2.7) simplify to the model equations (3.2).

A2.2 Separation of time scales

Assume that growth rates and dispersal patterns are identical for all types, i.e., $r_i \equiv r$, $M_i \equiv M_0$ and $V_i \equiv V_0$ for all i. We write the dynamics of this reference population $N_{0,T}$ as

$$\partial_t N_{0,T} = -\partial_x J_{0,T} + r N_{0,T}, \qquad \text{(A2.8)}$$

where the reference flux is given by $J_{0,T} = M_0 N_{0,T} - 1/2 \partial_x V_0 N_{0,T}$. Now suppose that dispersal patterns deviate only slightly from the reference pattern, $M_i = M_0 + m_i$ and $V_i = V_0 + v_i$, where m_i and v_i (and their derivatives) are of order $O(\varepsilon)$. Furthermore assume that $\partial_x p_i$ and $\partial_{xx} p_i$ stay bounded. This assumption is natural since local agglomerates flatten out by diffusion. Then, the population density dynamics, equation (3.2a), are dominated by the reference dynamics (A2.8), i.e., they differ only up to order $O(\varepsilon)$:

$$\begin{aligned}\partial_t N_T =& -\partial_x J_{0,T} + r N_T + \frac{\bar{v}}{2}\partial_{xx} N_T - \\ & - (\bar{m} - \partial_x \bar{v})\partial_x N_T - \left(\partial_x \bar{m} + \frac{\partial_{xx}\bar{v}}{2}\right) N_T \\ =& -\partial_x J_{0,T} + r N_T + O(\varepsilon),\end{aligned} \tag{A2.9}$$

where $\bar{m} = \sum m_j p_j$ and $\bar{v} = \sum v_j p_j$ are the average deviations from the reference values M_0 and V_0. Since $r_i \equiv r$ for all i, the right hand side of equation (3.2b) can be approximated by the reference flux as

$$\partial_t p_i \approx \frac{1}{N_T}\left(-\partial_x J_{0,i} + p_i \partial_x J_{0,T}\right), \tag{A2.10}$$

where $J_{0,i} = M_0 p_i N_{0,T} - 1/2 \partial_x V_0 p_i N_{0,T}$. Assuming that type frequencies spread out such that $\partial_x p_i$ and $\partial_{xx} p_i$ become negligibly small, expanding the right hand side of (A2.10) shows that $\partial_t p_i = O(\varepsilon)$.

A2.3 Stability of balanced dispersal

Consider the dynamics of two types in terms of (A2.6) for uniform growth rates $r_0 = r_I = r$, reading

$$\partial_t N_0 = -\partial_x J_0 + N_0 r, \tag{A2.11a}$$

$$\partial_t N_I = -\partial_x J_I + N_I r, \tag{A2.11b}$$

and assume that the original type N_0 follows a balanced dispersal strategy, i.e., $\partial_x V_0 \kappa - M_0 \kappa = const$. The dispersal strategy of the modified type N_I deviates from that of N_0 only slightly, $V_1 = V_0 + v$ and $M_1 = M_0 + m$. In the absence of the modifier, N_0 equilibrates at carrying capacity $N_0^* = \kappa$. I show that this equilibrium is asymptotically stable against invasion of non-balanced dispersal strategies.

At equilibrium, $r \equiv 0$. Setting $N_I(x,t) = \kappa e^{-\lambda t} Q(x)$, equation (A2.11b) transforms into an eigenvalue problem of Sturm-Liouville type (Courant and Hilbert, 1954; Weinstock, 1974):

$$0 = \frac{1}{2}\,\partial_x\left((V_0+v)\kappa\partial_x Q\right) + \partial_x(\Phi Q) + \lambda\kappa Q, \tag{A2.12}$$

where $\Phi = 1/2\partial_x(v\kappa) - m\kappa$. Upon multiplication with the integrating factor

$$\frac{2e^{\xi}}{(V_0+v)\kappa}, \qquad \text{where } \xi = \int \frac{\partial_x[(V_0+v)\kappa] + \Phi}{(V_0+v)\kappa} dx,$$

equation (A2.12) can be written in self-adjoint form

$$0 = \partial_x\left(e^{\xi}\partial_x Q\right) + \left(2e^{\xi}\frac{\partial_x\Phi}{(V_0+v)\kappa} + \lambda\frac{2e^{\xi}}{V_0+v}\right) Q. \tag{A2.13}$$

If Φ is constant, the eigenvalues of (A2.13) are known to constitute a non-negative sequence $0 \le \lambda_0 < \lambda_1 < ...$ (Weinstock, 1974). It is easy to see that $\lambda_0 = 0$ is an eigenvalue with constant eigenfunction $Q_0 \equiv const$. Therefore, if the modifier uses a balanced dispersal strategy ($\Phi \equiv const$), it is neutral with respect to the original type.

Now assume that $\Phi \neq const$. If m and v are small, $\partial_x\Phi$ is small and equation (A2.13) can be seen as a perturbation of the case $\Phi \equiv const$. Eigenvalues of (A2.13) depend continuously on the coefficients of the system (Courant and Hilbert, 1954). Thus, the following perturbation analysis is justified. I write $m = \varepsilon\tilde{m}$ and $v = \varepsilon\tilde{v}$. Then, $\Phi = \varepsilon\tilde{\Phi}$ and we consider the smallest eigenvalue and its eigenfunction to be a function of ε, i.e., $\lambda_0 = \lambda_0(\varepsilon)$ and $Q_0 = Q_0(\varepsilon)$. With this notation, the derivative $d\lambda_0/d\varepsilon$ determines the stability of the system.

Using the variational characterization of eigenvalues of (A2.13), $Q_0(\varepsilon)$ minimizes the functional

$$\int_\Omega e^{\xi}(\partial_x Q)^2 - \varepsilon\,\frac{2e^{\xi}\partial_x\tilde{\Phi}}{(V_0+v)\kappa}\,Q^2 dx, \tag{A2.14}$$

and its minimal value is $\lambda_0(\varepsilon)$. Since $\lambda_0(0) = 0$ and $Q_0(0) \equiv const$, the required derivative is

$$\frac{d\lambda_0}{d\varepsilon}(0) = \int_\Omega \frac{2\Phi^2}{(V_0+v)\kappa} e^{\int \Phi/[(V_0+v)\kappa]} dx - \left(e^{\int \Phi/[(V_0+v)\kappa]}\Phi\right)\Big|_\Omega. \tag{A2.15}$$

This expression is positive since the last term vanishes under reasonable assumptions on the boundaries of the habitat. Thus, the introduction of a non-balanced dispersal strategy causes the minimal eigenvalue to become positive and hence, the original population is protected from invasion by a non-balanced dispersal strategy.

A2.4 Genetic drift in a stepping stone model

We employ a stepping stone model (Kimura and Weiss, 1964) as a discrete analogue of the type frequency dynamics under type-dependent dispersal, equation (3.2b). The recursion for the type frequencies reads

$$p'_{(j)} = \frac{p_{(j)} + \frac{\mathcal{M}+m}{2}\left(p_{(j-1)} + p_{(j+1)} - 2p_{(j)}\right)}{1 + \frac{m}{2}\left(p_{(j-1)} + p_{(j+1)} - 2p_{(j)}\right)} \qquad j = 1, ..., \mathcal{J}, \tag{A2.16}$$

where the prime denotes frequencies measured in the next generation. With this notation, I assume that the habitat Ω consists of $\mathcal{J}$ equally spaced patches. Dispersal is described by migration rates $0 < \mathcal{M} < 1$ that determine the fraction of individuals leaving their patch to migrate to one of the adjacent patches (nearest-neighbour migration) with equal probability. These rates then translate into diffusiveness values of $V = \mathcal{M}(\Omega/\mathcal{J})^2$ and $M = 0$. The modifier type has frequency $p_{(j)}$ in patch j and migration rate $\mathcal{M} + m$, the original type thus has frequency $1 - p_{(j)}$ and migration rate $\mathcal{M}$.

If each of the $\mathcal{J}$ patches contains $\mathcal{N}$ individuals, the total number of individuals present in the habitat is $\Omega N_T = \mathcal{J}\mathcal{N}$. However, population size does not enter equation (A2.16) since it is assumed to be constant. This assumption can be justified by a specific population regulation mechanism or by taking m sufficiently small. Note that carrying capacity is considered to be spatially homogeneous and dispersal to be unconditional, hence population size is at carrying capacity at all times. Starting out from equation (A2.16), we can derive an expression for the change in the number of modifiers during one generation. For $m \ll \mathcal{M} \ll 1$, it reads

$$\begin{aligned}\Delta\mathcal{N}_I^{total} &= \sum_j \mathcal{N}\left(p'_{(j)} - p_{(j)}\right) = \\ &= -\frac{m\mathcal{N}}{2}\sum_j p_{(j)}\left(p_{(j-1)} + p_{(j+1)} - 2p_{(j)}\right).\end{aligned} \tag{A2.17}$$

This expression is equivalent to a discretization of the corresponding equation in the continuous setting, equation (3.7). If the habitat is homogeneous, the system is translation invariant at equilibrium. Then, taking the expectation of (A2.17) over a realization of the sampling process, we find that the expected change in total modifier abundance is given by equation (3.8).

The variance σ_p and the between-patch correlation ρ of type frequencies in space have been analysed under dispersal and selection, e.g., Felsenstein (1975); Nagylaki (1978), and under dispersal and mutation, e.g., Kimura and Weiss (1964); Weiss and Kimura (1965), ultimately yielding expressions for these quantities at stochastic equilibrium. Additional mechanisms like selection or mutation need to be evoked, since under random drift alone one type will eventually fix in the population, which leads to zero variance of type frequencies at equilibrium. In the articles mentioned above, only the presence of a single dispersal type in the population has been analysed. However, since the migration modification m is small, we will expand (3.8) only up to leading order in m such that this deficiency can be ignored.

I follow Kimura and Weiss (1964) to derive the variance of type frequencies, σ_p, and the correlation between type frequencies in adjacent patches, ρ. For the purpose of this calculation, I assume an infinite habitat where patches are indexed by $j \in \mathbb{Z}$. Let $\mathfrak{M}$ denote the migration matrix, i.e., $\mathfrak{M}_{ij}$ is the migration rate from patch i to patch j. For nearest-neighbour migration, set $\mathfrak{M}_{ij} = 1 - \mathcal{M}$ for $i = j$, $\mathfrak{M}_{ij} = \mathcal{M}/2$ for $j = i \pm 1$, and $\mathfrak{M}_{ij} = 0$ in all other cases. Denote the mutation rates to and from the focal type by ν_1 and $\nu_2 = \nu - \nu_1$, such that $\nu = \nu_1 + \nu_2$ is the total mutation rate. The dynamics of type frequencies $p_{(j)}$ is then given by

$$p'_{(j)} = (1 - \nu)\left(\mathfrak{M}.\mathbf{p}\right)_j + \nu_2 + \xi_j \tag{A2.18}$$

where $\mathbf{p} = (p_{(j)})_{j\in\mathbb{Z}}$ summarizes local type frequencies in a single vector. The random variable ξ_j describes genetic drift independently in each patch. It has zero mean and a variance of $p_{(j)}(1 - p_{(j)})/(2\mathcal{N})$.

From this, we may derive recursions for the expected type frequency, its variance and the covariance between patches – see also Fleming and Su (1974). Expected type frequencies settle at their homogeneous equilibrium determined solely by the mutation rates. Hence, I set $\mathbb{E}[p_{(j)}] = P$ uniformly in space. The remaining equations for the variances and covariances of gene frequencies can be solved assuming that correlations between patches decay geometrically with distance. For $\nu \ll \mathcal{M} \ll 1$ we obtain

$$\sigma_p = \frac{P(1-P)}{1 + 4\mathcal{N}\sqrt{2\mathcal{M}\nu}} \quad \text{and} \quad \rho = 1 - \frac{\sqrt{2\mathcal{M}\nu}}{\mathcal{M}}, \tag{A2.19}$$

see Kimura and Weiss (1964). Inserting into equation (3.8) produces

$$\mathbb{E}\left[\Delta \mathcal{N}_I^{total}\right] = m\mathcal{J}\mathcal{N}\frac{P(1-P)\sqrt{2\mathcal{M}\nu}}{\mathcal{M}(1+4\mathcal{N}\sqrt{2\mathcal{M}\nu})}. \tag{A2.20}$$

If the number of individuals per patch, $\mathcal{N}$, is large, the result simplifies as the denominator is approximately $4\mathcal{N}\mathcal{M}\sqrt{2\mathcal{M}\nu}$. Then, we may rewrite equation (A2.20), as

$$\mathbb{E}\left[\Delta \mathcal{N}_I^{total}\right] = \frac{m\mathcal{J}}{4\mathcal{M}}P(1-P).$$

Denote the average frequency of the modifier in the habitat by P. Then, dividing by the total population size $\mathcal{J}\mathcal{N}$, we obtain

$$\mathbb{E}\left[\Delta P\right] \approx \frac{m}{4\mathcal{N}\mathcal{M}}P(1-P). \tag{A2.21}$$

This expression is analogous to a haploid selection model with selection parameter $s = m/(4\mathcal{N}\mathcal{M})$.

A3 Frequency-independence and polymorphism

A3.1 Notation and assumptions

In this supplementary section, I formally prove that constant, frequency-independent selection eliminates genetic variation (c.f. the discussion in Section 1.3). If selection is also additive (alleles contribute additively to fitness), the result was shown by Kirzhner and Lyubich (1997). The proof presented here does not require additivity of selection, permitting epistatic interactions between alleles at different loci.

I assume that there are L genetic loci, indexed by $i \in \{1, ..., L\}$. Locus i has K_i possible allelic variants; I write $\mathcal{K} = \sum_{i=1}^{L} K_i$ for the total number of alleles across all loci. For $k \in \{1, ..., K_i\}$, denote the k-th allele on locus i by P_k^i. The frequency of allele P_k^i is p_k^i. Clearly, we have $\sum_{k=1}^{K_i} p_k^i = 1$ for every $i \in \{1, ..., L\}$. Furthermore, I denote the vector of allele frequencies at locus i by $\mathbf{p}^i$, and collect the allele frequencies at all loci in $\mathbf{p} = (\mathbf{p}^1, ..., \mathbf{p}^L)$.

A haploid genotype $\{P_{k_1}^1, ..., P_{k_L}^L\}$ is a list of alleles that sit on their respective loci ($k_i \in \{1, ..., K_i\}$). I assume that selection is weak relative to recombination, hence there is linkage equilibrium at all times. Then, the frequency of any genotype $\{P_{k_1}^1, ..., P_{k_L}^L\}$ is given by the product of the frequencies of the alleles it consists of, $\prod_{i=1}^{L} p_{k_i}^i$, and it suffices to follow the evolution of allele frequencies over time (rather than study the genotype frequencies).

Denote the fitness of a haploid genotype $\{P_{k_1}^1, ..., P_{k_L}^L\}$ by $w_{\{P_{k_1}^1, ..., P_{k_L}^L\}}$, and assume that selection is frequency-independent and constant in time. That is, the fitness values $w_{\{P_{k_1}^1, ..., P_{k_L}^L\}}$ are constant; they do not change over time directly (fluctuating selection), nor do their values depend on the allele frequencies. Note that I do not require any assumptions about the pattern of epistasis; the genotype fitnesses may contain any epistatic interactions between alleles.

The marginal fitness of an allele is the mean fitness of all genotypes containing the allele. Hence, for allele k_κ on locus i_λ, its marginal fitness is

$$w_{k_\kappa}^{i_\lambda} = \sum_{k_1=1}^{K_1} \cdots \sum_{k_{i_\lambda-1}=1}^{K_{i_\lambda-1}} \sum_{k_{i_\lambda+1}=1}^{K_{i_\lambda+1}} \cdots \sum_{k_L=1}^{K_L} \left(\prod_{i \neq i_\lambda} p_{k_i}^i w_{\{P_{k_1}^1, ..., P_{k_\kappa}^{i_\lambda}, ..., P_{k_L}^L\}} \right). \tag{A3.1}$$

It follows from the assumption of frequency-independent selection, that the marginal fitness of an allele does not depend on the frequencies of the alleles at its locus. In other words, for every locus i we have

$$\frac{\partial w_k^i}{\partial p_j^i} = 0 \qquad \text{for } j,k \in \{1,...,K_i\}. \tag{A3.2}$$

The mean fitness of the population is defined as the mean fitness of all genotypes, i.e.,

$$\bar{w} = \sum_{k_1=1}^{K_1} \cdots \sum_{k_L=1}^{K_L} \left(\prod_{i=1}^{L} p_{k_i}^i w_{\{P_{k_1}^1,...,P_{k_L}^L\}} \right). \tag{A3.3}$$

Clearly, we may write the mean fitness $\bar{w}$ in terms of the marginal fitnesses of the alleles at one locus, $\bar{w} = \sum_{k=1}^{K_i} p_k^i w_k^i$; this evaluates to the same value for any choice of $i \in \{1,...,L\}$.

To describe the evolution of allele frequencies, I consider the standard selection dynamics from population genetics in discrete time (generations). It neglects all other evolutionary forces (e.g., mutation) and just describes the impact of selection. In particular, there is no genetic drift, i.e., the population is practically infinite. The frequency of allele k on locus i in the next generation, $(p_k^i)'$, is calculated from the previous generation as

$$(p_k^i)' = p_k^i \frac{w_k^i}{\bar{w}} = f_k^i(\mathbf{p}). \tag{A3.4}$$

These dynamics respect the constraint $\sum_{k=1}^{K_i} p_k^i = 1$ for all times and every locus $i \in \{1,...,L\}$. A fully polymorphic equilibrium of equation (A3.4) is a vector $\hat{\mathbf{p}} = (\hat{\mathbf{p}}^1,...,\hat{\mathbf{p}}^L)$ of only non-zero entries that satisfy $f_k^i(\hat{\mathbf{p}}) = \hat{p}_k^i > 0$. It follows that at any polymorphic equilibrium we have $w_k^i = \bar{w}$ for all $i \in \{1,...,L\}$ and $k \in \{1,...,K_i\}$.

A3.2 Convergence to the set of equilibria

From the above assumptions on the marginal fitnesses, it follows that $\partial\bar{w}/\partial p_k^i = w_k^i$ for all i and k. Thus, from equation (A3.4), we may write the dynamics for allele k on locus i as

$$(p_k^i)' = \frac{p_k^i \frac{\partial \bar{w}}{\partial p_k^i}}{\sum_{j=1}^{K_i} p_j^i \frac{\partial \bar{w}}{\partial p_j^i}}. \tag{A3.5}$$

Furthermore, $\bar{w}$ is a linear combination of the allele frequencies at locus i, i.e., a homogeneous polynomial with positive coefficients (the marginal fitnesses of the alleles at locus i). Thus, the conditions for the inequality of Baum and Eagon (1967) are met. It follows that the mean fitness $\bar{w} = \bar{w}(\mathbf{p})$ is strictly increasing along trajectories of $\mathbf{p}$ under the dynamics (A3.4), remaining constant if and only if it has reached an equilibrium. Mathematically,

$$\bar{w}(\mathbf{p}') \geq \bar{w}(\mathbf{p}) \qquad \text{and} \qquad \bar{w}(\mathbf{p}') = \bar{w}(\mathbf{p}) \Longleftrightarrow \mathbf{p}' = \mathbf{p}.$$

The space of admissible $\mathbf{p}$ is a compact set, hence the values of $\bar{w}(\mathbf{p})$ are bounded from above. Thus, every trajectory of the dynamics (A3.4) converges to the set of its equilibrium points. This set may be complicated; nevertheless, the existence of other attractors (e.g. periodic orbits, chaotic attractors) can be excluded (Lyubich, 1992, Ch.9). If selection is additive, convergence to a given equilibrium was shown by Kirzhner and Lyubich (1997).

In the next section, I show that any polymorphic equilibria are unstable. As a consequence, every trajectory of the dynamics (A3.4) has to converge towards the boundary of the state space, where at least one of the alleles is lost from the system. Iterating the argument with the remaining alleles and those loci that stayed polymorphic shows that, eventually, every locus is fixed for a single allele, i.e., all genetic variation is lost.

A3.3 Stability of equilibria

The local behaviour of allele frequencies around an equilibrium $\hat{\mathbf{p}}$ is given by the linearisation of equation (A3.4) around $\hat{\mathbf{p}}$. The stability of $\hat{\mathbf{p}}$ is determined by the eigenvalues of the Jacobian matrix $J(\hat{\mathbf{p}})$. This matrix has dimensions $\mathcal{K} \times \mathcal{K}$ (recall that $\mathcal{K}$ is the total number of alleles at all loci), and its entry at position (m, n) is obtained from taking the derivative of the m-th function f_k^i with respect to the n-th variable p_j^l (counting contiguously across loci), evaluated at $\hat{\mathbf{p}}$. For example, the diagonal entries of $J(\hat{\mathbf{p}})$ are given by

$$(J(\hat{\mathbf{p}}))_{m,m} = \frac{\partial f_k^i(\hat{\mathbf{p}})}{\partial p_k^i}, \tag{A3.6}$$

where $m = \sum_{j=1}^{k-1} K_j + i$. If all eigenvalues of $J(\hat{\mathbf{p}})$ have a modulus less than one, the equilibrium $\hat{\mathbf{p}}$ is asymptotically stable; if the modulus of a single eigenvalue is greater

than one, it is unstable. In the case when the moduli of all eigenvalues equal one, further analysis would be needed. However, I will neglect this degenerate case, since it is highly unlikely.

Theorem (Instability of polymorphic equilibria)**.** *Under the assumptions stated in Section A3.1, i.e., linkage equilibrium and constant frequency-independent selection, any fully polymorphic equilibrium* $\hat{\mathbf{p}}$ *of the dynamics* (A3.4) *is unstable.*

For the proof, consider two simple lemmas:

Lemma 1. *Consider a polymorphic equilibrium* $\hat{\mathbf{p}}$ *of the dynamics* (A3.4)*. Then, for every locus* $i \in \{1, ..., L\}$*, there is at least one eigenvector* ν^i *of the Jacobian* $J(\hat{\mathbf{p}})$ *with associated eigenvalue* 0*, i.e.,* $J(\hat{\mathbf{p}}).\nu^i = 0$*.*

Proof. This is the case because the dynamics (A3.4) are a projection on the space of allele frequencies, $\sum_{k=1}^{K_i} p_k^i = 1$ for $i = 1, ..., L$. □

Lemma 2. *Consider a polymorphic equilibrium* $\hat{\mathbf{p}}$ *of the dynamics* (A3.4) *under the same assumptions as in Theorem A3.3. Then, the trace of the Jacobian* $J(\hat{\mathbf{p}})$ *(i.e., the sum of its diagonal entries) is*

$$\textit{tr}(J(\hat{\mathbf{p}})) = \mathcal{K} - L.$$

Proof. First, from equation (A3.4), we calculate the derivatives

$$\frac{\partial f_k^i(\hat{\mathbf{p}})}{\partial p_k^i} = 1 - \hat{p}_k^i.$$

In this calculation, I used that $\partial \bar{w}/\partial p_k^i = w_k^i$ (mean fitness as a linear combination of marginal fitnesses), $\partial w_k^i/\partial p_k^i = 0$ (frequency independence), and $w_k^i \equiv \bar{w}$ (equilibrium condition). It follows that the trace of $J(\mathbf{p})$ is

$$\begin{aligned}\text{tr}(J(\mathbf{p})) &= \sum_{i=1}^{L} \sum_{k_i=1}^{K_i} \frac{\partial f_{k_i}^i(\hat{\mathbf{p}})}{\partial p_{k_i}^i} = \sum_{i=1}^{L} \sum_{k_i=1}^{K_i} \left(1 - \hat{p}_{k_i}^i\right) = \\ &= \sum_{i=1}^{L} (K_i - 1) = \mathcal{K} - L.\end{aligned}$$

□

Proof of the Theorem. Consider a polymorphic equilibrium $\hat{\mathbf{p}}$ of equation (A3.4) and its Jacobian $J(\hat{\mathbf{p}})$. Because $J(\hat{\mathbf{p}})$ is a matrix with dimensions $\mathcal{K} \times \mathcal{K}$, it has $\mathcal{K}$ eigenvalues (counting multiplicities). Due to Lemma 1, at most $\mathcal{K} - L$ are non-zero. According to Lemma 2, the trace, and hence the sum of eigenvalues of $J(\hat{\mathbf{p}})$ is also $\mathcal{K} - L$. Hence, unless all eigenvalues equal one (the degenerate case), at least one of them has a modulus greater than one. Thus, the polymorphic equilibrium $\hat{\mathbf{p}}$ is unstable. □

A3.4 Summary

Start out with a population of haploid genotypes, consisting of multiple polymorphic loci. The central assumption is that selection is constant and frequency-independent, i.e., the genotypes have fixed fitness values. Furthermore, consider strong recombination to neglect linkage disequilibrium and study the evolution of allele frequencies under selection alone, i.e., the dynamics (A3.4).

In Section A3.2, I argued that the selection dynamics are simple in the sense that each trajectory converges to the set of equilibrium points of equation (A3.4). According to Section A3.3, however, each polymorphic equilibrium is unstable, hence trajectories converge to the boundary of the allele frequency space where at least one of the allele frequencies is zero. Thus, some alleles are removed from the population and the set of possible genotypes is reduced.

Repeating the argument on the reduced set of genotypes, i.e., restricting the system to the alleles on the remaining polymorphic loci, allows to iteratively remove alleles from the population. This procedure can be carried out until all loci become monomorphic, i.e., until only a single genotype remains. Thus, in the absence of mechanisms creating variation (e.g., mutation), the action of constant frequency-independent selection eventually deprives the population of all its genetic variation.